Supporting Information

for

Silane catecholate: versatile tools for self-assembled dynamic covalent bond chemistry

Yoshiteru Kawakami,[a] Tsuyoshi Ogishima,[a] Tomoki Kawara,[a] Shota Yamauchi,[a] Kazuhiko Okamoto,[a] Singo Nikaido,[a] Daiki Souma,[b] Ren-Hua Jin[b] and Yoshio Kabe*[a]

[a] Department of Chemistry, Faculty of Science, Kanagawa University 2946, Tsuchiya, Hiratsuka 259-1293, Japan.

[b] Department of Material and Life Chemistry, Faculty of Engineering, Kanagawa University 3-2-7, Rokkakubashi, Kanagawa-ku, Yokohama 221-8686 Japan.

1. General information and experimental procedures S2
2. Structural assignment and spectral data S17
3. Crystallographic data S62
4. MeCN-promoted DCC conditions for the formation of **4a**, **5a** and **6a** S64
5. ^{1}H NMR titration S74
6. Attempts to achieve gas adsorption within **4a**·4HNEt$_3$, **5a**·6Na, and **5a**·1.5(**8**) S85
7. Supporting references S89

1. General information and experimental procedures

All reactions were performed under an argon atmosphere unless otherwise specified. ^{1}H and ^{13}C NMR spectra were recorded at room temperature using a JEOL JNM-ECX 600R, JNM-ECS 400, or JNM-ECA 400 spectrometer. High resolution mass spectra (ESI) were recorded on a JEOL JMS-T100LC mass spectrometer using a reserpine and YOKUDELUNA calibration kit (JEOL) for accurate mass calibration. Commercially available solvents and reagents were purchased from Sigma-Aldrich, Wako, TCI, and KANTO. Anhydrous DMF was purchased from Wako. Tetrahydrofuran (THF) was distilled from lithium aluminum hydride (LAH). Methanol was distilled from calcium hydride, while acetonitrile was dried over MS3Å. Trimethoxysilanes, [$RSi(OMe)_3$, R = Ph, *p*-tolyl, Me, vinyl, $(CH_2)_3SH$, and $(CH_2)_3NMe_2$] were purchased from Shin-Etsu Chemical Co., Ltd. 9,10-Dimethyl-9,10-ethano-9,10-dihydro-2,3,6,7-tetrahydroxyanthracene (EAT) (**2**) was prepared from pyrocatechol and 2,5-hexanedione according to a literature method.[1)] Cyclotricatechylene (CTC) (**3**) was also synthesized according to a modified known procedure[2-5)] by hydrochloric acid catalyzed condensation of veratrole with trioxane to initially yield cyclotriveratrylene (CTV), followed by demethylation using Me_3SiCl/NaI in acetonitrile. Stoddart's blue box (**8**·$4PF_6$) and its synthetic precursor (**7**·$2PF_6$) were also prepared according to a modified literature method[6-7)] by *N*-alkylation of 1,1'-[1,4-phenylene-bis(methylene)]-bis(4,4'-bipyridinium) bis(hexafluorophosphate) with 1,4-bis(iodomethyl)benzene instead of the corresponding dibromide in the presence of 1,5-bi(2-(2-methoxyethoxy)ethoxy)naphthalene as template.

1.1. Synthesis of **4a**·$4HNEt_3$·2(**2**)·4THF

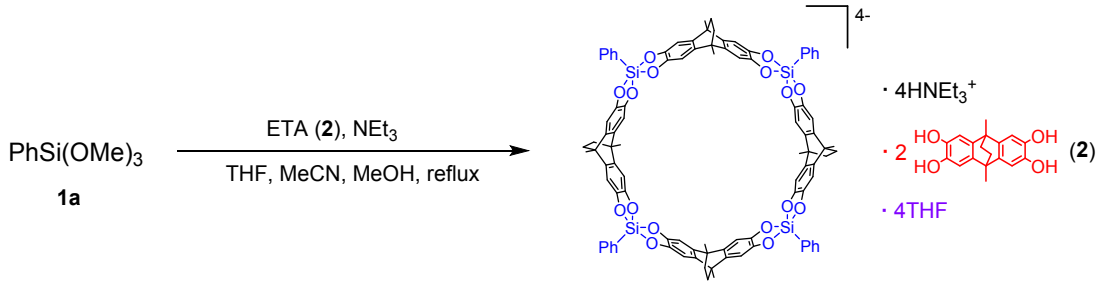

4a·$4HNEt_3$·2(**2**)·4THF

9,10-Dimethyl-9,10-ethano-9,10-dihydro-2,3,6,7-tetrahydroxyanthracene (EAT) etherate (**2**·Et_2O) (6.00 mmol, 2.24 g), $PhSi(OMe)_3$ (4.40 mmol, 0.872 g, 0.822 mL), and Et_3N (16.0 mmol, 1.62 g, 2.23 mL) were dissolved in 45 mL of THF, 15 mL of MeCN, and 15 mL of MeOH. The reaction mixture was stirred and refluxed under a nitrogen atmosphere for 2 days. The mixture was then cooled to room temperature, and the precipitate was collected by suction filtration. It was then washed with 20 mL of THF and dried under reduced pressure to give 2.52 g (0.871 mmol, 87.1%) of **4a**·$4HNEt_3$·2(**2**)·4THF as a white powder.

4a·4HNEt$_3$·2(**2**)·4THF: ^{1}H NMR (600MHz, DMSO-d_6) δ 8.66 (br, 4H, NH), 8.42 (s, 8H, OH), 7.51 (d, J = 6.4 Hz, 8H, *o*-CH), 7.13-7.09 (m, 12H, *p*-CH and *m*-CH), 6.59 (s, 8H, ArH), 6.41 (s, 16H, ArH), 3.59 (m, OCH$_2$, 16H), 2.85 (q, J = 7.2 Hz, 24H, NCH$_2$), 1.75 (m, OCH$_2$<u>CH$_2$</u>, 16H), 1.67 (s, 12H, CH$_3$), 1.64 (brs, 24H, CH$_3$), 1.39 (s, 8H, CH$_2$), 1.35 (brs, 16H, CH$_2$), 1.00 (t, J = 7.2 Hz, 36H, NCH$_2$<u>CH$_3$</u>); ^{13}C NMR (150MHz, DMSO-d_6) δ 146.77 (C), 142.77 (*ipso*-C), 141.74 (C), 137.63 (C), 136.25 (C), 134.77 (*o*-CH), 127.45 (*p*-CH), 126.62 (*m*-CH), 108.77 (CH), 103.08 (CH), 67.04 (OCH$_2$), 45.55 (NCH$_2$), 40.25 (C), 39.94 (C), 36.27 (CH$_2$), 36.24 (CH$_2$), 25.14 (OCH$_2$<u>CH$_2$</u>), 19.24 (CH$_3$), 18.52 (CH$_3$), 8.49 (NCH$_2$<u>CH$_3$</u>); ^{29}Si NMR (120MHz, DMSO-d_6) δ -86.91 (PhSiO$_4$); HRMS (ESI-, MeOH) m/z calcd for $C_{138}H_{129}N_1O_{24}Si_4$ [M+HNEt$_3$+H+2(**2**)]$^{2-}$ 1147.89908, found 1147.89793.

1.2. Preparation of **4a**·4HNEt$_3$

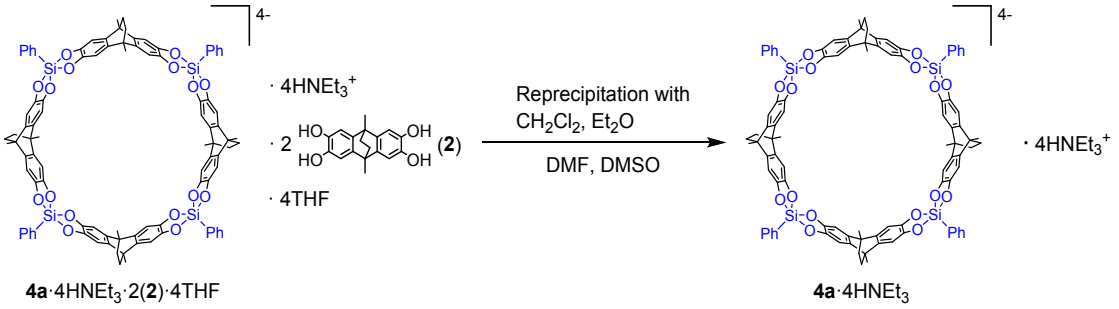

Compound **4a**·4HNEt$_3$·2(**2**)·4THF (2.00 mmol, 5.78 g) was dissolved in 50 mL of DMSO and 50 mL of DMF upon heating. Further addition of 100 mL of CH$_2$Cl$_2$ and 300 mL of Et$_2$O led to the precipitation of a white powder. The powder was collected by suction filtration and dried under reduced pressure to give 2.71 g (1.35 mmol, 67.5%) of **4a**·4HNEt$_3$.

4a·4HNEt$_3$: ^{1}H NMR (600MHz, DMSO-d_6) δ 8.62 (br, 4H, NH), 7.52 (d, J = 6.4 Hz, 8H, *o*-CH), 7.14-7.11 (m, 12H, *p*-CH and *m*-CH), 6.42 (s, 16H, ArH), 2.81 (q, J = 7.2 Hz, 24H, NCH$_2$), 1.65 (brs, 24H, CH$_3$), 1.37 (brs, 16H, CH$_2$), 0.98 (t, J = 7.2 Hz, 36H, NCH$_2$<u>CH$_3$</u>); ^{13}C NMR (150MHz, DMSO-d_6) δ 146.74 (C), 142.76 (*ipso*-C), 136.20 (C), 134.74 (*o*-CH), 127.40 (*p*-CH), 126.58 (*m*-CH), 103.03 (CH), 45.52 (NCH$_2$), 40.21 (C), 36.24 (CH$_2$), 19.21 (CH$_3$), 8.43 (NCH$_2$<u>CH$_3$</u>); ^{29}Si NMR (120MHz, DMSO-d_6) δ -86.85 (PhSiO$_4$); HRMS (ESI-, MeOH) m/z calcd for $C_{102}H_{93}N_1O_{16}Si_4$ [M+HNEt$_3$+H]$^{2-}$ 849.77857, found 849.77934.

1.3. Synthesis of **4a**·4HNEt$_2$Bn·2(**2**)·4THF

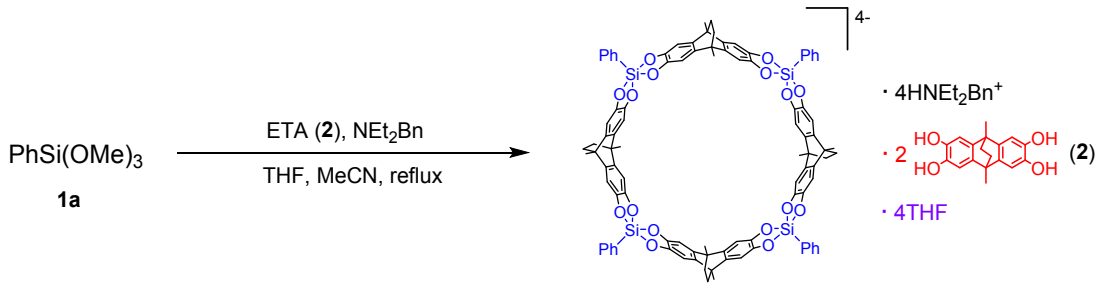

4a·4HNEt$_2$Bn·2(**2**)·4THF

9,10-Dimethyl-9,10-ethano-9,10-dihydro-2,3,6,7-tetrahydroxyanthracene (EAT) (**2**) (2.00 mmol, 0.597 g), PhSi(OMe)$_3$ (2.10 mmol, 0.416 g, 0.392 mL), and NEt$_2$Bn (6.00 mmol, 0.979 g, 1.08 mL) were dissolved in 15 mL of THF and 5 mL of MeCN. The reaction mixture was stirred and refluxed under a nitrogen atmosphere for 1 day. The mixture was then cooled to room temperature, and the precipitate was collected by suction filtration. It was washed with 10 mL of THF and dried under reduced pressure to give 0.665 g (0.212 mmol, 63.7%) of **4a**·4HNEt$_2$Bn·2(**2**)·4THF as a white powder.

4a·4HNEt$_2$Bn·2(**2**)·4THF: ^{1}H NMR (600MHz, DMSO-d_6) δ 8.98 (br, 4H, NH), 8.42 (s, 8H, OH), 7.51 (d, J = 6.4 Hz, 8H, *o*-CH), 7.36-7.30 (m, 20H, NCH$_2$<u>Ph</u>), 7.13-7.10 (m, 12H, *p*-CH and *m*-CH), 6.60 (s, 8H, ArH), 6.41 (s, 16H, ArH), 4.06 (d, J = 5.3 Hz, 8H, N<u>CH$_2$</u>Ph), 3.59 (m, OCH$_2$, 16H), 2.88-2.75 (m, 16H, NCH$_2$), 1.75 (m, OCH$_2$<u>CH$_2$</u>, 16H), 1.67 (s, 12H, CH$_3$), 1.64 (brs, 24H, CH$_3$), 1.40 (s, 8H, CH$_2$), 1.36 (brs, 16H, CH$_2$), 0.95 (t, J = 7.2 Hz, 24H, NCH$_2$<u>CH$_3$</u>); ^{13}C NMR (150MHz, DMSO-d_6) δ 146.80 (C), 142.77 (*ipso*-C), 141.78 (C), 137.67 (C), 136.33 (C), 134.79 (*o*-CH), 130.80 (NBn, *o*-CH), 129.93 (NBn, *ipso*-C), 129.38 (NBn, *p*-CH), 128.87 (NBn, *m*-CH), 127.48 (*p*-CH), 126.64 (*m*-CH), 108.80 (CH), 103.14 (CH), 67.05 (OCH$_2$), 55.00 (N<u>CH$_2$</u>Ph), 45.85 (NCH$_2$), 40.28 (C), 39.97 (C), 36.29 (CH$_2$), 36.27 (CH$_2$), 25.16 (OCH$_2$<u>CH$_2$</u>), 19.25 (CH$_3$), 18.54 (CH$_3$), 8.24 (NCH$_2$<u>CH$_3$</u>); ^{29}Si NMR (120MHz, DMSO-d_6) δ -86.72 (PhSiO$_4$); HRMS (ESI-, MeOH) m/z calcd for $C_{143}H_{131}N_1O_{24}Si_4$ [M+HNEt$_2$Bn+H+2(**2**)]$^{2-}$ 1178.90691, found 1178.90791.

1.4. Synthesis of **4a**·4HNMe$_2$Bn·2THF

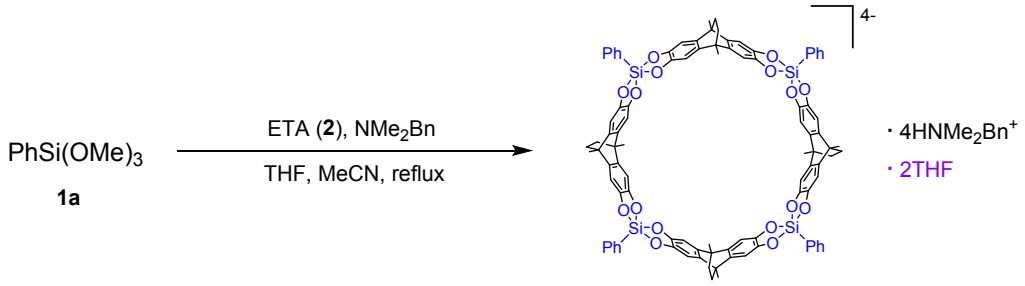

4a·4HNMe$_2$Bn·2THF

9,10-Dimethyl-9,10-ethano-9,10-dihydro-2,3,6,7-tetrahydroxyanthracene (EAT) (**2**) (2.00 mmol, 0.597 g), PhSi(OMe)$_3$ (2.10 mmol, 0.416 g, 0.392 mL), and NMe$_2$Bn (6.00 mmol, 0.811 g, 0.901 mL) were dissolved in 15 mL of THF and 5 mL of MeCN. The reaction mixture was stirred and refluxed under a nitrogen atmosphere for 2 day. The mixture was then cooled to room temperature, and the precipitate was collected by suction filtration. It was then washed with 10 mL of THF and dried under reduced pressure to give 0.845 g (0.369 mmol, 73.8%) of **4a**·4HNMe$_2$Bn·2THF as a white powder.

4a·4HNMe$_2$Bn·2THF: ^{1}H NMR (600MHz, DMSO-d_6) δ 9.36 (br, 4H, NH), 7.51 (d, J = 6.4 Hz, 8H, *o*-CH), 7.36-7.31 (m, 20H, NCH$_2$<u>Ph</u>), 7.13-7.09 (m, 12H, *p*-CH and *m*-CH), 6.41 (s, 16H, ArH), 4.06 (brs, 8H, N<u>CH$_2$</u>Ph), 3.59 (m, OCH$_2$, 8H), 2.51 (s, 24H, NCH$_3$), 1.75 (m, OCH$_2$<u>CH$_2$</u>, 8H), 1.64 (brs, 24H, CH$_3$), 1.36 (brs, 16H, CH$_2$); ^{13}C NMR (150MHz, DMSO-d_6) δ 146.71 (C), 142.76 (*ipso*-C), 136.24 (C), 134.70 (*o*-CH), 130.67 (NBn, *o*-CH), 130.52 (NBn, *ipso*-C), 129.34 (NBn, *p*-CH), 128.82 (NBn, *m*-CH), 127.39 (*p*-CH), 126.58 (*m*-CH), 103.08 (CH), 67.00 (OCH$_2$), 59.92 (N<u>CH$_2$</u>Ph), 41.79 (NCH$_3$), 40.21 (C), 36.21 (CH$_2$), 25.10 (OCH$_2$<u>CH$_2$</u>), 19.20 (CH$_3$); ^{29}Si NMR (120MHz, DMSO-d_6) δ -86.86 (PhSiO$_4$); HRMS (ESI-, MeOH) m/z calcd for $C_{105}H_{91}N_1O_{16}Si_4$ [M+HNMe$_2$Bn+H]$^{2-}$ 866.77075, found 866.76976.

1.5. Synthesis of **4a**·4HNMe$_2$Bu·2THF

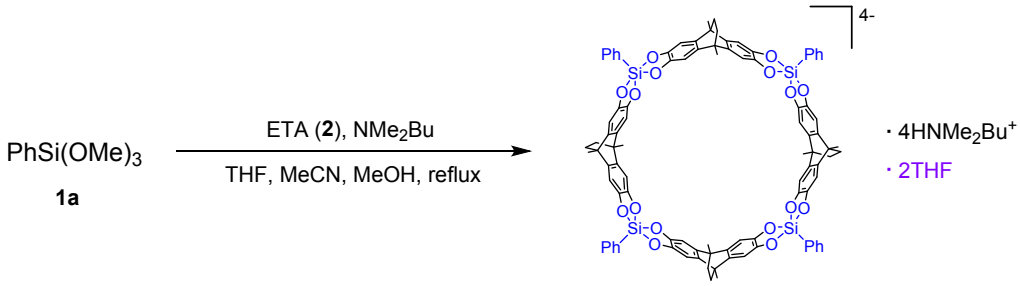

4a·4HNMe$_2$Bu·2THF

9,10-Dimethyl-9,10-ethano-9,10-dihydro-2,3,6,7-tetrahydroxyanthracene (EAT) (**2**) (2.00 mmol, 0.597 g), PhSi(OMe)$_3$ (2.20 mmol, 0.436 g, 0.411 mL), and NMe$_2$Bu (6.00 mmol, 0.607 g, 0.842

mL) were dissolved in 15 mL of THF, 5 mL of MeCN, and 5 mL of MeOH. The reaction mixture was stirred and refluxed under a nitrogen atmosphere for 2 days. The mixture was then cooled to room temperature, and the precipitate was collected by suction filtration. It was then washed with 10 mL of THF and dried under reduced pressure to give 0.624 g (0.290 mmol, 58.0%) of **4a**·4HNMe$_2$Bu·2THF as a white powder.

4a·4HNMe$_2$Bu·2THF: ^{1}H NMR (600MHz, DMSO-d_6) δ 8.98 (br, 4H, NH), 7.51 (d, J = 6.4 Hz, 8H, *o*-CH), 7.13-7.10 (m, 12H, *p*-CH and *m*-CH), 6.41 (s, 16H, ArH), 3.59 (m, OCH$_2$, 8H), 2.81 (brt, J = 8.1 Hz, 8H, N$\underline{CH_2}$CH$_2$CH$_2$CH$_3$), 2.56 (s, 24H, NCH$_3$), 1.75 (m, OCH$_2\underline{CH_2}$, 8H), 1.64 (brs, 24H, CH$_3$), 1.45-1.39 (m, 8H, NCH$_2\underline{CH_2}$CH$_2$CH$_3$), 1.35 (brs, 16H, CH$_2$), 1.42 (sext, J = 7.5 Hz, 8H, NCH$_2$CH$_2\underline{CH_2}$CH$_3$), 1.42 (t, J = 7.4 Hz, 12H, NCH$_2$CH$_2$CH$_2\underline{CH_3}$); ^{13}C NMR (150MHz, DMSO-d_6) δ 146.70 (C), 142.79 (*ipso*-C), 136.21 (C), 134.77 (*o*-CH), 127.38 (*p*-CH), 126.57 (*m*-CH), 103.06 (CH), 67.00 (OCH$_2$), 56.54 (N$\underline{CH_2}$CH$_2$CH$_2$CH$_3$), 42.29 (NCH$_3$), 40.20 (C), 36.24 (CH$_2$), 25.85 (NCH$_2\underline{CH_2}$CH$_2$CH$_3$), 25.11 (OCH$_2\underline{CH_2}$), 19.20 (CH$_3$), 19.13 (NCH$_2$CH$_2\underline{CH_2}$CH$_3$), 13.41 (NCH$_2$CH$_2$CH$_2\underline{CH_3}$); ^{29}Si NMR (120MHz, DMSO-d_6) δ -87.02 (PhSiO$_4$); HRMS (ESI-, MeOH) m/z calcd for $C_{102}H_{93}N_1O_{16}Si_4$ $[M+HNMe_2Bu+H]^{2-}$ 849.77857, found 849.77895.

1.6. Synthesis of **4a**·4TMEDAH·2THF

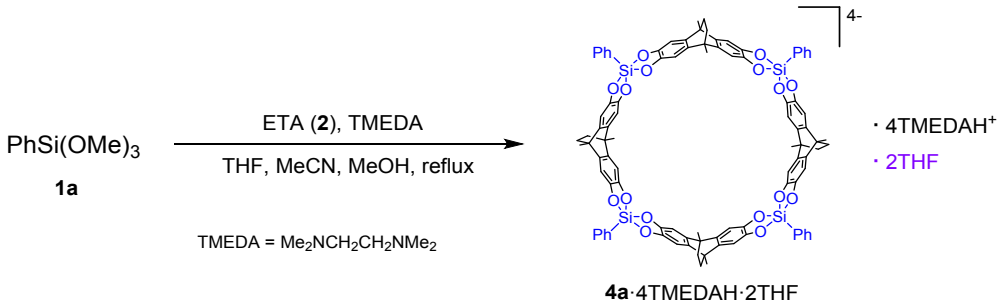

9,10-Dimethyl-9,10-ethano-9,10-dihydro-2,3,6,7-tetrahydroxyanthracene (EAT) etherate (**2**·Et$_2$O) (2.00 mmol, 0.745 g), PhSi(OMe)$_3$ (2.20 mmol, 0.436 g, 0.411 mL), and TMEDA (6.00 mmol, 0.697 g, 0.900 mL) were dissolved in 15 mL of THF, 5 mL of MeCN, and 5 mL of MeOH. The reaction mixture was stirred and refluxed under a nitrogen atmosphere for 1 day. The mixture was then cooled to room temperature, and the precipitate was collected by suction filtration. It was then washed with 10 mL of THF and dried under reduced pressure to give 0.877 g (0.397 mmol, 79.4%) of **4a**·4 TMEDAH·2THF as a white powder.

4a·4 TMEDAH·2THF: ^{1}H NMR (600MHz, DMSO-d_6) δ 7.51 (d, J = 6.4 Hz, 8H, *o*-CH), 7.13-7.10 (m, 12H, *p*-CH and *m*-CH), 6.41 (s, 16H, ArH), 3.59 (m, OCH$_2$, 8H), 2.58 (s, 16H, NCH$_2$CH$_2$N),

2.29 (s, 48H, NCH_3), 1.75 (m, $OCH_2\underline{CH_2}$, 8H), 1.64 (brs, 24H, CH_3), 1.35 (brs, 16H, CH_2); ^{13}C NMR (150MHz, DMSO-d_6) δ 146.73 (C), 142.83 (*ipso*-C), 136.20 (C), 134.81 (*o*-CH), 127.39 (*p*-CH), 126.59 (*m*-CH), 103.09 (CH), 67.02 (OCH_2), 53.38 (NCH_2CH_2N), 43.71 (NCH_3), 40.22 (C), 36.25 (CH_2), 25.12 ($OCH_2\underline{CH_2}$), 19.23 (CH_3); ^{29}Si NMR (120MHz, DMSO-d_6) δ -87.02 ($PhSiO_4$); HRMS (ESI-, MeOH) m/z calcd for $C_{109}H_{114}N_4O_{17}Si_4$ $[M+2(HNMe_2CH_2CH_2NMe_2)+MeOH]^{2-}$ 931.36280, found 931.36222.

1.7. Synthesis of **4a**·4HNEt$_3$·2(**2**)·2Anthracene·THF

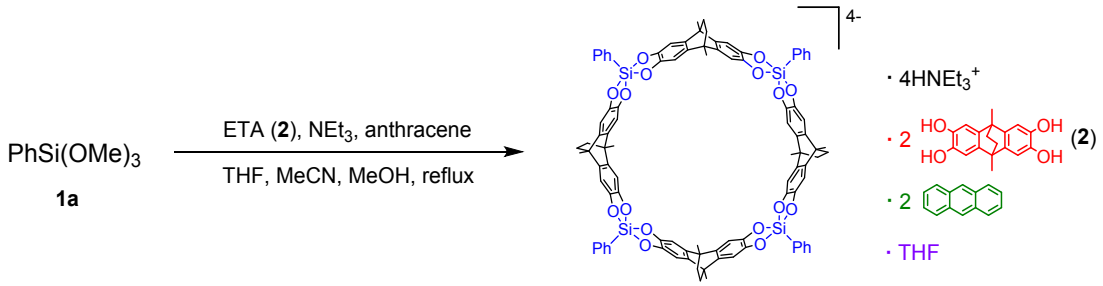

4a·4HNEt$_3$·2(**2**)·2anthracene·THF

9,10-Dimethyl-9,10-ethano-9,10-dihydro-2,3,6,7-tetrahydroxyanthracene (EAT) (**2**) (2.00 mmol, 0.597 g), $PhSi(OMe)_3$ (2.10 mmol, 0.416 g, 0.392 mL), and Et_3N (6.00 mmol, 0.607 g, 0.836 mL) with anthracene (4.00 mmol, 0.713 g) were dissolved in 15 mL of THF, 5 mL of MeCN, and 5 mL of MeOH. The reaction mixture was stirred and refluxed under a nitrogen atmosphere for 2 days. The mixture was then cooled to room temperature, and the precipitate was collected by suction filtration. It was then washed with 20 mL of THF and dried under reduced pressure to give 0.886 g (0.292 mmol, 87.6%) of **4a**·2(**2**)·4HNEt$_3$·2Anthracene·THF as a white powder.

4a·4HNEt$_3$·2(**2**)·2Anthracene·THF: ^1H NMR (600MHz, DMSO-d_6) δ 8.66 (br, 4H, NH), 8.57 (s, 4H, 9,10-CH), 8.41 (s, 8H, OH), 8.08 (dd, , J = 6.4, 3.3 Hz, 8H, 1,4,5,8-CH), 7.53-7.49 (m, 16H, *o*-CH, 2,3,6,7-CH), 7.13-7.09 (m, 12H, *p*-CH and *m*-CH), 6.59 (s, 8H, ArH), 6.41 (s, 16H, ArH), 3.59 (m, OCH_2, 4H), 2.86 (q, J = 7.3 Hz, 24H, NCH_2), 1.75 (m, $OCH_2\underline{CH_2}$, 4H), 1.67 (s, 12H, CH_3), 1.63 (brs, 24H, CH_3), 1.39 (s, 8H, CH_2), 1.35 (brs, 16H, CH_2), 1.01 (t, J = 7.3 Hz, 36H, $NCH_2\underline{CH_3}$); ^{13}C NMR (150MHz, DMSO-d_6) δ 146.79 (C), 142.78 (*ipso*-C), 141.75 (C), 137.64 (C), 136.27 (C), 134.78 (*o*-CH), 131.20 (C), 128.03 (1,4,5,8-CH), 127.45 (*p*-CH), 126.62 (*m*-CH), 126.02 (9,10-CH), 125.54 (2,3,6,7-CH), 108.78 (CH), 103.09 (CH), 67.03 (OCH_2), 45.54 (NCH_2), 40.26 (C), 39.95 (C), 36.27 (CH_2), 36.23 (CH_2), 25.13 ($OCH_2\underline{CH_2}$), 19.24 (CH_3), 18.52 (CH_3), 8.43 ($NCH_2\underline{CH_3}$); ^{29}Si NMR (120MHz, DMSO-d_6) δ -86.94 ($PhSiO_4$); HRMS (ESI-, MeOH) m/z calcd for $C_{138}H_{129}N_1O_{24}Si_4$ $[M+HNEt_3+H+2(\mathbf{2})]^{2-}$ 1147.89908, found 1147.89916.

1.8. Synthesis of **4b**·4HNEt$_3$·2THF

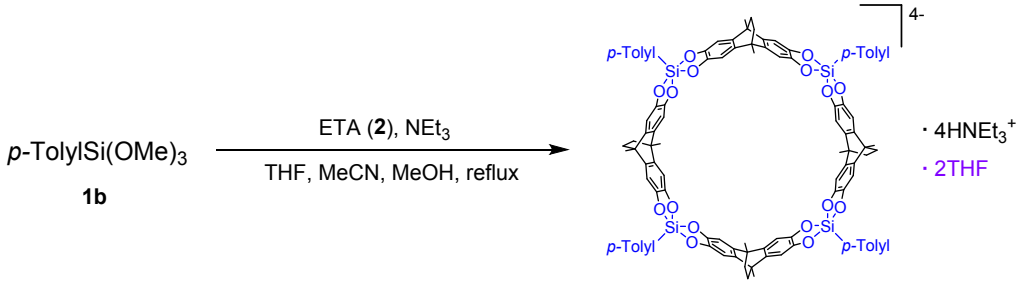

4b·4HNEt$_3$·2THF

9,10-Dimethyl-9,10-ethano-9,10-dihydro-2,3,6,7-tetrahydroxyanthracene (EAT) (**2**) (2.00 mmol, 0.597 g), *p*-tolylSi(OMe)$_3$ (2.10 mmol, 0.446 g, 0.432 mL), and Et$_3$N (6.00 mmol, 0.607 g, 0.836 mL) were dissolved in 15 mL of THF, 5 mL of MeCN, and 5 mL of MeOH. The reaction mixture was stirred and refluxed under a nitrogen atmosphere for 2 days. The mixture was then cooled to room temperature, and the precipitate was collected by suction filtration. It was then washed with 10 mL of THF and dried under reduced pressure to give 0.599 g (0.271 mmol, 54.2%) of **4b**·4HNEt$_3$·2THF as a white powder.

4b·4HNEt$_3$·2THF: 8.63 (br, 4H, NH), 7.41 (d, J = 7.8 Hz, 8H, *o*-CH), 6.93 (d, J = 7.8 Hz, 8H, *m*-CH), 6.40 (s, 16H, ArH), 3.59 (m, OCH$_2$, 8H), 2.82 (q, J = 7.3 Hz, 24H, NCH$_2$), 2.17 (s, 12H, Ar$\underline{CH_3}$), 1.75 (m, OCH$_2\underline{CH_2}$, 8H), 1.63 (brs, 24H, CH$_3$), 1.35 (brs, 16H, CH$_2$), 0.98 (t, J = 7.3 Hz, 36H, NCH$_2\underline{CH_3}$); ^{13}C NMR (150MHz, DMSO-d_6) δ 146.79 (C), 139.16 (C), 136.33 (C), 136.12 (C), 135.06 (*o*-CH), 127.24 (*m*-CH), 102.98 (CH), 67.00 (OCH$_2$), 45.57 (NCH$_2$), 40.20 (C), 36.29 (CH$_2$), 25.11 (OCH$_2\underline{CH_2}$), 20.97 (Ar$\underline{CH_3}$), 19.22 (CH$_3$), 8.48 (NCH$_2\underline{CH_3}$); ^{29}Si NMR (120MHz, DMSO-d_6) δ -86.57 (*p*-TolylSiO$_4$); HRMS (ESI-, MeOH) m/z calcd for $C_{106}H_{101}N_1O_{16}Si_4$ $[M+HNEt_3+H]^{2-}$ 877.80987, found 877.80782.

1.9. Synthesis of **5a**·6HNEt$_3$

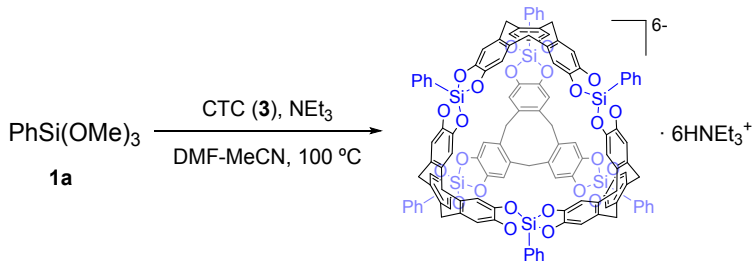

5a·6HNEt$_3$

Cyclotricatechylene (CTC) (**3**) (2.00 mmol, 0.733 g), PhSi(OMe)$_3$ (3.30 mmol, 0.654 g, 0.616 mL),

and Et_3N (9.00 mmol, 0.911 g, 1.25 mL) were dissolved in 20 mL of DMF and 10 mL of MeCN. The reaction mixture was stirred and heated at 100 ºC overnight under a nitrogen atmosphere. After cooling to room temperature, all the volatiles were removed under reduced pressure. The resulting residue was redissolved in 20 mL of THF and 10 mL of MeCN. Addition of Et_2O (200 mL) led to the precipitation of a brownish powder, which was collected by suction filtration and dried under reduced pressure to give 1.27 g (0.473 mmol, 94.6%) of **5a**·6HNEt$_3$ as a light brown powder.

5a·6HNEt$_3$: ^{1}H NMR δ 8.59 (br, 6H, NH), 7.36 (d, J = 6.6 Hz, 12H, *o*-CH), 7.14-7.07 (m, 18H, *p*-CH and *m*-CH), 6.49 (s, 24H, ArH), 4.44 (d, J = 13.1 Hz, 12H, ArCH$_2$Ar), 3.12 (d, J = 13.1 Hz, 12H, ArCH$_2$Ar), 2.85-2.79 (m, 36H, NCH$_2$), 0.95 (t, J = 7.2 Hz, 54H, CH$_3$); ^{13}C NMR δ 148.49 (C), 142.31 (*ipso*-C), 133.64 (*o*-CH), 128.82 (C), 127.40 (*p*-CH), 126.65 (*m*-CH), 110.33 (CH), 45.65 (NCH$_2$), 35.59 (ArCH$_2$Ar), 8.47 (CH$_3$); ^{29}Si NMR δ -86.94 (PhSiO$_4$); HRMS (ESI-, MeOH) m/z calcd for $C_{144}H_{142}N_4O_{24}Si_6$ [M+4HNEt$_3$]$^{2-}$ 1239.43148, found 1239.43078.

1.10. Synthesis of **6a**·9HNEt$_3$

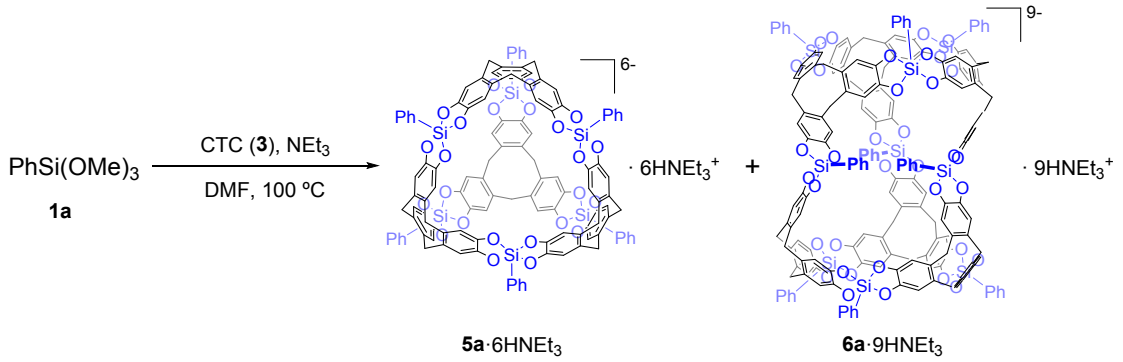

Cyclotricatechylene (CTC) (**3**) (2.00 mmol, 0.733 g), PhSi(OMe)$_3$ (3.30 mmol, 0.614 g, 0.616 mL), and Et_3N (9.00 mmol, 0.911 g, 1.25 mL) were dissolved in 30 mL of DMF. The reaction mixture was stirred and heated at 100 ºC overnight under a nitrogen atmosphere. After cooling to room temperature, 400 mL of THF was added and a small amount of black precipitate was formed and immediately filtered off. Then, the solution was left standing for 2 h until precipitation of a brown crystalline solid occurred. The solid was filtered and redissolved in 20 mL of THF and 10 mL of MeCN. Addition of Et_2O led to the precipitation of a brownish powder, whichwas collected by suction filtration and dried under reduced pressure to give 0.487 g (0.121 mmol, 36.3%) of **6a**·9HNEt$_3$ as a light brown powder.

The residual DMF-THF filtrate was evaporated under reduced pressure and treated as described above (section 1.10) to give 0.797 g (0.297 mmol, 59.4%) of **5a**·6HNEt$_3$ as a light brown powder.

6a·9HNEt$_3$: ^{1}H NMR δ 8.43 (br, 9H, NH), 7.35 (d, J = 6.6 Hz, 12H, *o*-CH), 7.22 (d, J = 6.8 Hz, 6H, *o*-CH'), 7.13-7.06 (m, 18H, *p*-CH and *m*-CH), 6.63 (t, J = 7.2 Hz, 6H, *m*-CH'), 6.55 (s, 12H, ArH), 6.47 (s, 12H, ArH), 6.42 (s, 12H, ArH), 6.38 (t, J = 7.6 Hz, 3H, *p*-CH'), 4.55 (d, J = 12.4 Hz, 6H, ArCH$_2$Ar), 4.44 (d, J = 12.6 Hz, 12H, ArCH$_2$Ar), 3.22-3.06 (m, 18H, ArCH$_2$Ar), 2.61 (q, J = 7.0 Hz, 54H, NCH$_2$), 0.88 (t, J = 7.0 Hz, 81H, CH$_3$); ^{13}C NMR δ 148.51 (C), 148.47 (C), 148.36 (C), 142.33 (*ipso*-C), 141.35 (*ipso*-C'), 133.70 (*o*-CH), 133.35 (*o*-CH'), 129.89 (C), 129.11 (C), 127.64 (C), 127.33 (*p*-CH), 127.22 (*p*-CH'), 126.61 (*m*-CH), 126.22 (*m*-CH'), 111.16 (CH), 110.44 (CH), 110.35 (CH), 45.48 (NCH$_2$), 36.28 (ArCH$_2$Ar), 35.67 (ArCH$_2$Ar), 8.41 (CH$_3$); ^{29}Si NMR δ -86.34 (3PhSiO$_4$), -86.85 (6PhSiO$_4$); HRMS (ESI-, MeOH) m/z calcd for $C_{216}H_{214}N_6O_{36}Si_9$ [M+6HNEt$_3$+H]$^{2-}$ 1859.65113, found 1859.64986.

1.11. Synthesis of **5b**·6HNEt$_3$

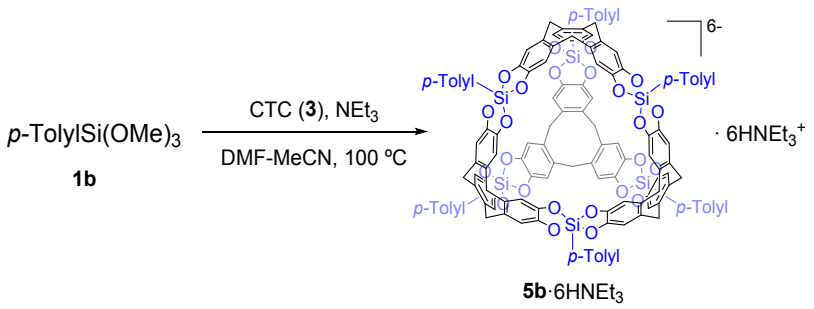

Cyclotricatechylene (CTC) (**3**) (2.00 mmol, 0.733 g), *p*-TolylSi(OMe)$_3$ (3.30 mmol, 0.701 g, 0.678 mL), and Et$_3$N (9.00 mmol, 0.911 g, 1.25 mL) were dissolved in 20 mL of DMF and 10 mL of MeCN. The reaction mixture was stirred and heated at 100 ºC overnight under a nitrogen atmosphere. After cooling to room temperature, all the volatiles were removed under reduced pressure. The resulting residue was redissolved in 20 mL of THF and 10 mL of MeCN. Addition of Et$_2$O (200 mL) led to the precipitation of a brownish powder, which was collected by suction filtration and dried under reduced pressure to give 1.38 g (0.498 mmol, 99.6%) of **5b**·6HNEt$_3$ as an off-white powder.

5b·6HNEt$_3$: ^{1}H NMR δ 8.63 (br, 6H, NH), 7.28 (d, J = 7.7 Hz, 12H, *o*-CH), 6.93 (d, J = 7.7 Hz, 12H, *m*-CH), 6.50 (s, 24H, ArH), 4.47 (d, J = 13.0 Hz, 12H, ArCH$_2$Ar), 3.15 (d, J = 13.0 Hz, 12H, ArCH$_2$Ar), 2.86 (m, 36H, NCH$_2$), 0.97 (t, J = 7.2 Hz, 54H, CH$_3$); ^{13}C NMR δ 148.54 (C), 138.77 (*ipso*-C), 136.28 (*p*-C), 133.80 (*o*-CH), 128.77 (C), 127.32 (*m*-CH), 110.29 (CH), 45.71 (NCH$_2$), 35.63 (ArCH$_2$Ar), 21.05 (Ar$\underline{CH_3}$), 8.48 (CH$_3$); ^{29}Si NMR δ -86.40 (*p*-TolylSiO$_4$); HRMS (ESI-, MeOH) m/z calcd for $C_{150}H_{154}N_4O_{24}Si_6$ [M+4HNEt$_3$]$^{2-}$ 1281.47843, found 1281.47666.

1.12. Synthesis of **5c**·6HNEt$_3$

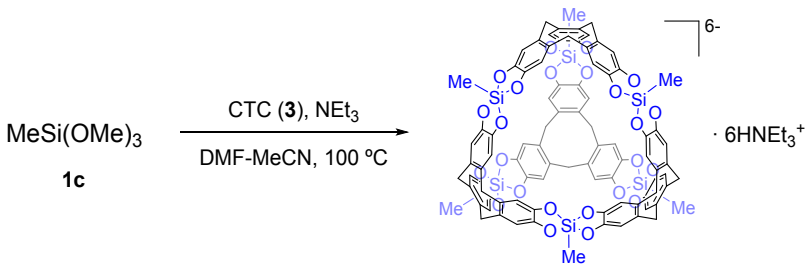

5c·6HNEt$_3$

Cyclotricatechylene (CTC) (**3**) (2.00 mmol, 0.733 g), MeSi(OMe)$_3$ (3.30 mmol, 0.450 g, 0.471 mL), and Et$_3$N (9.00 mmol, 0.911 g, 1.25 mL) were dissolved in 20 mL of DMF and 10 mL of MeCN. The reaction mixture was stirred and heated at 100 ºC overnight under a nitrogen atmosphere. After cooling to room temperature, all the volatiles were removed under reduced pressure. The resulting residue was redissolved in 30 mL of THF and 15 mL of MeCN. Addition of Et$_2$O (300 mL) led to the precipitation of a brownish powder, which was collected by suction filtration and dried under reduced pressure to give 1.15 g (0.497 mmol, 99.4%) of **5c**·6HNEt$_3$ as an off-white powder.

5c·6HNEt$_3$: ^{1}H NMR δ 8.54 (br, 6H, NH), 6.36 (s, 24H, ArH), 4.43 (d, J = 13.1 Hz, 12H, ArCH$_2$Ar), 3.09 (d, J = 13.1 Hz, 12H, ArCH$_2$Ar), 2.76 (q, J = 7.2 Hz, 36H, NCH$_2$), 0.91 (t, J = 7.2 Hz, 54H, CH$_3$), -0.29 (SiCH$_3$); ^{13}C NMR δ 148.27 (C), 128.48 (C), 110.17 (CH), 45.58 (NCH$_2$), 35.62 (ArCH$_2$Ar), 8.43 (CH$_3$), -0.22 (SiCH$_3$); ^{29}Si NMR δ -75.02 (MeSiO$_4$); HRMS (ESI-, MeOH) m/z calcd for $C_{114}H_{130}N_4O_{24}Si_6$ [M+4HNEt$_3$]$^{2-}$ 1053.38453, found 1053.38564.

1.13. Synthesis of **5d**·6HNEt$_3$

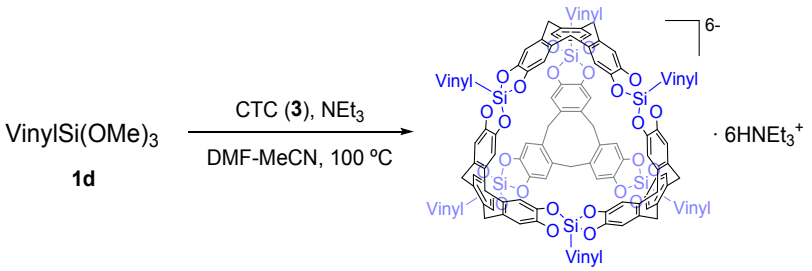

5d·6HNEt$_3$

Cyclotricatechylene (CTC) (**3**) (2.00 mmol, 0.733 g), VinylSi(OMe)$_3$ (3.30 mmol, 0.489 g, 0.505 mL), and Et$_3$N (9.00 mmol, 0.911 g, 1.25 mL) were dissolved in 20 mL of DMF and 10 mL of MeCN. The reaction mixture was stirred and heated at 100 ºC 1 day under a nitrogen atmosphere. After cooling to room temperature, all the volatiles were removed under reduced pressure. The resulting residue was redissolved in 20 mL of THF and 10 mL of MeCN. Addition of Et$_2$O (200 mL)

led to the precipitation of a brownish powder. The powder was collected by suction filtration and dried under reduced pressure to give 1.14 g (0.478 mmol, 94.6%) of **5d**·6HNEt$_3$ as a light brown powder.

5d·6HNEt$_3$: ^{1}H NMR δ 8.57 (br, 6H, NH), 6.40 (s, 24H, ArH), 5.78 (dd, J = 20.0, 14.6 Hz, 6H, SiCH), 5.46 (dd, J = 14.6, 5.0 Hz, 6H, CH=$\underline{CH_2}$), 5.42 (dd, J = 20.0, 5.0 Hz, 6H, CH=$\underline{CH_2}$), 4.44 (d, J = 13.1 Hz, 12H, ArCH$_2$Ar), 3.12 (d, J = 13.1 Hz, 12H, ArCH$_2$Ar), 2.81 (m, 36H, NCH$_2$), 0.95 (t, J = 7.2 Hz, 54H, CH$_3$); ^{13}C NMR δ 148.31 (C), 140.75 (SiCH), 128.61 (C), 128.58 (CH=$\underline{CH_2}$), 110.20 (CH), 45.62 (NCH$_2$), 35.58 (ArCH$_2$Ar), 8.43 (CH$_3$); ^{29}Si NMR δ -87.64 (VinylSiO$_4$); HRMS (ESI-, MeOH) m/z calcd for $C_{120}H_{130}N_4O_{24}Si_6$ [M+4HNEt$_3$]$^{2-}$ 1089.38453, found 1089.38557.

1.14. Synthesis of **5e**·6HNEt$_3$

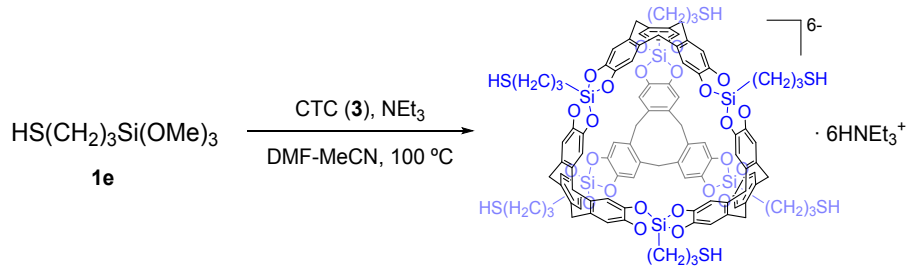

Cyclotricatechylene (CTC) (**3**) (2.00 mmol, 0.733 g), HS(CH$_2$)$_3$Si(OMe)$_3$ (3.30 mmol, 0.648 g, 0.613 mL), and Et$_3$N (9.00 mmol, 0.911 g, 1.25 mL) were dissolved in 20 mL of DMF and 10 mL of MeCN. The reaction mixture was stirred and heated at 100 ºC 1 day under a nitrogen atmosphere. After cooling to room temperature, all the volatiles were removed under reduced pressure. The resulting residue was redissolved in 20 mL of THF and 10 mL of MeCN. Addition of Et$_2$O (200 mL) led to the precipitation of a brownish powder, which was collected by suction filtration and dried under reduced pressure to give 1.31 g (0.490 mmol, 98.0%) of **5e**·6HNEt$_3$ as an off-white powder.

5e·6HNEt$_3$: ^{1}H NMR δ 8.56 (br, 6H, NH), 6.38 (s, 24H, ArH), 4.42 (d, J = 13.1 Hz, 12H, ArCH$_2$Ar), 3.10 (d, J = 13.1 Hz, 12H, ArCH$_2$Ar), 2.79 (q, J = 7.2 Hz, 36H, NCH$_2$), 2.25 (q, J = 7.4 Hz, 12H, CH$_2$S), 1.93 (t, J = 7.8 Hz, 6H, SH), 1.37 (quin, J = 7.8 Hz, 12H, $\underline{CH_2}$CH$_2$S), 0.91 (t, J = 7.2 Hz, 54H, CH$_3$), 0.36 (t, J = 8.3 Hz, 12H, SiCH$_2$); ^{13}C NMR δ 148.48 (C), 128.48 (C), 110.08 (CH), 45.66 (NCH$_2$), 35.62 (ArCH$_2$Ar), 29.34 (CH$_2$S), 27.57 ($\underline{CH_2}$CH$_2$S), 16.55 (SiCH$_2$), 8.46 (CH$_3$); ^{29}Si NMR δ -76.39 (HS(CH$_2$)$_3$SiO$_4$); HRMS (ESI-, MeOH) m/z calcd for $C_{126}H_{154}N_4O_{24}S_6Si_6$ [M+4HNEt$_3$]$^{2-}$ 1233.39464, found 1233.39472.

1.15. Synthesis of **5a**·6Na

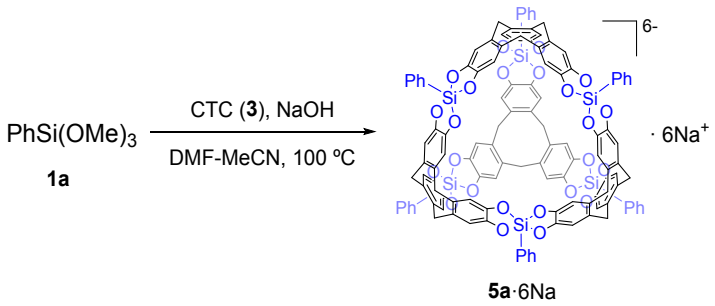

Cyclotricatechylene (CTC) (**3**) (2.00 mmol, 0.733 g), $PhSi(OMe)_3$ (3.30 mmol, 0.654 g, 0.616 mL), and NaOH (3.10 mmol, 0.124 g) were dissolved in 20 mL of DMF and 10 mL of MeCN. The reaction mixture was stirred and heated at 100 ºC overnight under a nitrogen atmosphere. After cooling to room temperature, all the volatiles were removed under reduced pressure. The resulting crude product was dissolved in 5 mL of MeOH. After addition of 100 mL of benzene, the mixture was left standing for 1 h until a small amount of black precipitate was formed and filtered off. The solvent was removed under reduced pressure and the residue was redissolved in 10 mL of THF. Addition of Et_2O (100 mL) led to the precipitation of a white powder, which was collected by suction filtration and dried under reduced pressure to give 0.948 g (0.429 mmol, 85.8%) of **5a**·6Na as an off-white powder.

5a·6Na: ^{1}H NMR δ7.38 (d, J = 6.6 Hz, 12H, *o*-CH), 7.14-7.07 (m, 18H, *p*-CH and *m*-CH), 6.51 (s, 24H, ArH), 4.45 (d, J = 13.1 Hz, 12H, $ArCH_2Ar$), 3.11 (d, J = 13.1 Hz, 12H, $ArCH_2Ar$); ^{13}C NMR δ 148.23 (C), 141.87 (*ipso*-C), 133.62 (*o*-CH), 128.87 (C), 127.65 (*p*-CH), 126.74 (*m*-CH), 110.76 (CH), 35.74 ($ArCH_2Ar$); ^{29}Si NMR δ -87.17 ($PhSiO_4$); HRMS (ESI-, MeOH) m/z calcd for $C_{124}H_{94}Na_4O_{28}Si_6$ $[M+4Na+4MeOH]^{2-}$ 1145.20690, found 1145.20624.

1.16. Synthesis of **5c**·6Na

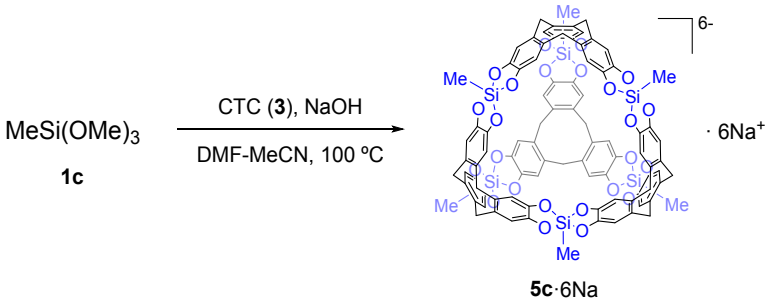

Cyclotricatechylene (CTC) (**3**) (2.00 mmol, 0.733 g), $MeSi(OMe)_3$ (3.30 mmol, 0.450 g, 0.471

mL), and NaOH (3.10 mmol, 0.124 g) were dissolved in 20 mL of DMF and 10 mL of MeCN. The reaction mixture was stirred and heated at 100 ºC overnight under a nitrogen atmosphere. After cooling to room temperature, all the volatiles were removed under reduced pressure. The resulting crude product was dissolved in 20 mL of MeOH and 20 mL of THF. After addition of 100 mL of benzene, the mixture was left standing for 30 min until a small amount of black precipitate was formed and filtered off. The solvent was removed under reduced pressure and the residue was redissolved in 10 mL of MeOH. Addition of Et_2O (200 mL) led to the precipitation of a white powder, which was collected by suction filtration and dried under reduced pressure to give 0.897 g (0.488 mmol, 97.6%) of **5a**·6Na as an off-white powder.

5c·6Na: ^{1}H NMR δ 6.41 (s, 24H, ArH), 4.45 (d, J = 13.1 Hz, 12H, $ArCH_2Ar$), 3.09 (d, J = 13.1 Hz, 12H, $ArCH_2Ar$), -0.25 ($SiCH_3$); ^{13}C NMR δ 147.97 (C), 128.62 (C), 110.72 (CH), 35.82 ($ArCH_2Ar$), -0.16 ($SiCH_3$); ^{29}Si NMR δ -75.16 ($MeSiO_4$); HRMS (ESI-, MeOH) m/z calcd for $C_{94}H_{82}Na_4O_{28}Si_6$ $[M+4Na+4MeOH]^{2-}$ 959.15995, found 959.16131.

1.17. Synthesis of **5f**·6Na

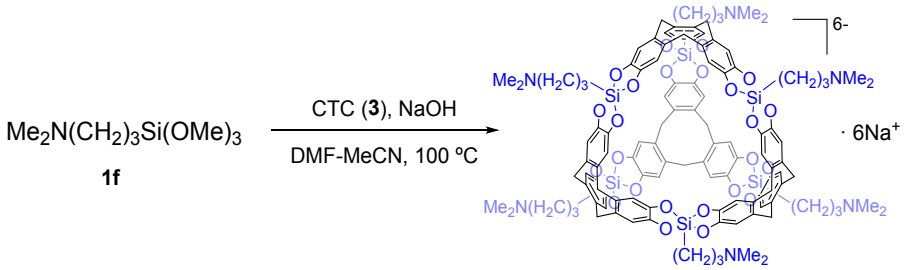

Cyclotricatechylene (CTC) (**3**) (2.00 mmol, 0.733 g), $Me_2N(CH_2)_3Si(OMe)_3$ (3.30 mmol, 0.684 g, 0.722 mL), and NaOH (3.10 mmol, 0.124 g) were dissolved in 20 mL of DMF and 10 mL of MeCN. The reaction mixture was stirred and heated at 100 ºC overnight under a nitrogen atmosphere. After cooling to room temperature, small amount of precipitate was formed and removed by filtration. All the volatiles were then removed under reduced pressure from filtrate. The resulting crude product was dissolved in 15 mL of MeOH and 5 mL of MeCN. Addition of Et_2O (400 mL) led to the precipitation of a pink white powder, which was collected by suction filtration and dried under reduced pressure to give 1.04 g (0.459 mmol, 91.8%) of **5f**·6Na as a pink white powder.

5f·6Na: ^{1}H NMR δ 6.42 (s, 24H, ArH), 4.44 (d, J = 13.1 Hz, 12H, $ArCH_2Ar$), 3.09 (d, J = 13.1 Hz, 12H, $ArCH_2Ar$), 1.98 (s, 36H, NCH_3), 1.94 (t, J = 7.5 Hz, 12H, CH_2N), 1.21 (quin, J = 7.8 Hz, 12H, $SiCH_2\underline{CH_2}CH_2N$), 0.25 (t, J = 8.3 Hz, 12H, $SiCH_2$); ^{13}C NMR δ 148.31 (C), 128.63 (C), 110.70

(CH), 63.25 (CH_2N), 45.41 (NCH_3), 36.00 ($ArCH_2Ar$), 22.28 ($SiCH_2\underline{CH_2}CH_2N$), 14.79 ($SiCH_2$); ^{29}Si NMR δ -75.66 ($Me_2N(CH_2)_3SiO_4$). MS spectrum of **5f**·6Na was not detectable due to degradation of its ionic species in mass spectrometer.

1.18. Cation exchange of **5a**·6HNEt$_3$

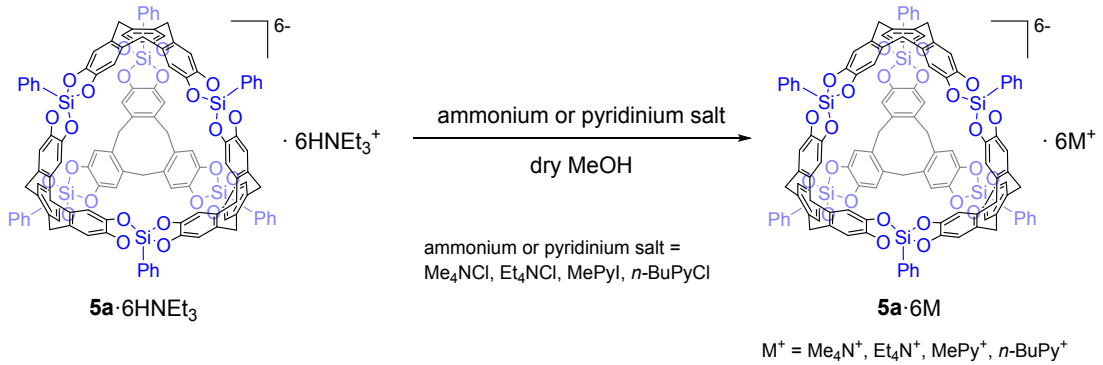

1.18.1. Cation exchange of **5a**·6HNEt$_3$ with Me_4NCl

Compound **5a**·6HNEt$_3$ (0.100 mmol, 269 mg) was dissolved in 130 mL of dry MeOH in 200 mL flask. Then, Me_4NCl (1.20 mmol, 132 mg) was placed in a 25 mL volumetric flask and diluted with dry MeOH to a total volume of 25 mL, thus yielding a 48 mM Me_4NCl solution. The Me_4NCl solution was added dropwise to the solution of **5a**·6HNEt$_3$ over 25 min. The precipitate was collected by suction filtration and dried to give 177 mg (70.3 μmol, 70.3%) of **5a**·6Me_4N as a brown powder.

5a·6Me_4N: ^1H NMR δ 7.36 (d, J = 6.6 Hz, 12H, *o*-CH), 7.13-7.04 (m, 18H, *p*-CH and *m*-CH), 6.51 (s, 24H, ArH), 4.43 (d, J = 13.1 Hz, 12H, $ArCH_2Ar$), 3.11 (d, J = 13.1 Hz, 12H, $ArCH_2Ar$), 2.77 (brs, 72H, NCH_3); ^{13}C NMR δ 148.64 (C), 142.29 (*ipso*-C), 133.64 (*o*-CH), 128.85 (C), 127.45 (*p*-CH), 126.67 (*m*-CH), 110.38 (CH), 54.34 (NCH_3), 35.49 ($ArCH_2Ar$); ^{29}Si NMR δ -86.83 ($PhSiO_4$); HRMS (ESI-, MeOH) m/z calcd for $C_{136}H_{126}N_4O_{24}Si_6$ $[M+4Me_4N]^{2-}$ 1183.36888, found 1183.37118.

1.18.2. Cation exchange of **5a**·6HNEt$_3$ with Et_4NCl

Compound **5a**·6HNEt$_3$ (0.100 mmol, 269 mg) was dissolved in 120 mL of dry MeOH in 200 mL flask. Then, Et_4NCl (1.20 mmol, 199 mg) was placed in a 25 mL volumetric flask and diluted with dry MeOH to a total volume of 25 mL, thus yielding a 48 mM Et_4NCl solution. The Et_4NCl solution was added dropwise to the solution of **5a**·6HNEt$_3$ over 10 min. The precipitate was collected by suction filtration and dried to give 171 mg (59.9 μmol, 59.9%) of **5a**·6Et_4N as a brown powder.

5a·6Et_4N: ^{1}H NMR δ 7.35 (d, *J* = 6.5 Hz, 12H, *o*-CH), 7.13-7.05 (m, 18H, *p*-CH and *m*-CH), 6.48 (s, 24H, ArH), 4.43 (d, *J* = 13.0 Hz, 12H, $ArCH_2Ar$), 3.11 (d, *J* = 13.0 Hz, 12H, $ArCH_2Ar$), 2.92 (br, 36H, NCH_2), 0.90 (br, 54H, CH_3); ^{13}C NMR δ 148.28 (C), 142.28 (*ipso*-C), 133.68 (*o*-CH), 128.83 (C), 127.38 (*p*-CH), 126.58 (*m*-CH), 110.25 (CH), 51.30 (NCH_2), 35.53 ($ArCH_2Ar$), 6.77 (CH_3); ^{29}Si NMR δ -86.76 ($PhSiO_4$); HRMS (ESI-, MeOH) m/z calcd for $C_{152}H_{158}N_4O_{24}Si_6$ $[M+4Et_4N]^{2-}$ 1295.49408, found 1295.49291.

1.18.3. Cation exchange of **5a**·6$HNEt_3$ with *N*-MePyI

Compound **5a**·6$HNEt_3$ (0.100 mmol, 269 mg)) was dissolved in 120 mL of dry MeOH in 200 mL flask. Then, *N*-MePyI (1.20 mmol, 265 mg) was placed in a 25 mL volumetric flask and diluted with dry MeOH to a total volume of 25 mL, thus yielding a 48 mM *N*-MePyI solution. The *N*-MePyI solution was added dropwise to the solution of **5a**·6$HNEt_3$ over 10 min. The precipitate was collected by suction filtration and dried to give 213 mg (80.8 μmol, 80.8%) of **5a**·6MePy as a brown powder.

5a·6MePy: ^{1}H NMR δ 8.63 (br, 12H, 2-CH), 8.59 (br, 6H, 4-CH), 7.81 (br, 12H, 3-CH), 7.44 (d, *J* = 6.5 Hz, 12H, *o*-CH), 7.17-7.09 (m, 18H, *p*-CH and *m*-CH), 6.73 (s, 24H, ArH), 4.50 (d, *J* = 13.1 Hz, 12H, $ArCH_2Ar$), 4.02 (s, 18H, NCH_3), 3.20 (d, *J* = 13.1 Hz, 12H, $ArCH_2Ar$); ^{13}C NMR δ 148.23 (C), 145.33 (4-CH), 144.97 (2-CH), 141.65 (*ipso*-C), 133.63 (*o*-CH), 129.34 (C), 127.64 (*p*-CH), 127.39 (3-CH), 126.77 (*m*-CH), 110.66 (CH), 48.01 (NCH_3), 35.46 ($ArCH_2Ar$); ^{29}Si NMR δ -86.26 ($PhSiO_4$); HRMS (ESI-, MeOH) m/z calcd for $C_{144}H_{110}N_4O_{24}Si_6$ $[M+4MeNC_5H_5]^{2-}$ 1223.30628, found 1223.30773.

1.18.4. Cation exchange of **5a**·6$HNEt_3$ with *N*-BuPyCl

Compound **5a**·6$HNEt_3$ (0.100 mmol, 269 mg) was dissolved in 120 mL of dry MeOH in 200 mL flask. Then, *N*-BuPyCl (1.20 mmol, 206 mg) was placed in a 25 mL volumetric flask and diluted with dry MeOH to a total volume of 25 mL, thus yielding a 48 mM *N*-BuPyCl solution. The *N*-BuPyCl solution was added dropwise to the solution of **5a**·6$HNEt_3$ over 45 min. The precipitate was collected by suction filtration and dried to give 214 mg (74.1 μmol, 74.1%) of **5a**·6BuPy as a dark brown powder.

5a·6BuPy: ^{1}H NMR δ 8.88 (br, 18H, 2-CH and 4-CH), 8.00 (br, 12H, 3-CH), 7.47 (br, 12H, *o*-CH), 7.14 (br, 18H, *p*-CH and *m*-CH), 6.77 (br, 24H, ArH), 4.50 (br, 12H, $ArCH_2Ar$), 4.36 (br, 10H,

NCH_2), 3.23 (br, 12H, $ArCH_2Ar$), 1.49 (br, 10H, $NCH_2\underline{CH_2}$), 0.51 (br, 25H, $NCH_2CH_2\underline{CH_2CH_3}$), -0.40 (br, 2H, NCH_2'), -1.58 (br, 2H, $NCH_2\underline{CH_2}$'), -2.12 (br, 2H, $NCH_2CH_2\underline{CH_2}CH_3$'), -2.25 (br, 3H, $NCH_2CH_2CH_2\underline{CH_3}$'); ^{13}C NMR δ 148.05 (C), 145.88 (4-CH), 144.23 (2-CH), 141.50 (*ipso*-C), 133.77 (*o*-CH), 129.46 (C), 128.11 (3-CH), 127.71 (*p*-CH), 126.81 (*m*-CH), 110.80 (CH), 60.76 (NCH_2), 35.52 ($ArCH_2Ar$), 32.72 ($NCH_2\underline{CH_2}$), 17.94 ($NCH_2CH_2\underline{CH_2}CH_3$), 12.89 $NCH_2CH_2CH_2\underline{CH_3}$); ^{29}Si NMR δ -86.17 (br, $PhSiO_4$); HRMS (ESI-, MeOH) m/z calcd for $C_{156}H_{134}N_4O_{24}Si_6$ $[M+4BuNC_5H_5]^{2-}$ 1307.40018, found 1307.39803.

2. Structural assignment and spectral data

2.1. Structual assignment and spectral data for **4a**,**b**·4HNR_3·n(**2**)·m(anthracene)·l(THF) (HNR_3 = $HNEt_3$, $HNEt_2Bn$, $HNMe_2Bn$, $HNMe_2Bu$, TMEDAH ($HNMe_2CH_2CH_2NMe_2$); n = 0, 2; m = 0, 2; l = 1, 2, 4)

The ^1H and ^{13}C NMR spectra of **4a** showed a 1:1 ratio of the 9,10-dimethyl-9,10-ethano-9,10-dihydroanthracene and silyl phenyl unit excluding the peaks driving from the $HNEt_3^+$ counter ions, complexed **2**, and THF (Figure S1 and S2). ^{29}Si NMR showed a peak at -86.9 ppm, which is characteristic of an aryl-substituted penta-coordinated anionic silane biscatecholate (Figure S3). On the basis of the integrals of the peaks in the ^1H NMR spectra of Figure S1, a 1:4:2:4 molar ratio of **4a**, $HNEt_3^+$, **2**, and THF was observed that remained invariant throughout the experimental procedureand can be attributed to the molecular complex **4a**·4$HNEt_3$·2(**2**)·4THF. The formation of **4a**·4$HNEt_3$·2(**2**)·4THF was also confirmed by ESI-mass spectroscopy (Figure S4). A negative ion peak of the molecular complex was found at m/z 1147.8, which corresponds to $[M+HNEt_3+H+2(\mathbf{2})]^{2-}$. Pure **4a**·4$HNEt_3$ was obtained after redissolving the product in DMSO/DMF followed by precipitation with CH_2Cl_2/Et_2O to remove compound **2**.

The ^1H, ^{13}C, and DEPT135 NMR spectra of pure **4a** consisted of the 9,10-dimethyl-9,10-ethano-9,10-dihydroanthracene and silyl phenyl unit in a 1:1 ratio without compound **2** (Figure S5, S6 and S7), while ^{29}Si NMR showed the same value as that of the molecular complex (Figure S8). The formation of **4a**·4$HNEt_3$ was also confirmed by ESI-mass spectroscopy. The negative ion spectrum showed apparent molecular ions that were consistent with $[M+HNEt_3+H]^{2-}$ at m/z 849.8 (where M is the tetraanion core) (Figure S9). All NMR and ESI-mass spectroscopic data were supported the formation of the cyclic tetramer of silane catecholate **4a**·4$HNEt_3$.

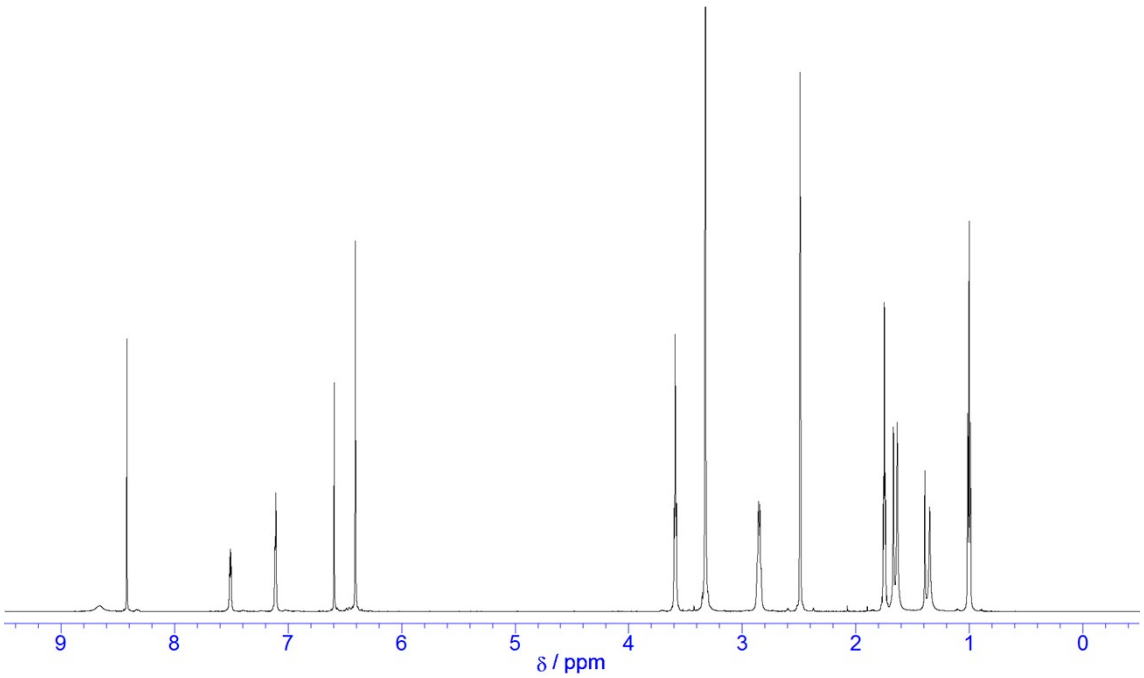

Figure S1. ^{1}H NMR spectrum of **4a**·4HNEt$_3$·2(**2**)·4THF (600 MHz, DMSO-d_6).

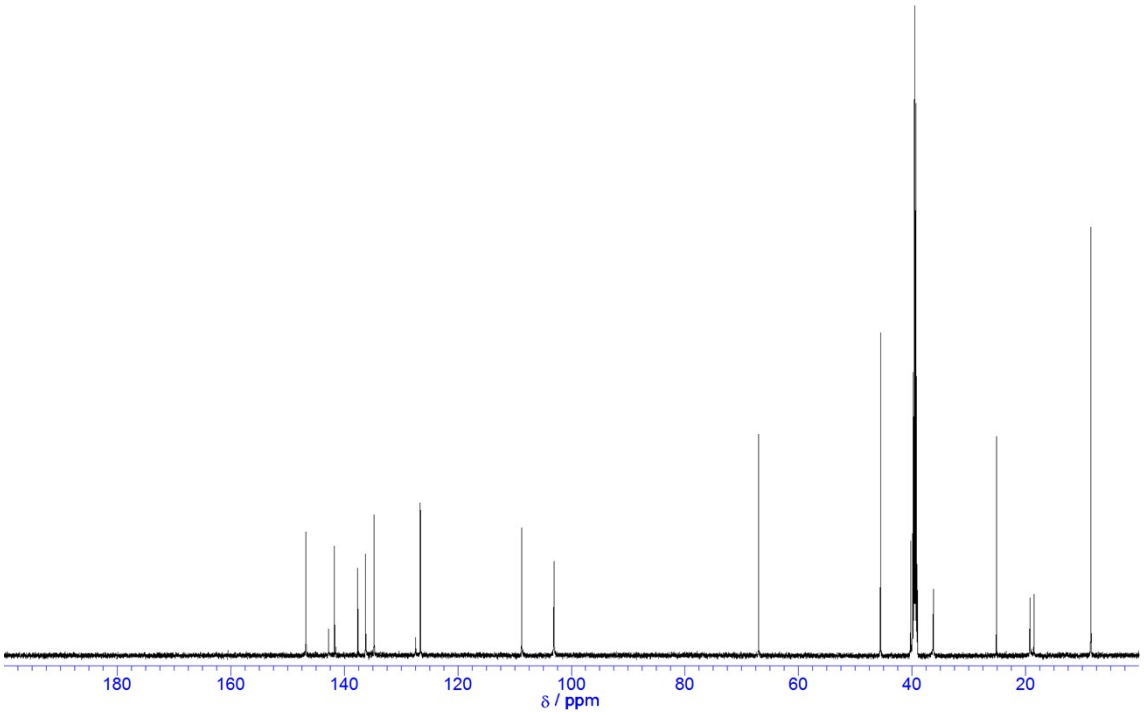

Figure S2. ^{13}C NMR spectrum of **4a**·4HNEt$_3$·2(**2**)·4THF (150 MHz, DMSO-d_6).

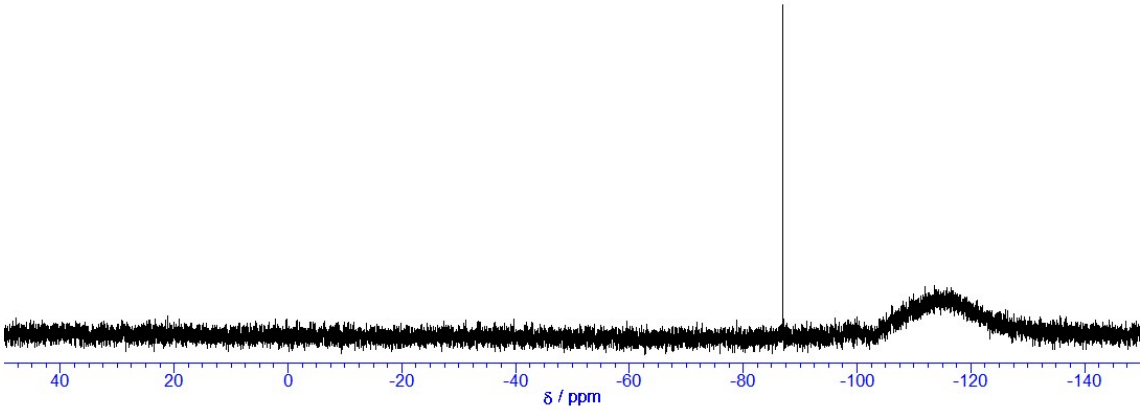

Figure S3. ^{29}Si NMR spectrum of **4a**·4HNEt$_3$·2(**2**)·4THF (120 MHz, DMSO-d_6).

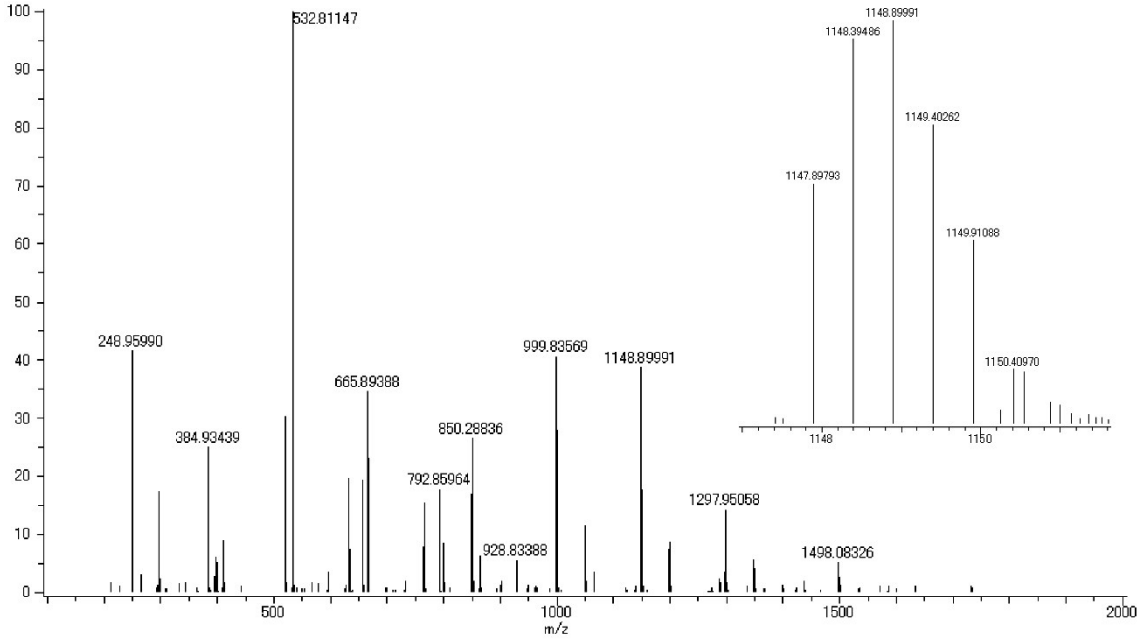

Figure S4. ESI-MS spectrum of **4a**·4HNEt$_3$·2(**2**)·4THF (MeOH).

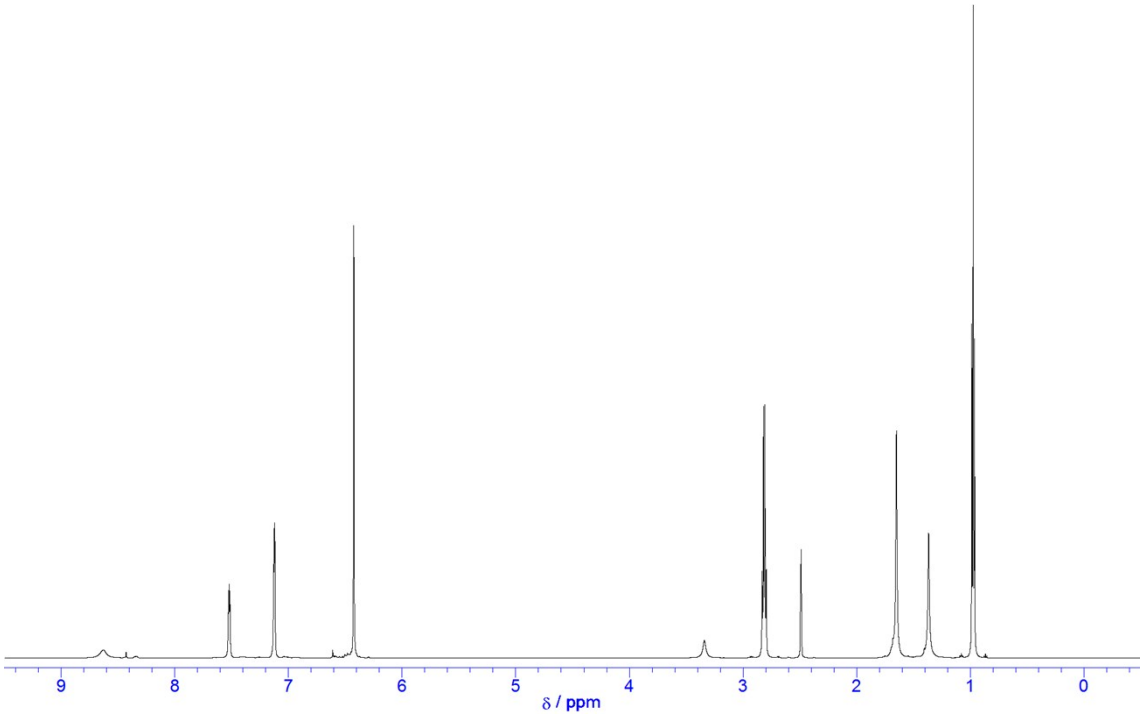

Figure S5. ^{1}H NMR spectrum of **4a**·4HNEt$_3$ (600 MHz, DMSO-d_6).

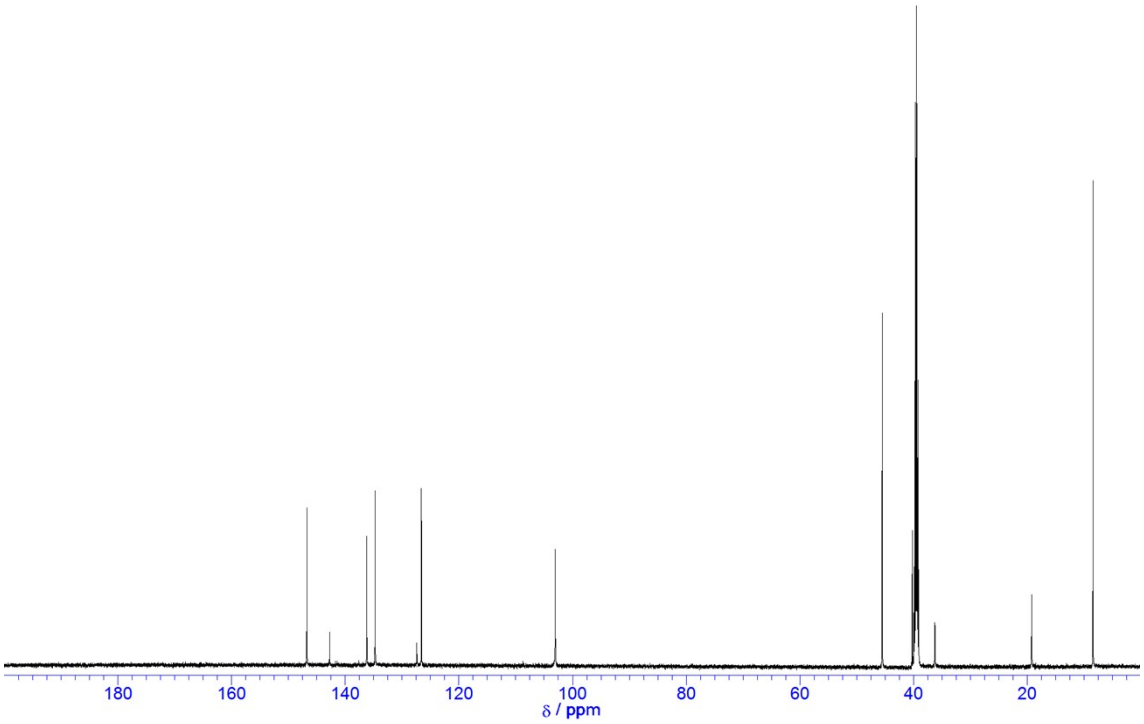

Figure S6. ^{13}C NMR spectrum of **4a**·4HNEt$_3$ (150 MHz, DMSO-d_6).

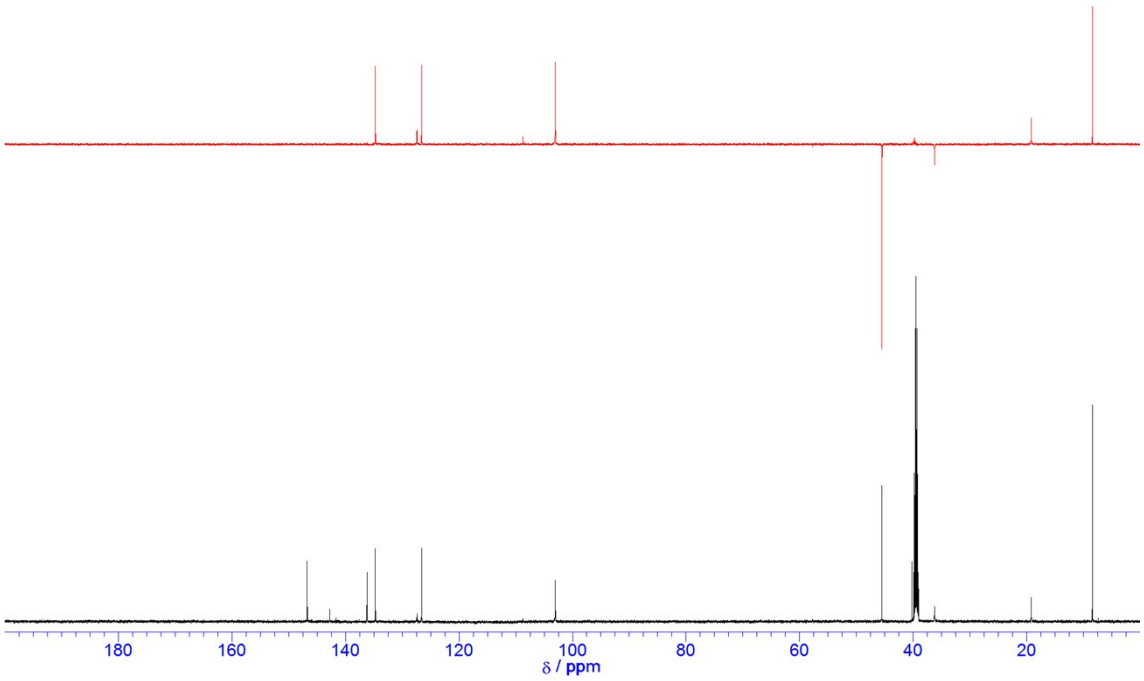

Figure S7. ^{13}C and DEPT135 NMR spectra of **4a**·4HNEt$_3$ (150 MHz, DMSO-d_6).

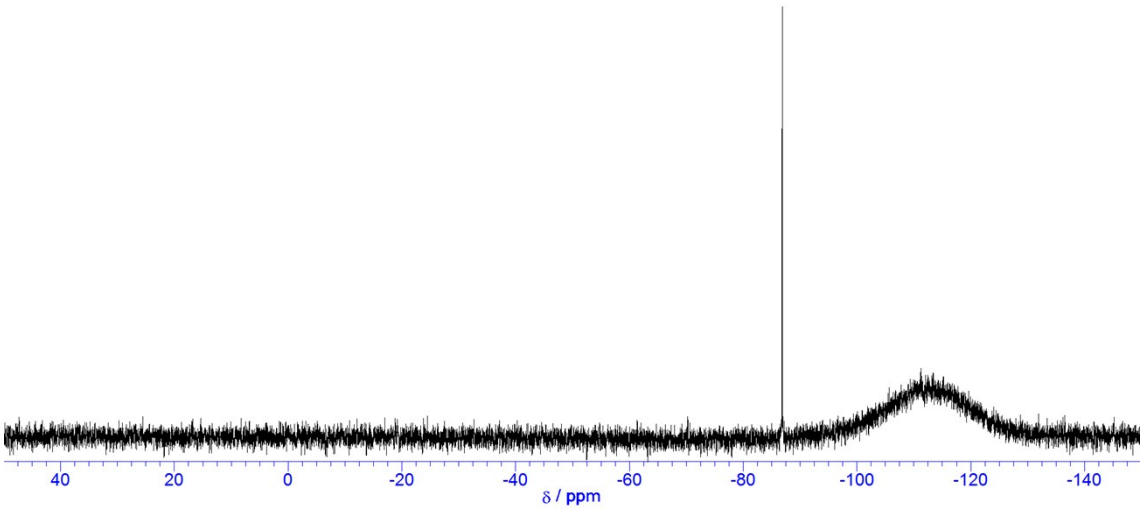

Figure S8. ^{29}Si NMR spectrum of **4a**·4HNEt$_3$ (120 MHz, DMSO-d_6).

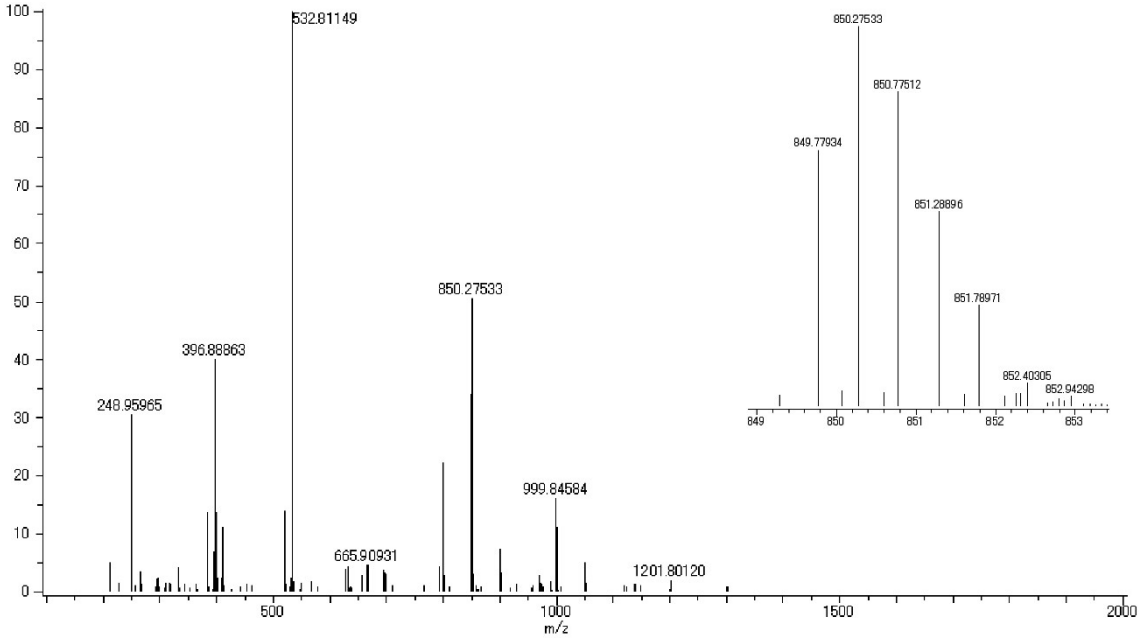

Figure S9. ESI-MS spectrum of **4a**·4HNEt$_3$ (MeOH).

The replacement of triethylamine with diethylbenzylamine, dimethylbenzylamine, dimethylbutylamine, and tetramethylethylenediamine (TMEDA) resulted in macrocycle formation, i.e., **4a**·4HNEt$_2$Bn·2(**2**)·4THF, **4a**·4HNMe$_2$Bn·2THF, **4a**·4HNMe$_2$Bu·2THF, and **4a**·4HTMEDA·2THF. These macrocycles with different ammonium cations were fully characterized by ^{1}H, ^{13}C, and ^{29}Si NMR as well as ESI-mass spectroscopy (Figure S10-S25).

With regard to molecular complex **4a** with reactant **2**, it is noteworthy that the addition of anthracene to the reaction of **1a** and **2** with Et$_3$N produced a macrocycle complex including anthracene, i.e., **4a**·4HNEt$_3$·2(**2**)·2anthracene·THF (Figure S26-S29). Hence, it can be assumed that reactant **2** and anthracene may act as template for macrocycle formation.

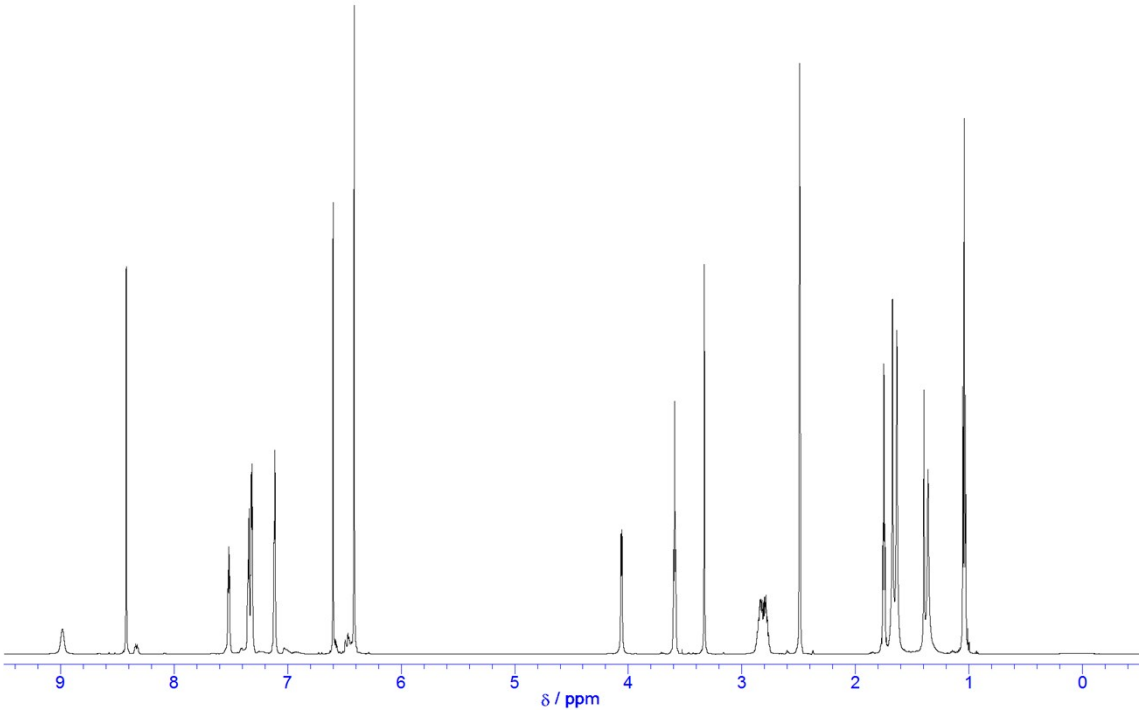

Figure S10. ^{1}H NMR spectrum of **4a**·4HNEt$_2$Bn·2(**2**)·4THF (600 MHz, DMSO-d_6).

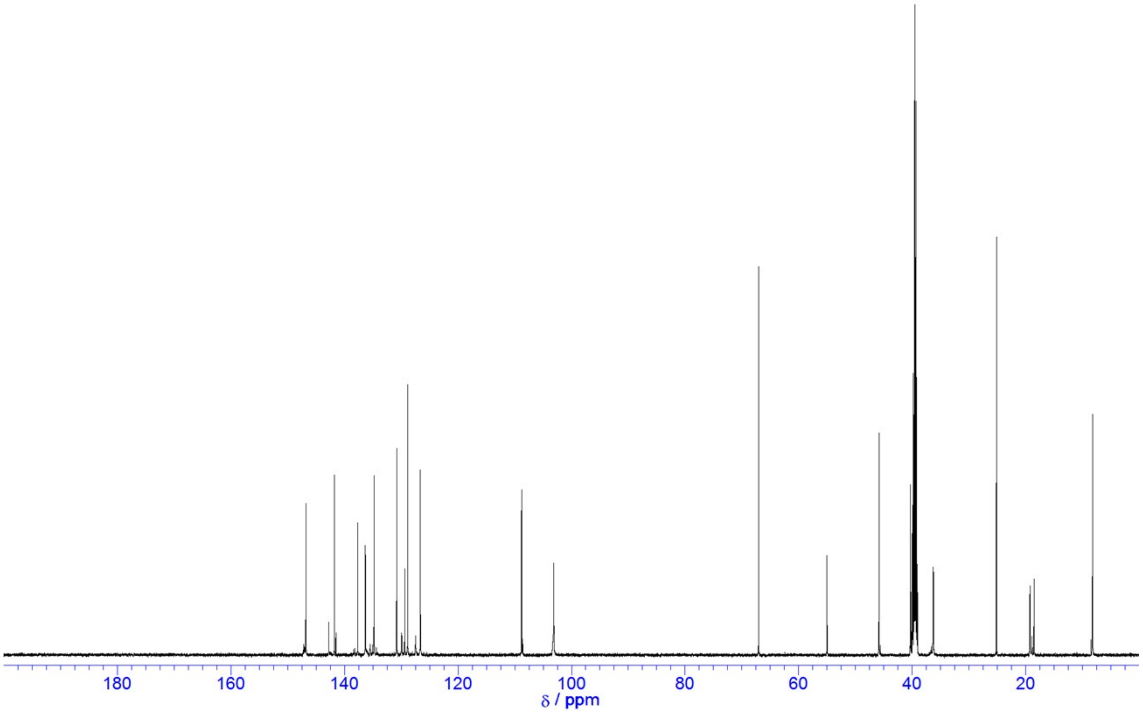

Figure S11. ^{13}C NMR spectrum of **4a**·4HNEt$_2$Bn·2(**2**)·4THF (150 MHz, DMSO-d_6).

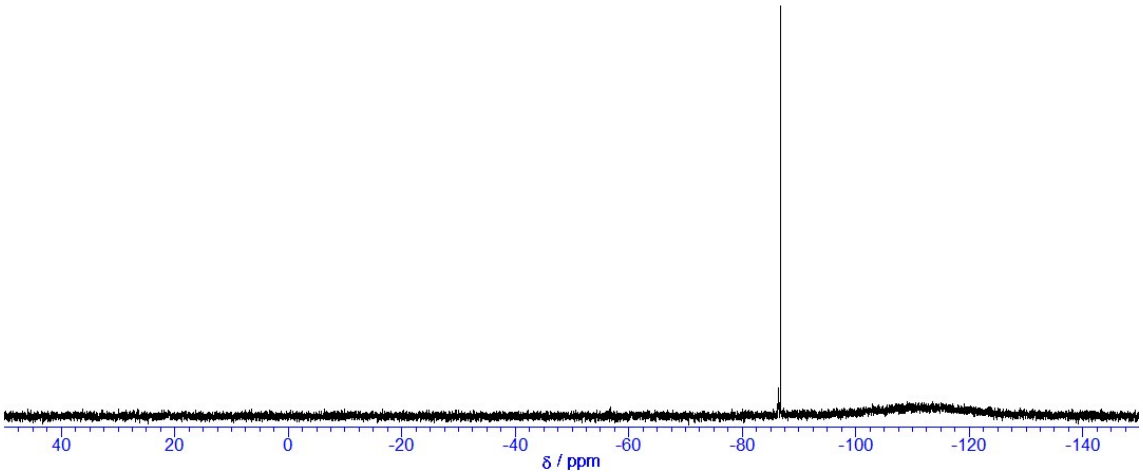

Figure S12. ^{29}Si NMR spectrum of **4a**·4HNEt$_2$Bn·2(**2**)·4THF (120 MHz, DMSO-d_6).

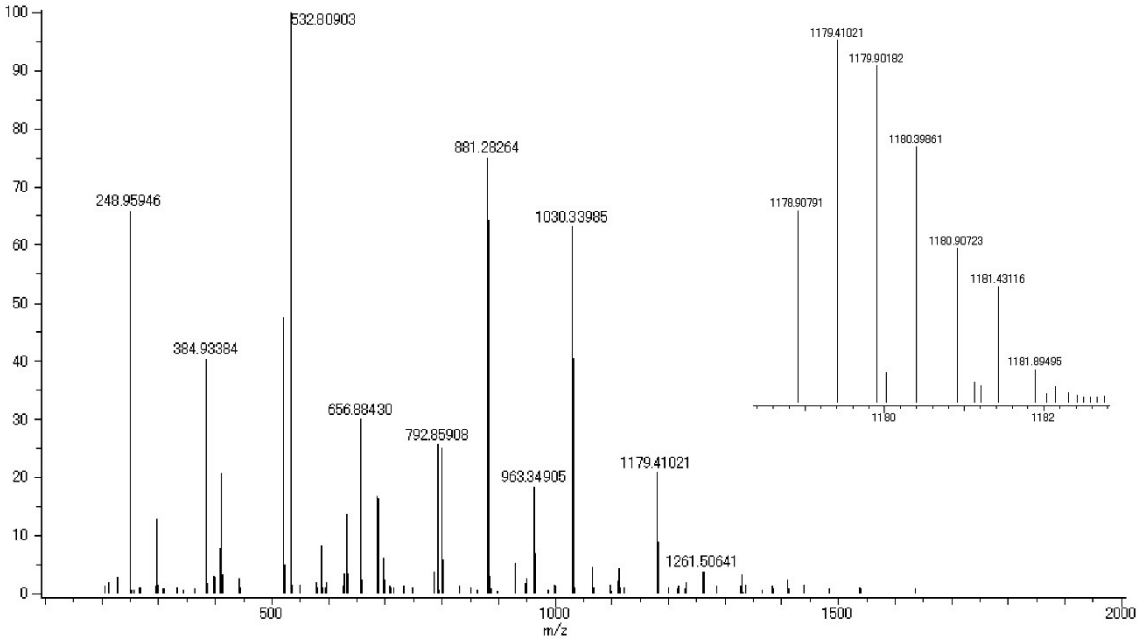

Figure S13. ESI-MS spectrum of **4a**·4HNEt$_2$Bn·2(**2**)·4THF (MeOH).

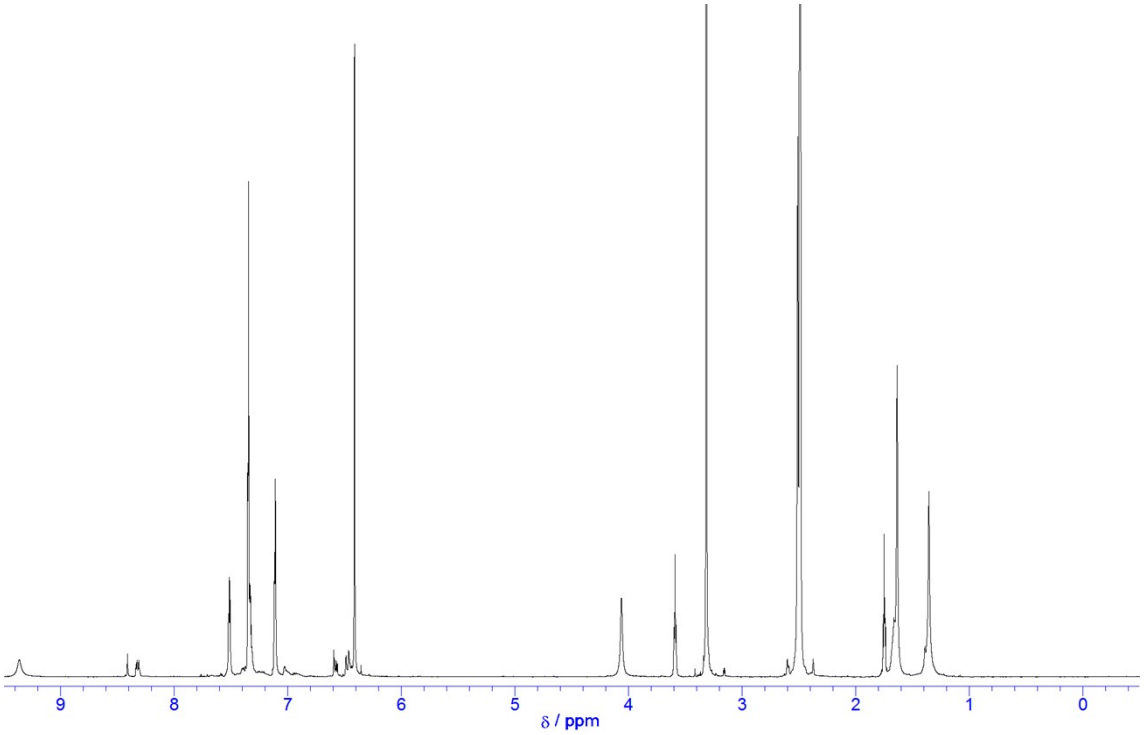

Figure S14. ^{1}H NMR spectrum of **4a**·4HNMe$_2$Bn·2THF (600 MHz, DMSO-d_6).

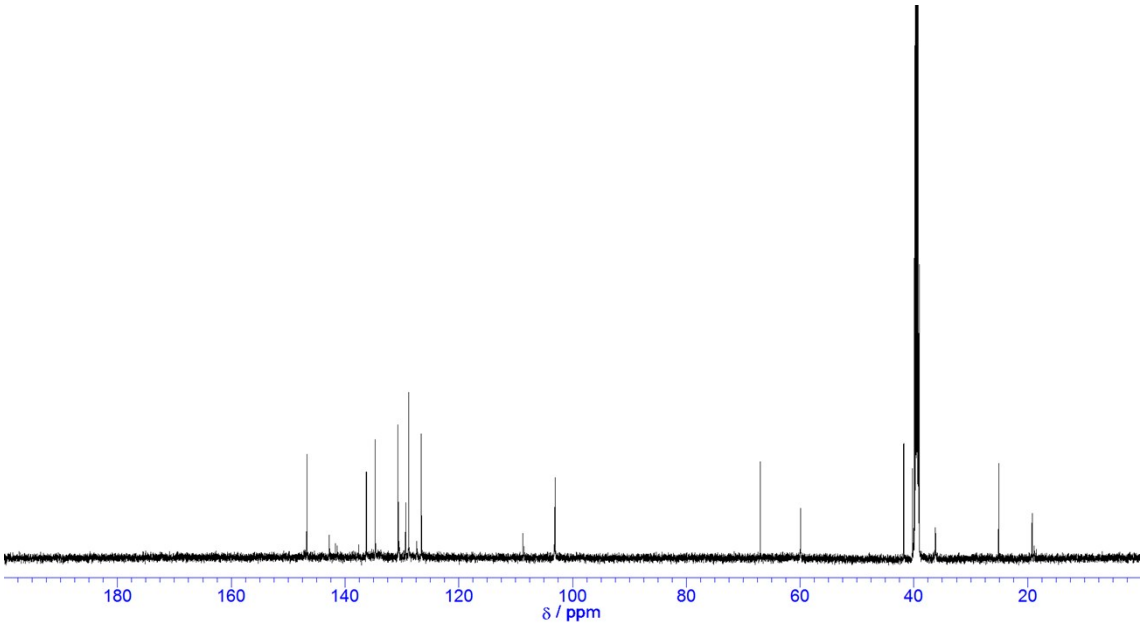

Figure S15. ^{13}C NMR spectrum of **4a**·4HNMe$_2$Bn·2THF (150 MHz, DMSO-d_6).

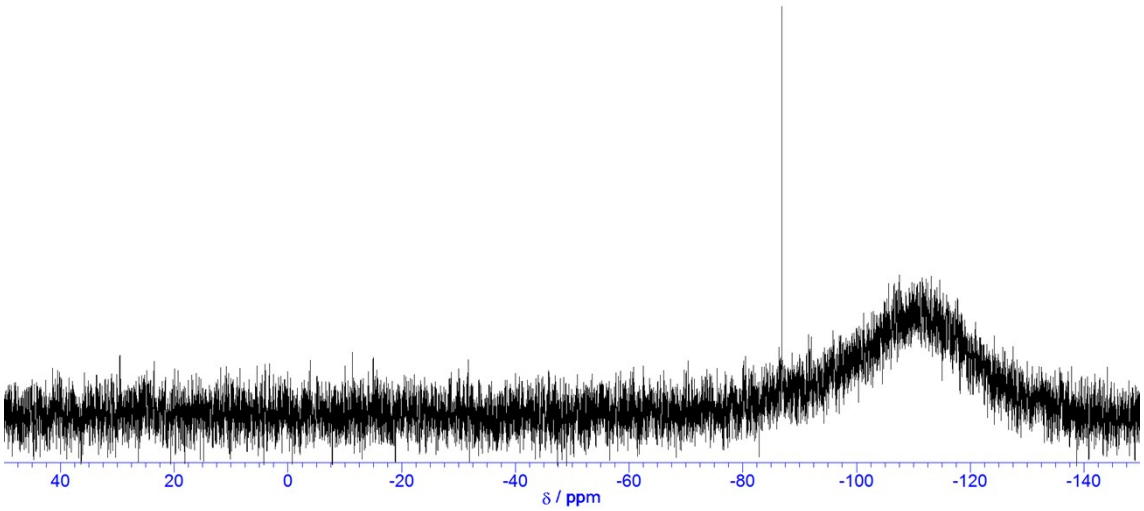

Figure S16. ^{29}Si NMR spectrum of **4a**·4HNMe$_2$Bn·2THF (120 MHz, DMSO-d_6).

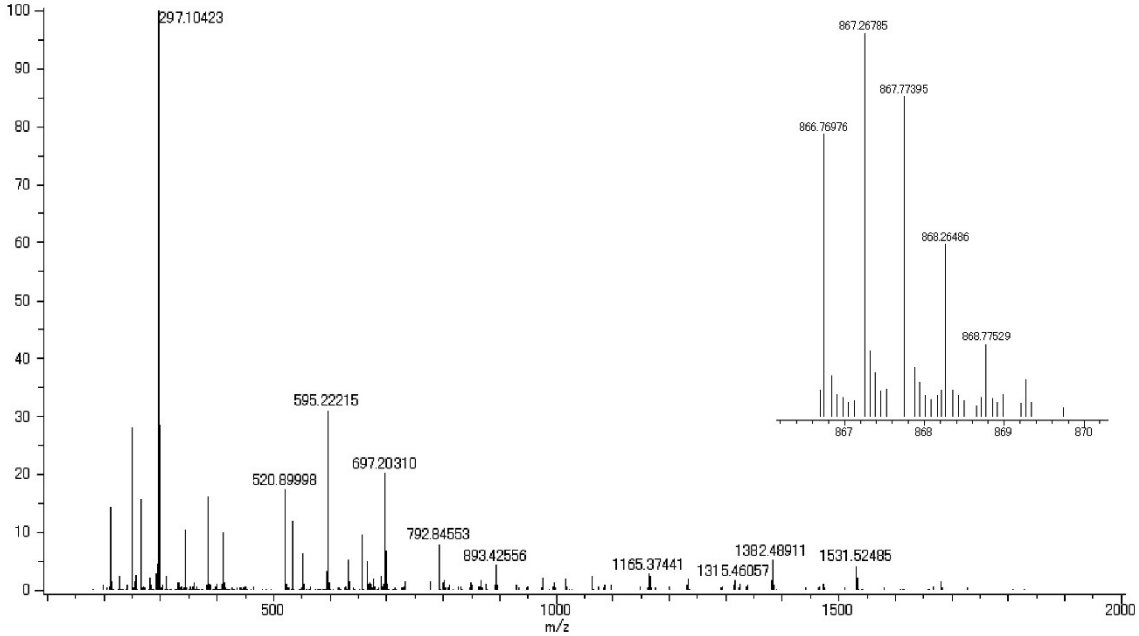

Figure S17. ESI-MS spectrum of **4a**·4HNMe$_2$Bn·2THF (MeOH).

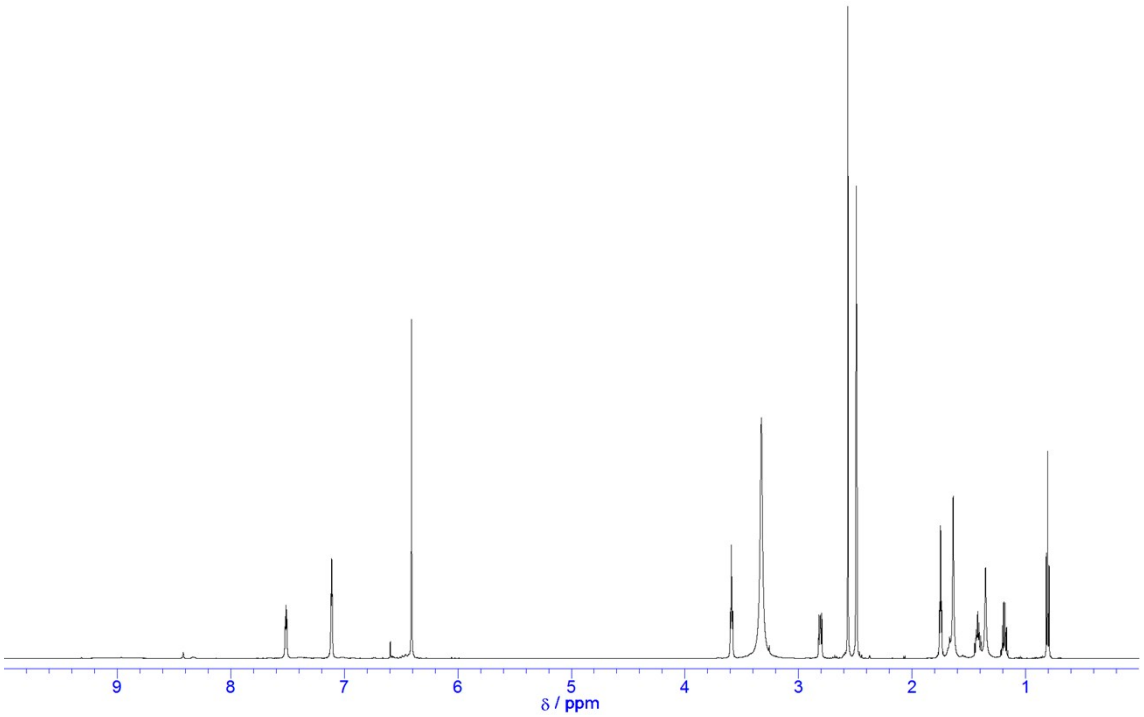

Figure S18. ^{1}H NMR spectrum of **4a**·4HNMe$_2$Bu·2THF (600 MHz, DMSO-d_6).

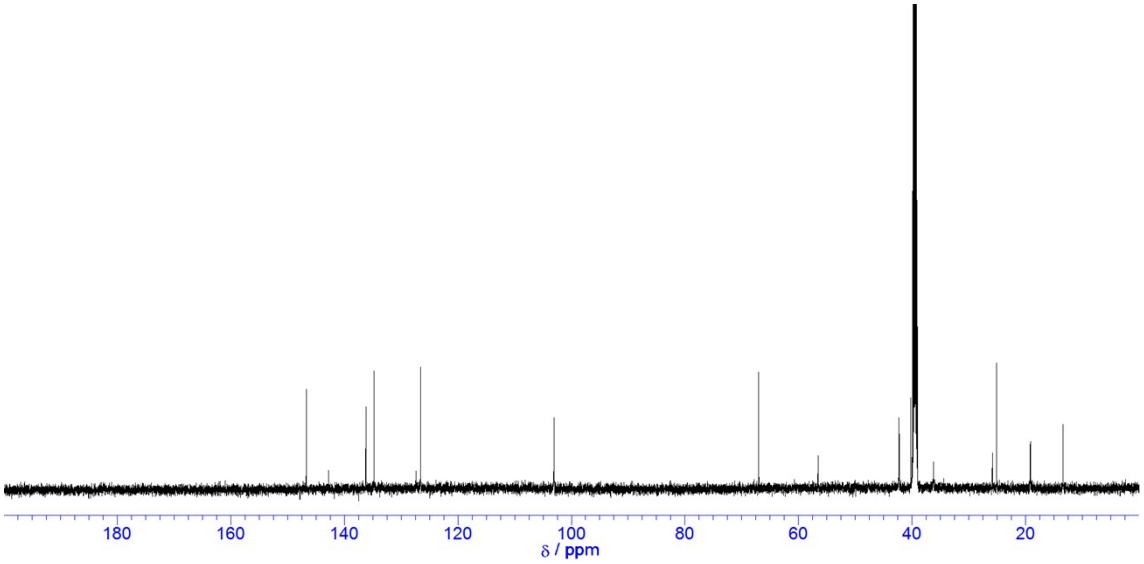

Figure S19. ^{13}C NMR spectrum of **4a**·4HNMe$_2$Bu·2THF (150 MHz, DMSO-d_6).

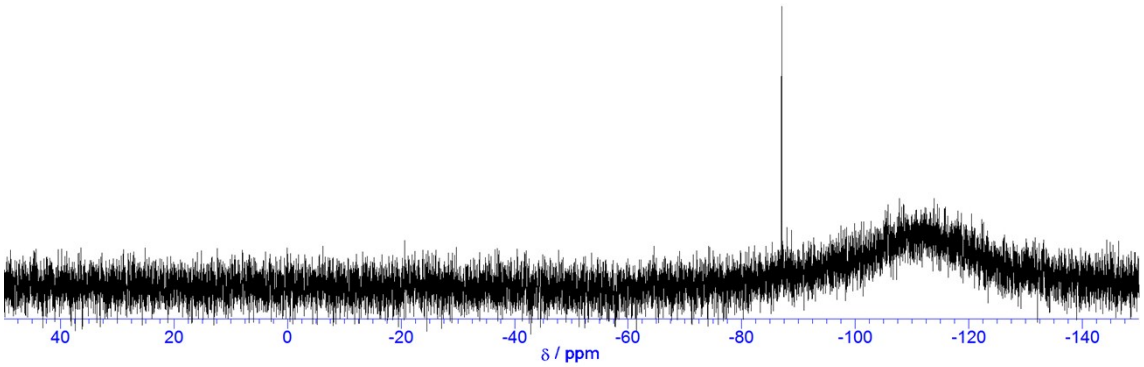

Figure S20. ^{29}Si NMR spectrum of **4a**·4HNMe$_2$Bu·2THF (120 MHz, DMSO-d_6).

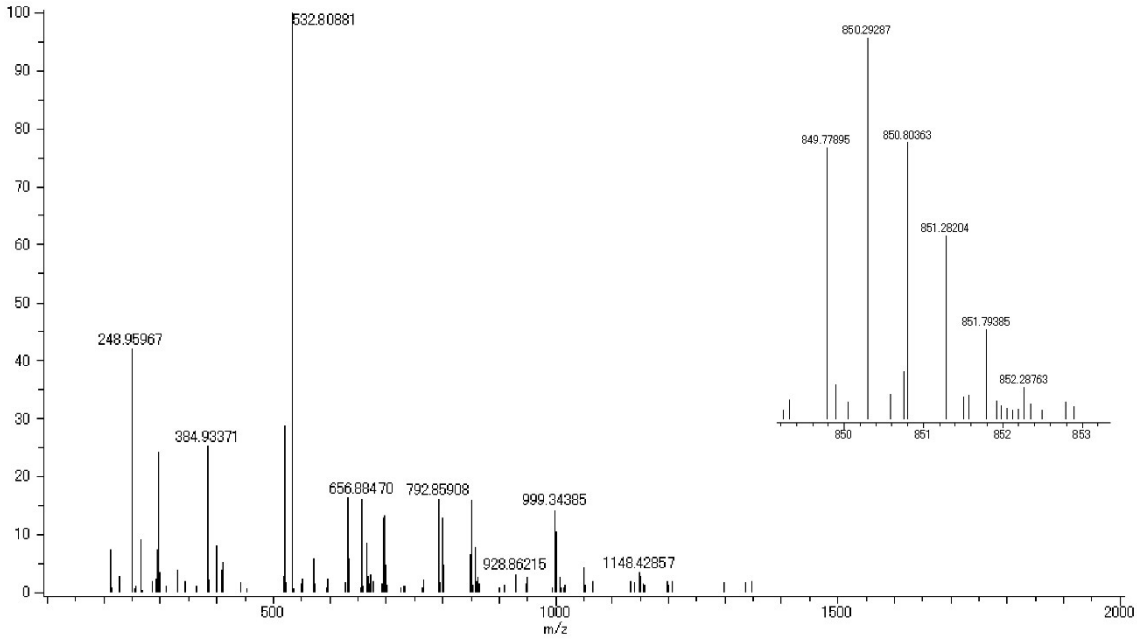

Figure S21. ESI-MS spectrum of **4a**·4HNMe$_2$Bu·2THF (MeOH).

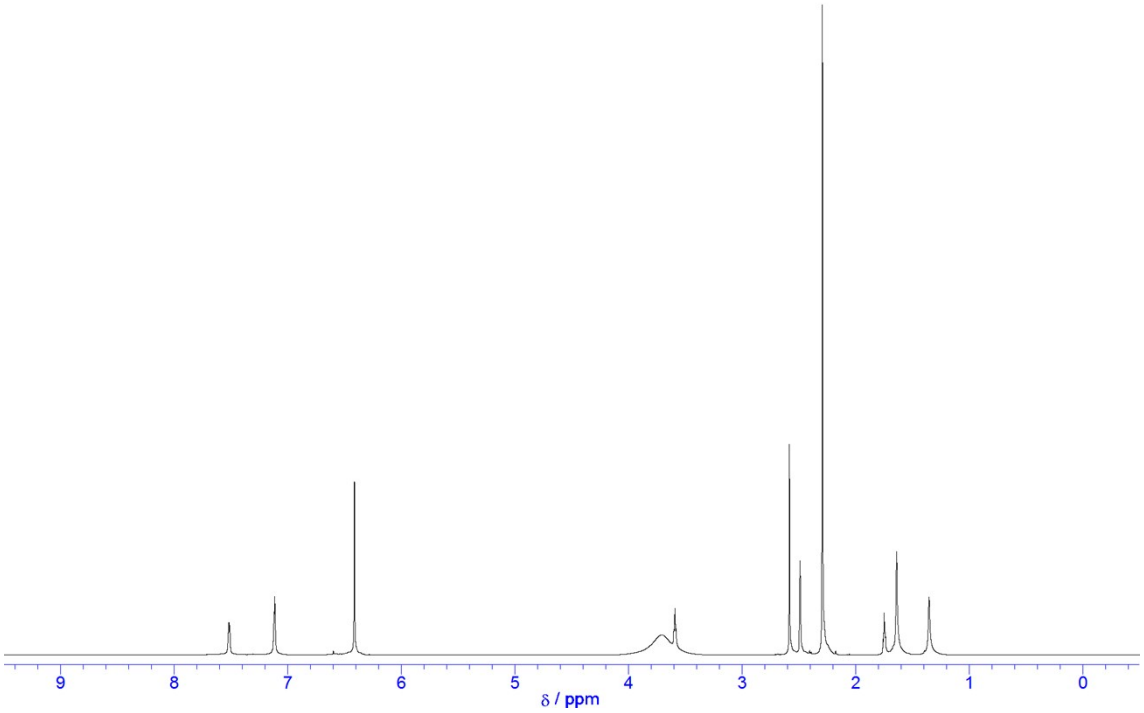

Figure S22. ^{1}H NMR spectrum of **4a**·4TMEDAH·2THF (600 MHz, DMSO-d_6).

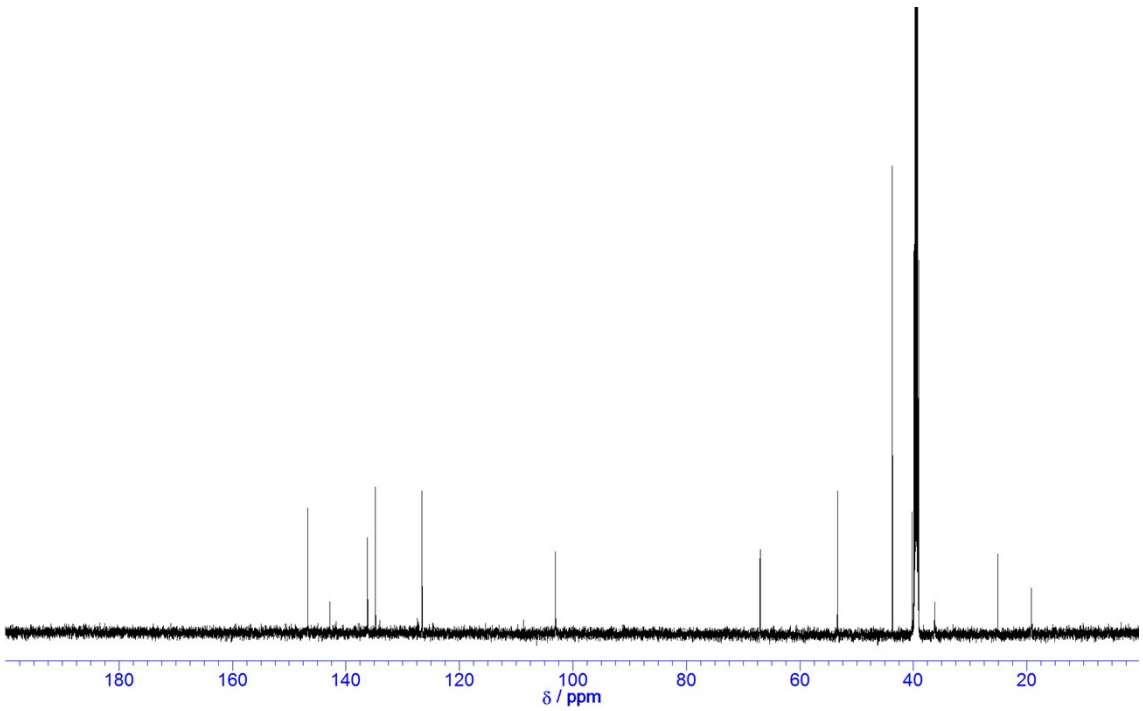

Figure S23. ^{13}C NMR spectrum of **4a**·4TMEDAH·2THF (150 MHz, DMSO-d_6).

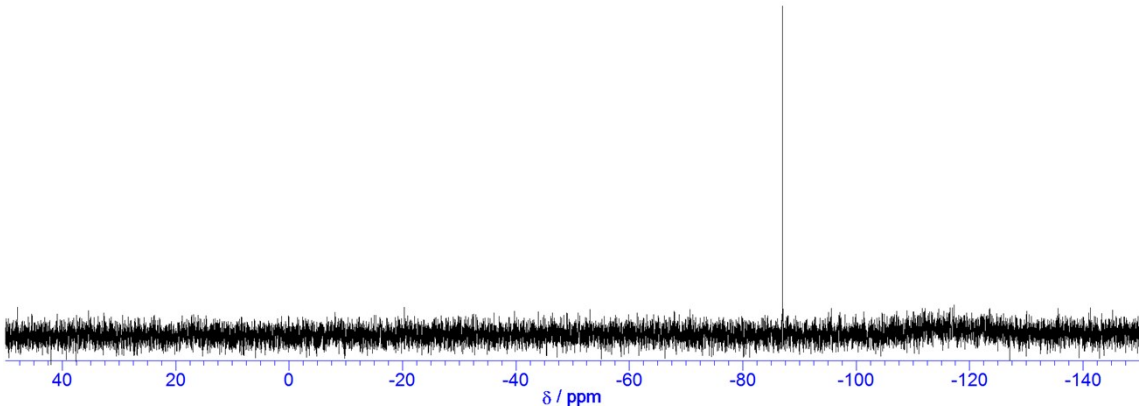

Figure S24. ^{29}Si NMR spectrum of **4a**·4TMEDAH·2THF (120 MHz, DMSO-d_6).

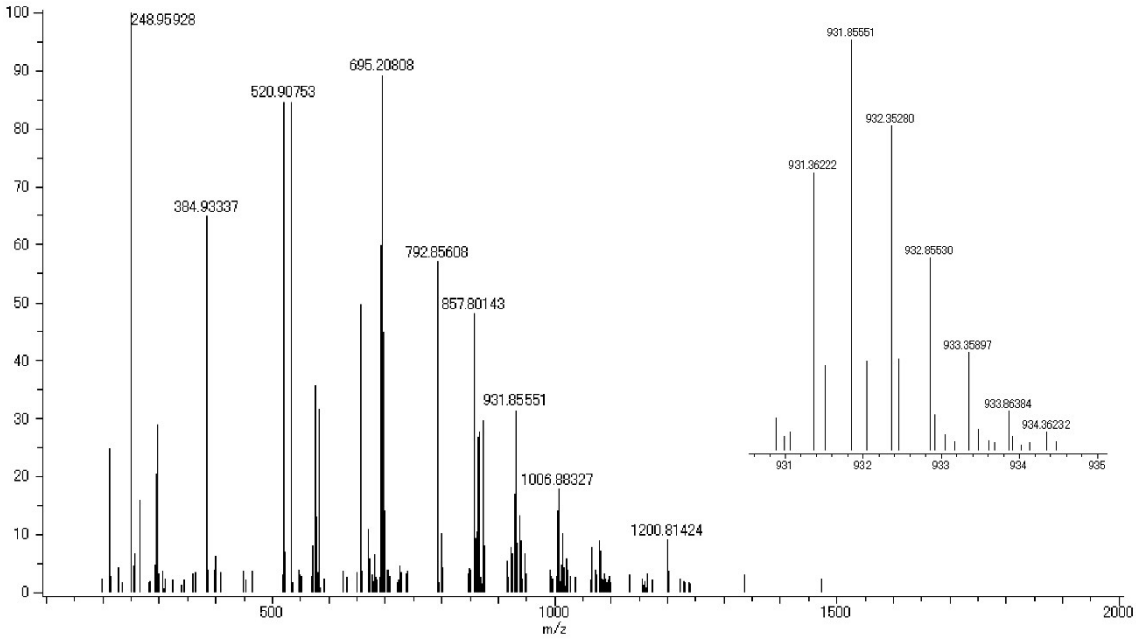

Figure S25. ESI-MS spectrum of **4a**·4TMEDAH·2THF (MeOH).

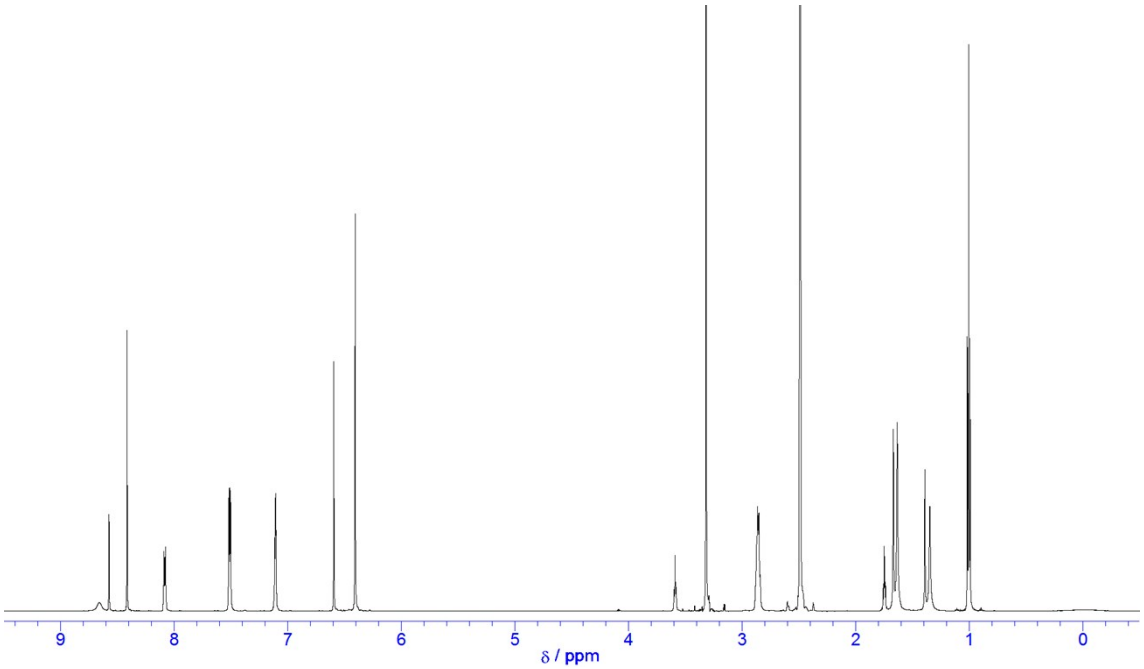

Figure S26. ^{1}H NMR spectrum of **4a**·4HNEt$_3$·2(**2**)·anthracene·4THF (600 MHz, DMSO-d_6).

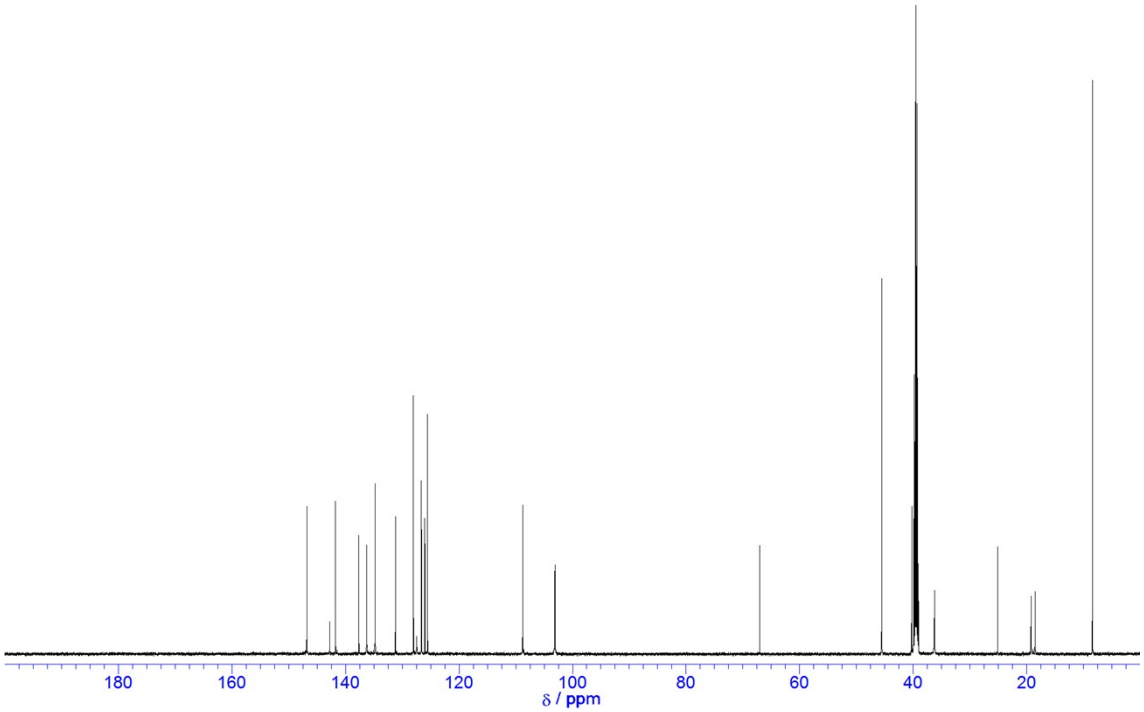

Figure S27. ^{13}C NMR spectrum of **4a**·4HNEt$_3$·2(**2**)·anthracene·4THF (150 MHz, DMSO-d_6).

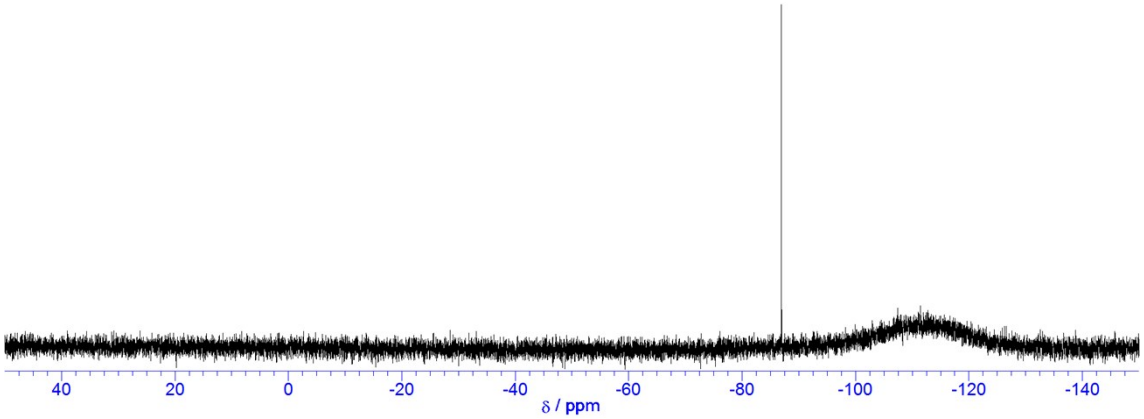

Figure S28. ^{29}Si NMR spectrum of **4a**·4HNEt$_3$·2(**2**)·anthracene·4THF (120 MHz, DMSO-d_6).

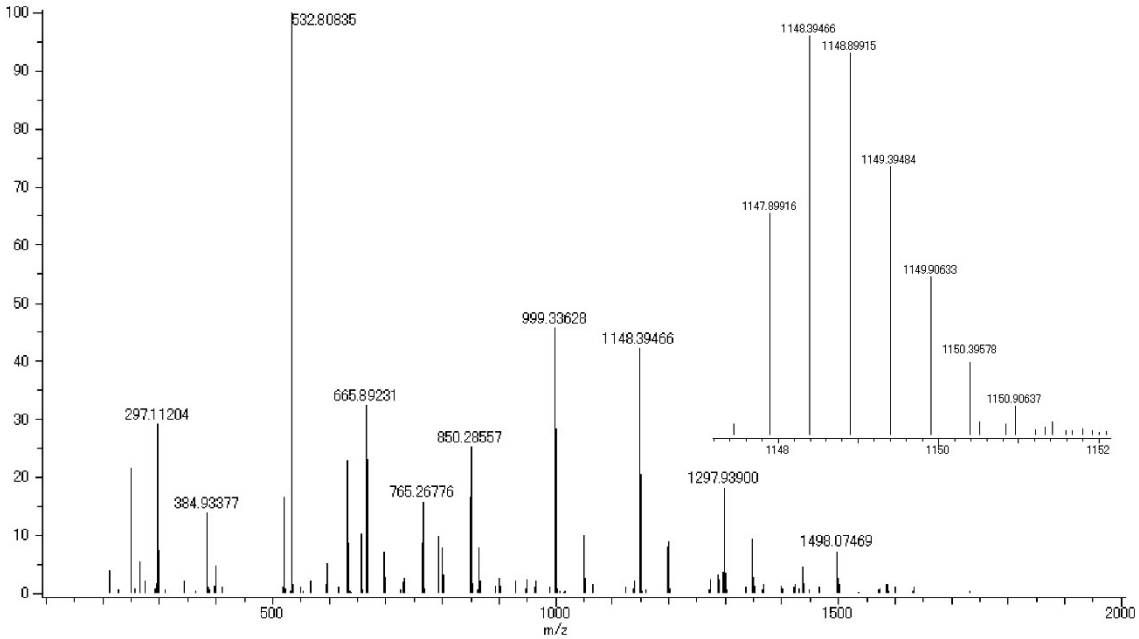

Figure S29. ESI-MS spectrum of **4a**·4HNEt$_3$·2(**2**)·anthracene·4THF (MeOH).

The replacement of *p*-tolylSi(OMe)$_3$ with PhSi(OMe)$_3$ resulted in the formation of a macrocycle possessing a *p*-tolyl group, i.e., **4b**·4HNEt$_3$·2(**2**)·2THF (Figure S30-S33).

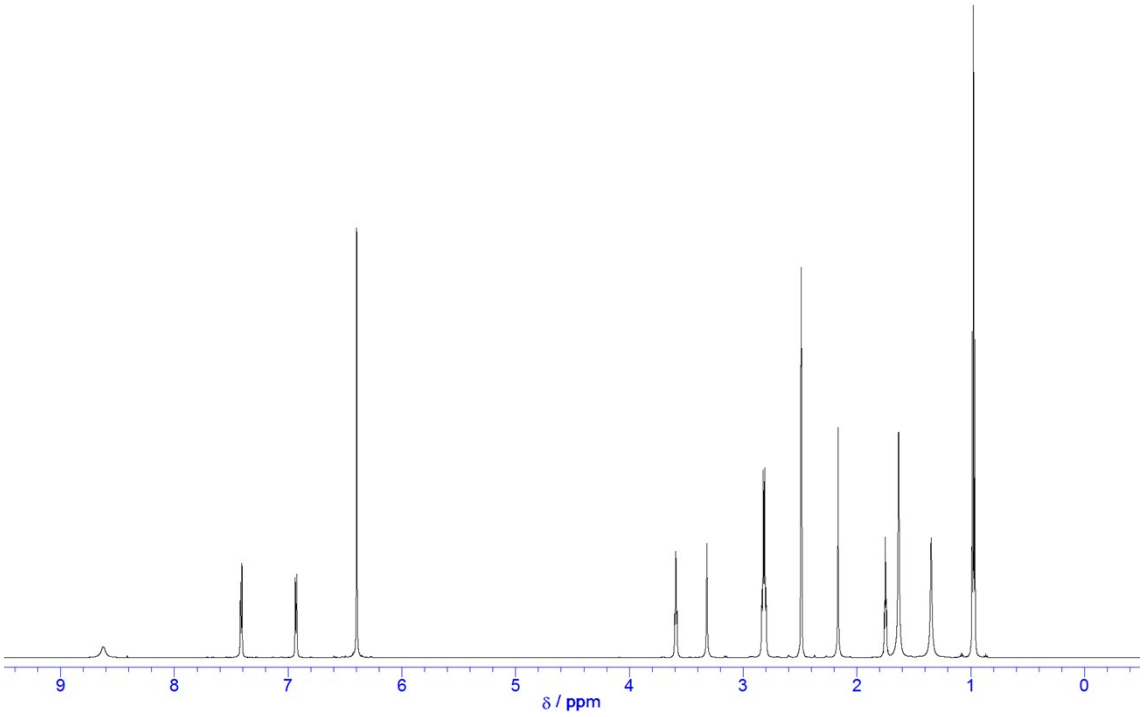

Figure S30. ^{1}H NMR spectrum of **4b**·4HNEt$_3$·2THF (600 MHz, DMSO-d_6).

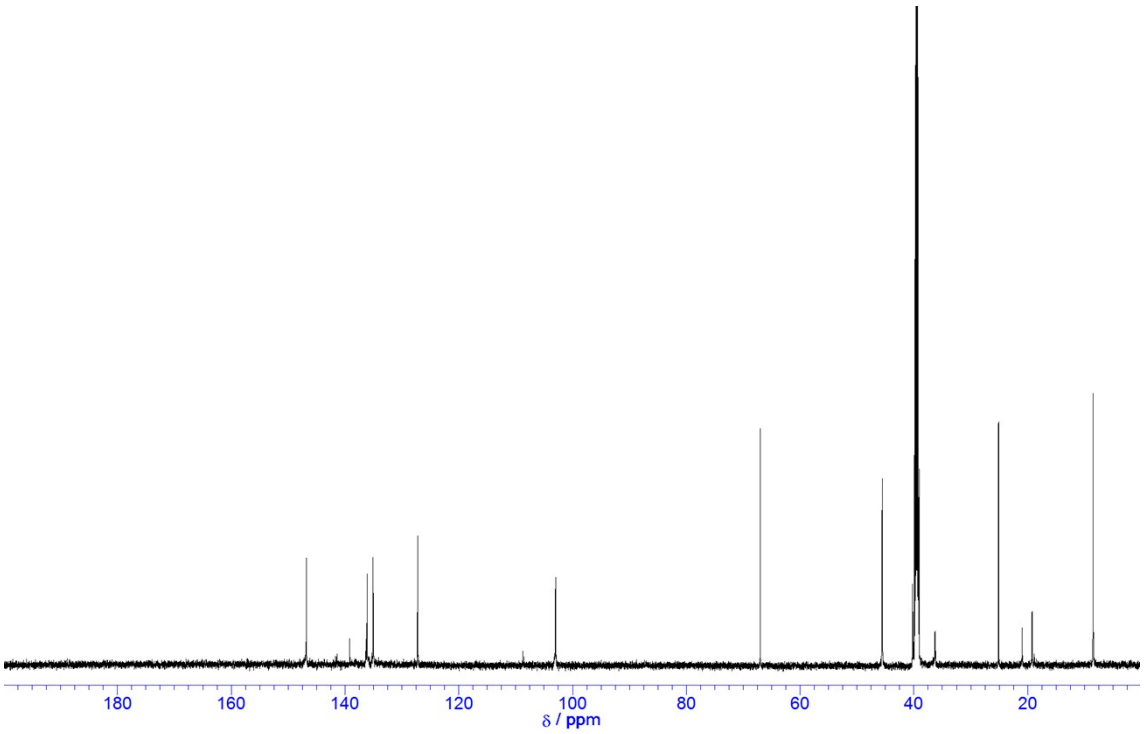

Figure S31. ^{13}C NMR spectrum of **4b**·4HNEt$_3$·2THF (150 MHz, DMSO-d_6).

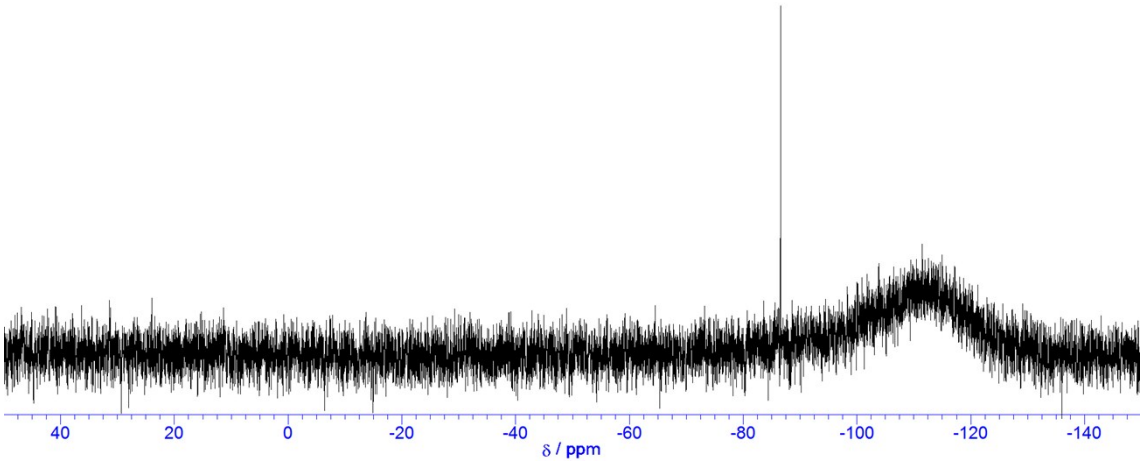

Figure S32. ^{29}Si NMR spectrum of **4b**·4HNEt$_3$·2THF (120 MHz, DMSO-d_6).

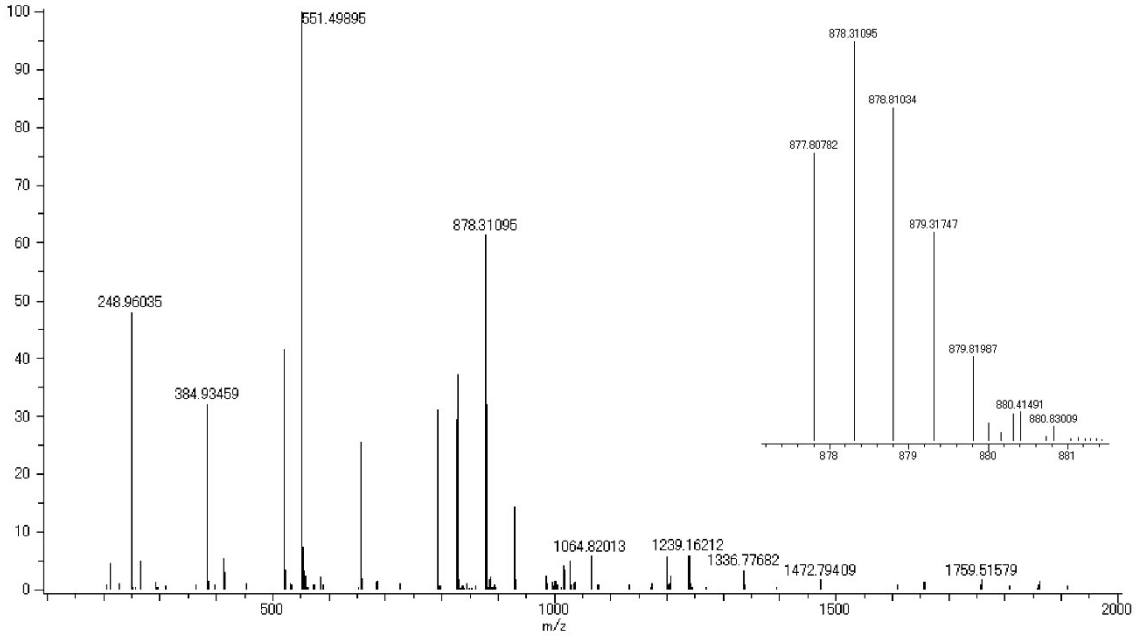

Figure S33. ESI-MS spectrum of **4b**·4HNEt$_3$·2THF (MeOH).

2.2. Structual assignment and spectral data of **5a-f** and **6a**

The ^{1}H, ^{13}C, and DEPT135 NMR spectra of both **5a** and **6a** showed a 2:3:3 molar ratio of cyclotricatechylene (CTC), silyl phenyl and HNEt$_3^+$ counter ion (Figure S34, S35, S36, S39, and S40). The ^{29}Si NMR spectra of **5a** and **6a** showed peak at -86.94 ppm and -86.34, -86.85 ppm, respectively, corresponding to a penta-coordinated anionic silane biscatecholate (Figure S37 and S41). The ESI mass spectra of **5a** and **6a** also showed molecular ions that were consistent with

$[M+4HNEt_3]^{2-}$ at m/z 1239.4 for **5a** (M = hexaanion core) and $[M+7HNEt_3]^{2-}$ at m/z 1859.6 for **6a** (M = nonaanion core) (Figure S38 and S42).

The spectral results of **5a** indicated a tetrameric tetrahedral cage structure of this silane catecholate compound, where the CTC units are situated at the vertices of the tetrahedron with the silane catecholate bridging them along each tetrahedral edge.

The spectral data obtained for **6a** also confirmed a hexameric prismatic cage structure, which is concaved inward placing three phenyl groups inside a nanocage. Upon a closer inspection of the ^{1}H NMR spectrum of **6a** (Figure S39), six sets of phenyl protons could be seen at almost the same chemical shift as those of **5a** (Figure S34) at 7.36 ppm (*o*-CH) and 7.14-7.07 ppm (*m*-, *p*-CH). The remaining three sets of phenyl protons were shifted to higher fields, i.e., at 7.22 ppm (*o*-CH'), 6.63 ppm (*m*-CH'), and 6.38 ppm (*p*-CH') owing to the three phenyl groups located inside of magnetically anisotropic nanocage accounting for the eighteen aromatic rings of CTC.

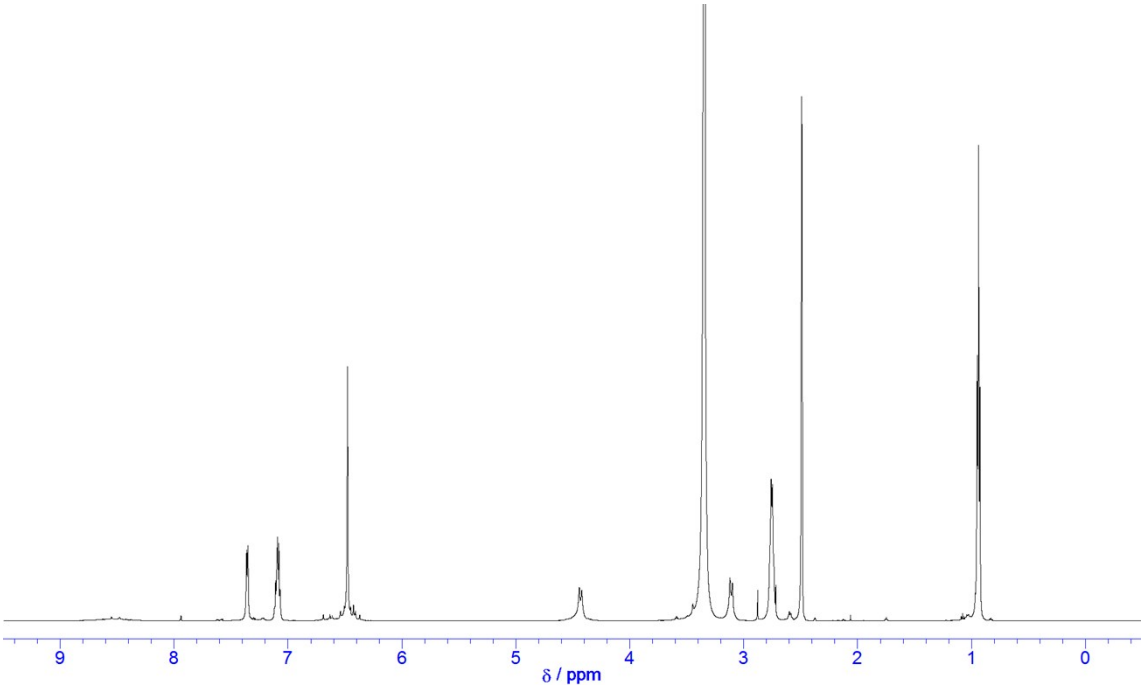

Figure S34. ^{1}H NMR spectrum of **5a**·6HNEt$_3$ (600 MHz, DMSO-d_6).

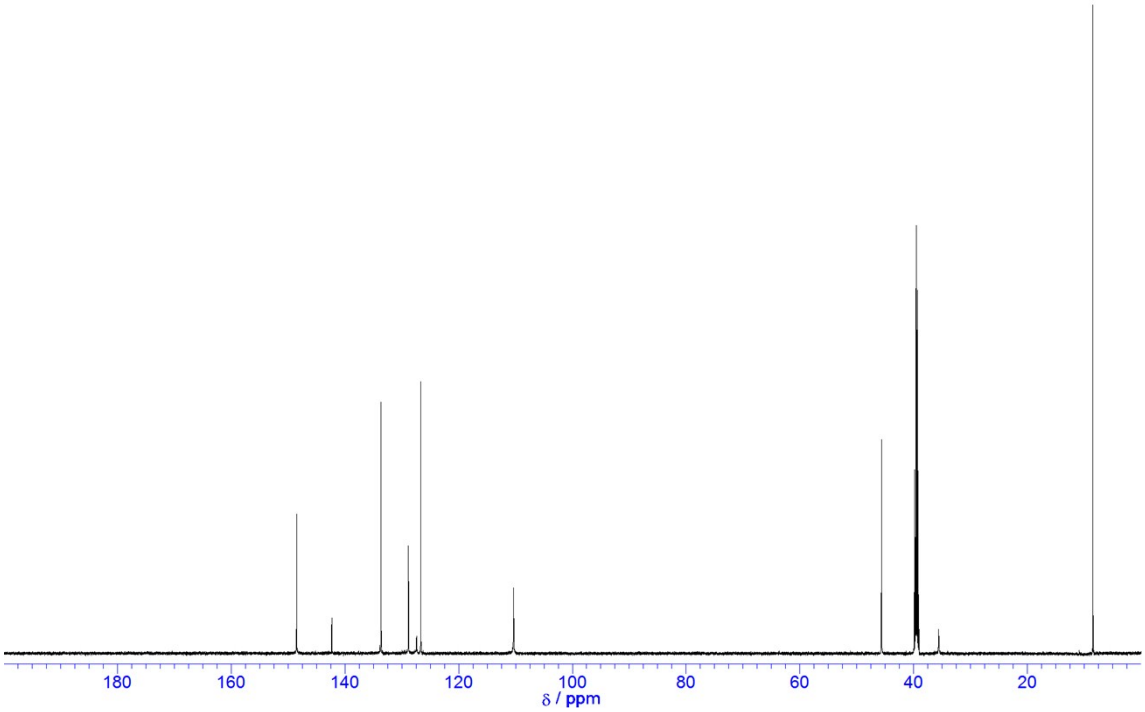

Figure S35. ^{13}C NMR spectrum of **5a**·6HNEt$_3$ (150 MHz, DMSO-d_6).

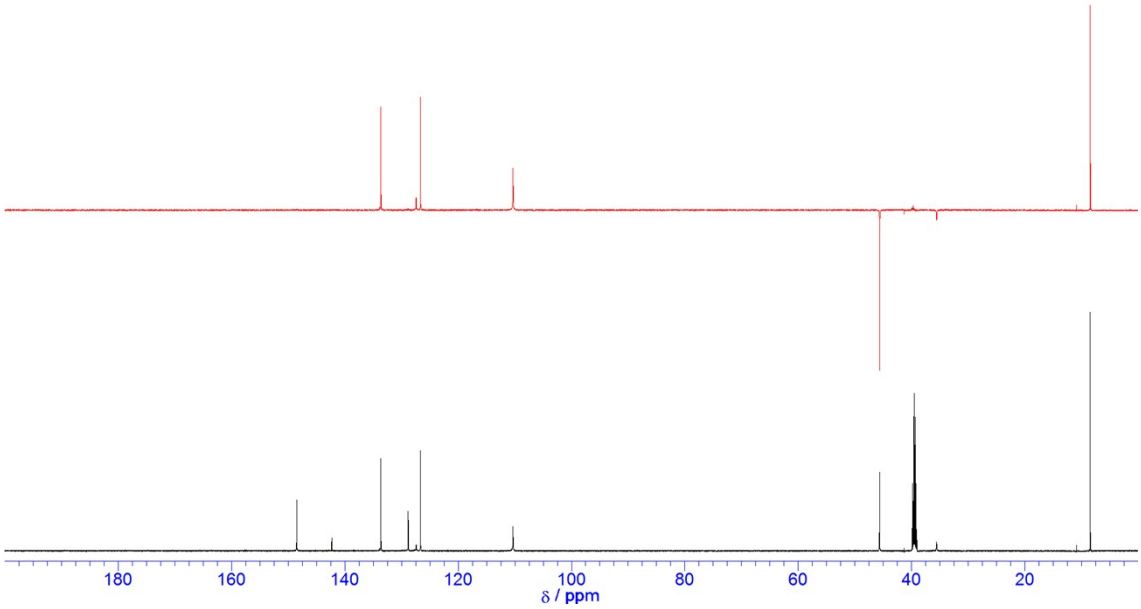

Figure S36. ^{13}C and DEPT135 NMR spectra of **5a**·6HNEt$_3$ (150 MHz, DMSO-d_6).

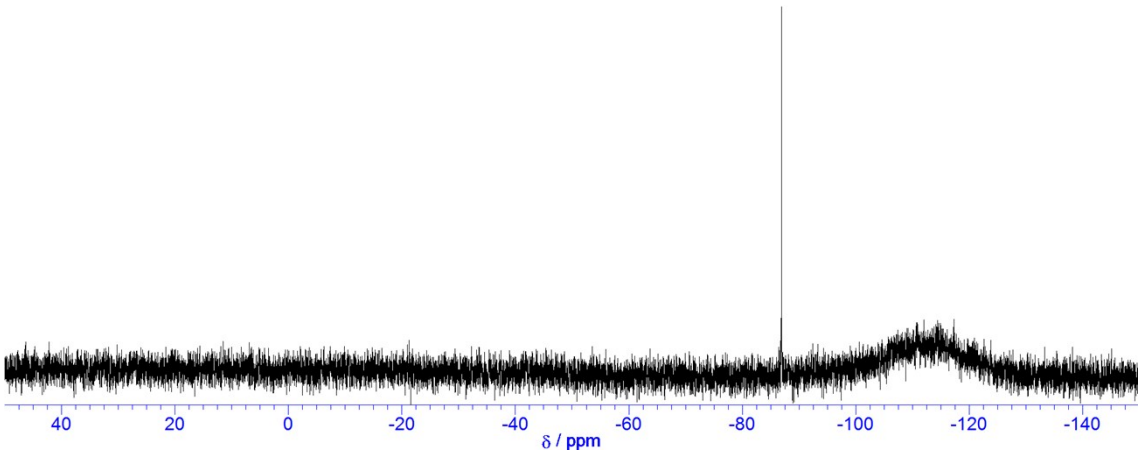

Figure S37. ^{29}Si NMR spectrum of **5a**·6HNEt$_3$ (120 MHz, DMSO-d_6).

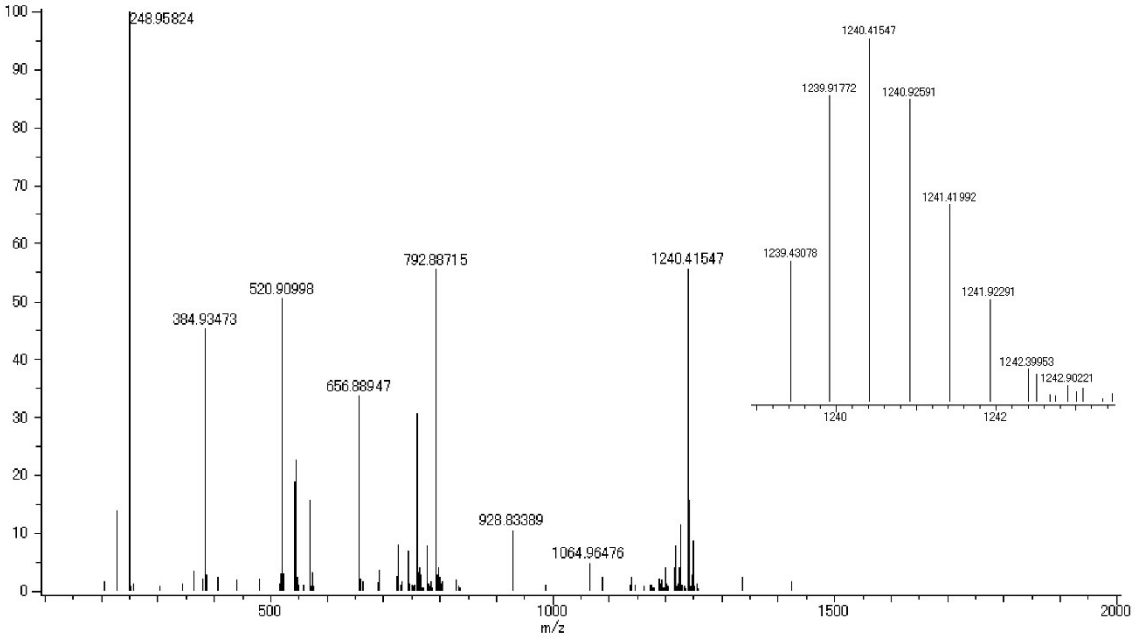

Figure S38. ESI-MS spectrum of **5a**·6HNEt$_3$ (MeOH).

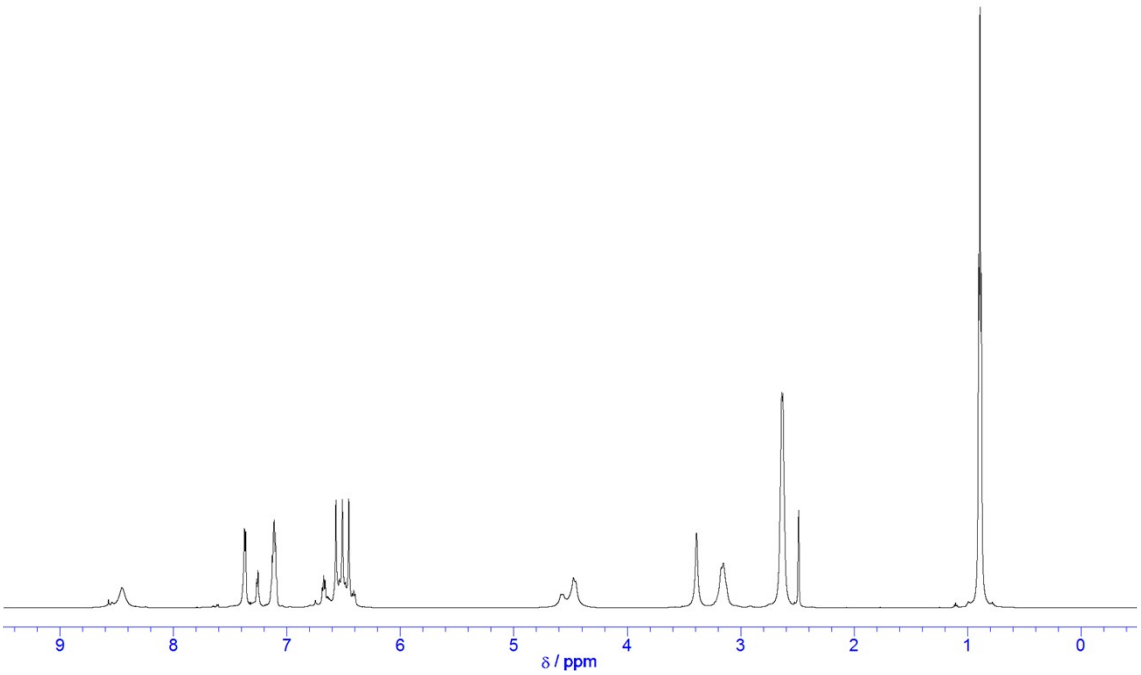

Figure S39. ^{1}H NMR spectrum of **6a**·9HNEt$_3$ (600 MHz, DMSO-d_6).

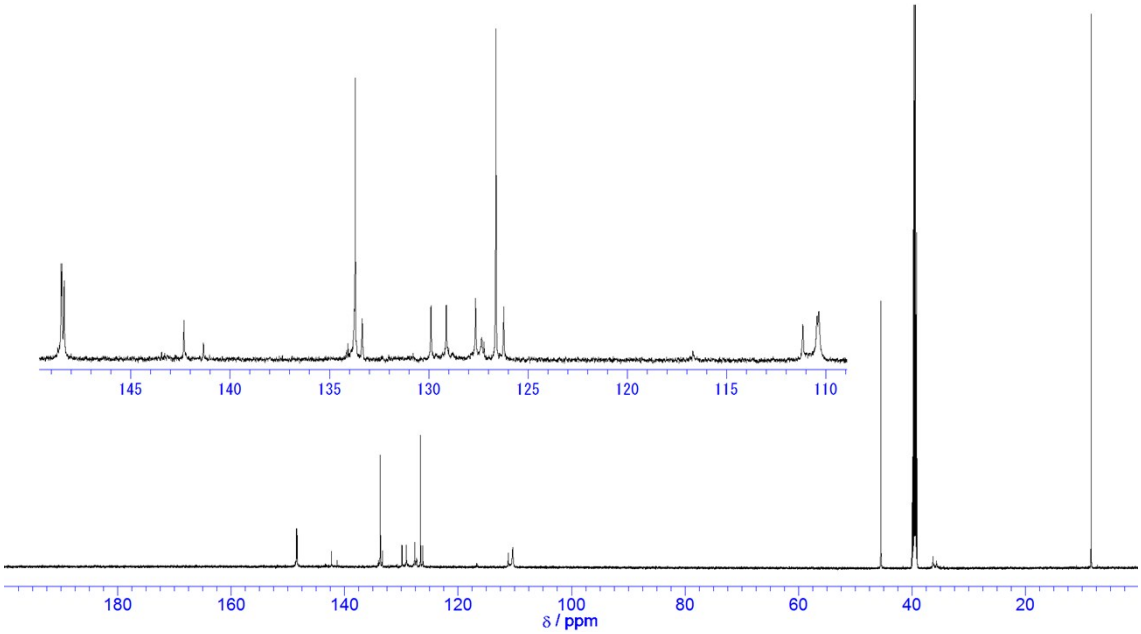

Figure S40. ^{13}C NMR spectrum of **6a**·9HNEt$_3$ (150 MHz, DMSO-d_6).

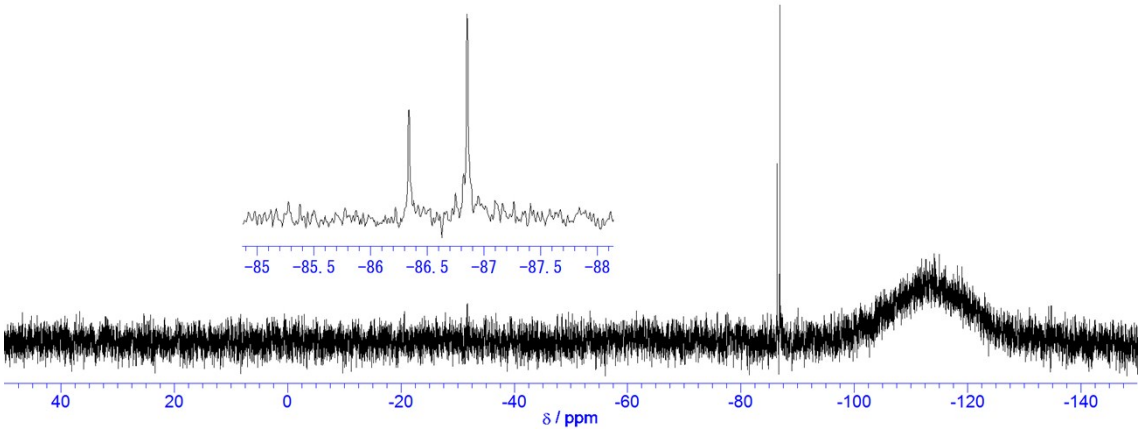

Figure S41. ^{29}Si NMR spectrum of **6a**·9HNEt$_3$ (120 MHz, DMSO-d_6).

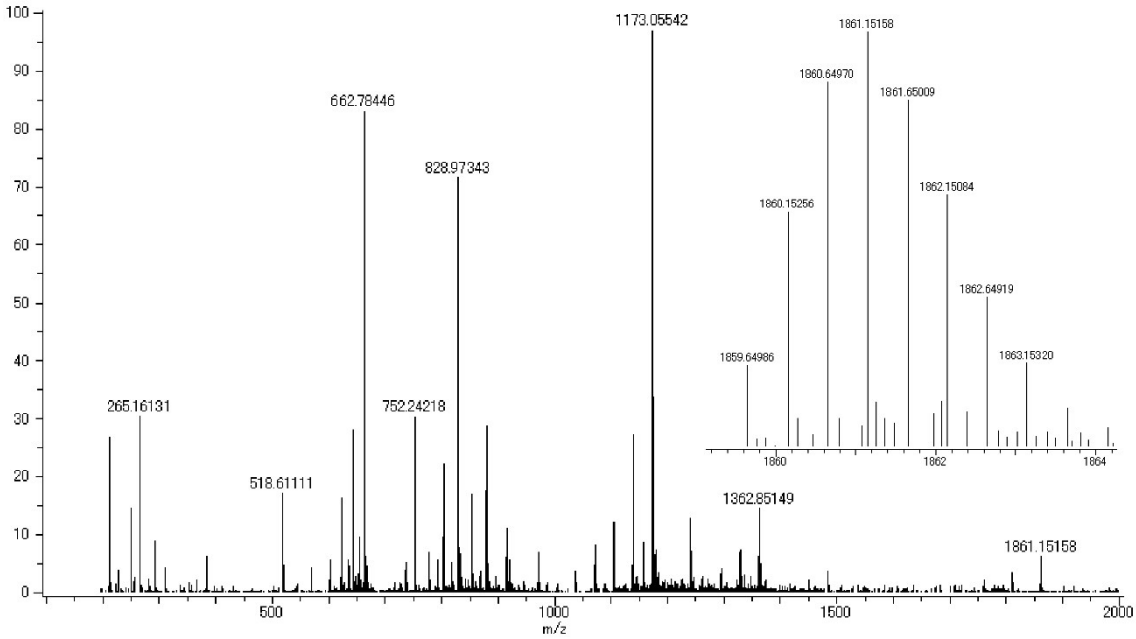

Figure S42. ESI-MS spectrum of **6a**·9HNEt$_3$ (MeOH).

The replacement of the phenyl group in RSi(OMe)$_3$ with *p*-tolyl, methyl, vinyl, and (CH$_2$)$_3$SH resulted in the formation of tetrahedral nanocages, i.e., **5b**·6HNEt$_3$, **5c**·6HNEt$_3$, **5d**·6HNEt$_3$, and **5e**·6HNEt$_3$, respectively (Figure S43-S59). By using NaOH instead of Et$_3$N, the ammonium cation could also be replaced by Na$^+$ affording **5a**·6Na and **5c**·6Na (Figure S60-S67).

The reaction of H$_2$NCONH(CH$_2$)$_3$Si(OMe)$_3$, H$_2$N(CH$_2$)$_3$Si(OMe)$_3$, and Me$_2$N(CH$_2$)$_3$Si(OMe)$_3$ with CTC and Et$_3$N led to a complex mixture of intermediate oligomers, which was insoluble due to the cation-anion interactions between (CH$_2$)$_3$NHR$_2^+$ and the silane catecholate anions, thus impeding the further reaction progress. On the other hand, the reaction of Me$_2$N(CH$_2$)$_3$Si(OMe)$_3$ with CTC and

NaOH yielded tetrameric cage **5f**·6Na (Figure S68-S70).

These anionic nanocages with different substituents at the silicon atoms were fully characterized by ^{1}H, ^{13}C, and ^{29}Si NMR as well as ESI-mass spectroscopy.

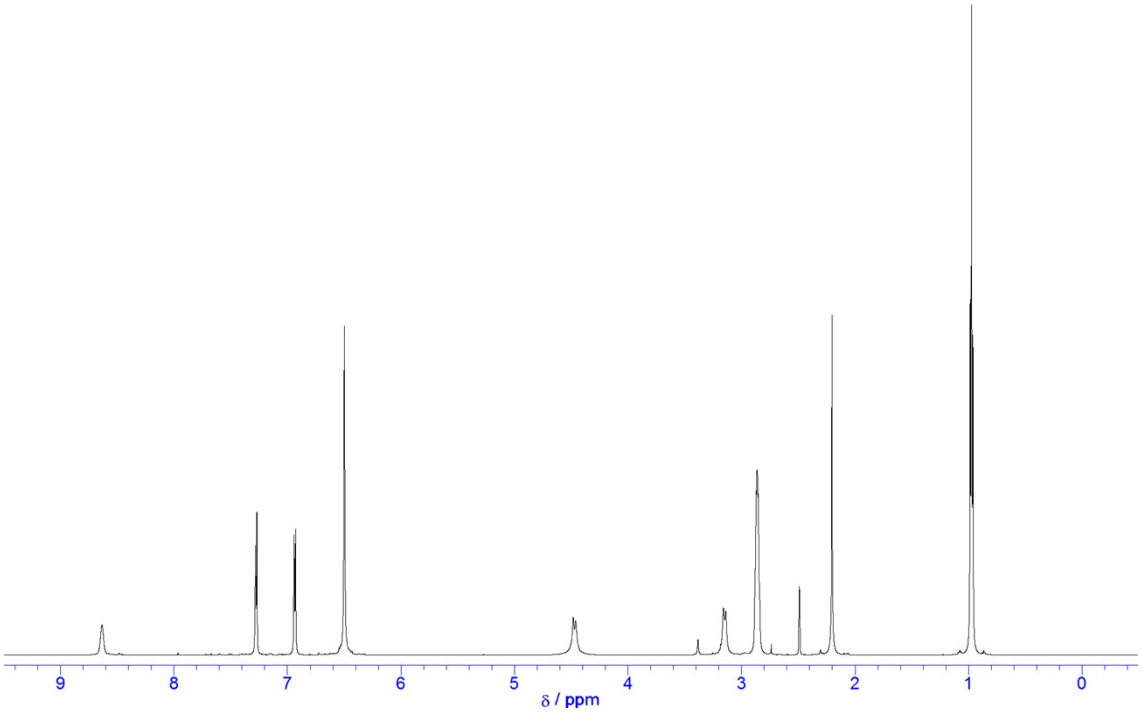

Figure S43. ^{1}H NMR spectrum of **5b**·6HNEt$_3$ (600 MHz, DMSO-d_6).

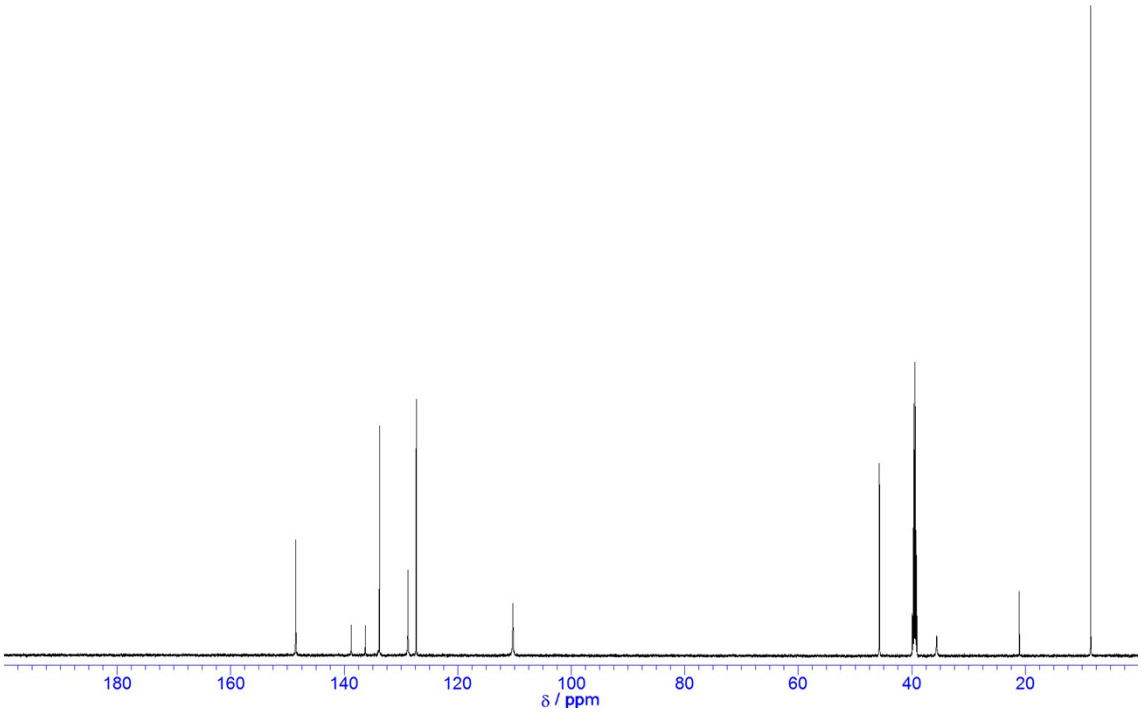

Figure S44. ^{13}C NMR spectrum of **5b**·6HNEt$_3$ (150 MHz, DMSO-d_6).

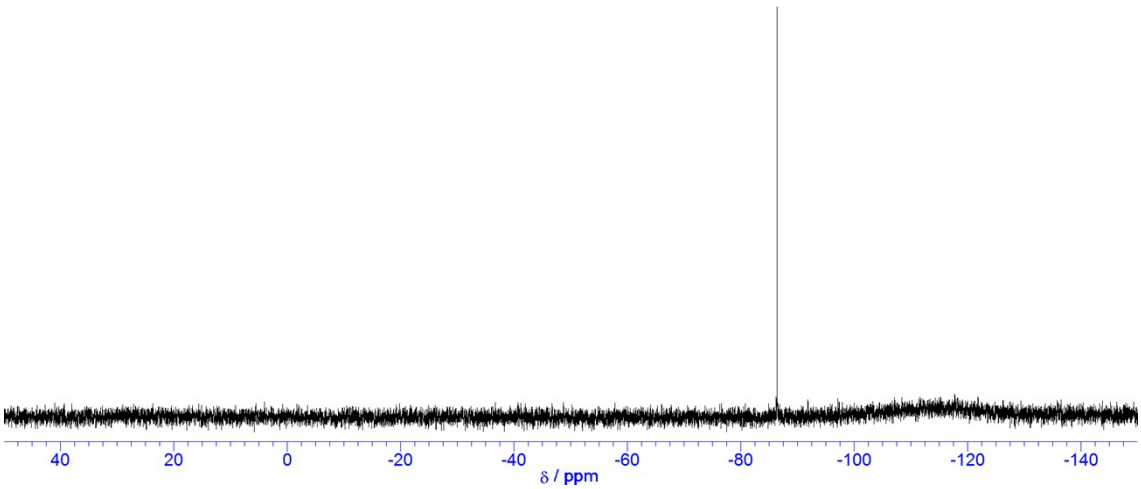

Figure S45. ^{29}Si NMR spectrum of **5b**·6HNEt$_3$ (120 MHz, DMSO-d_6).

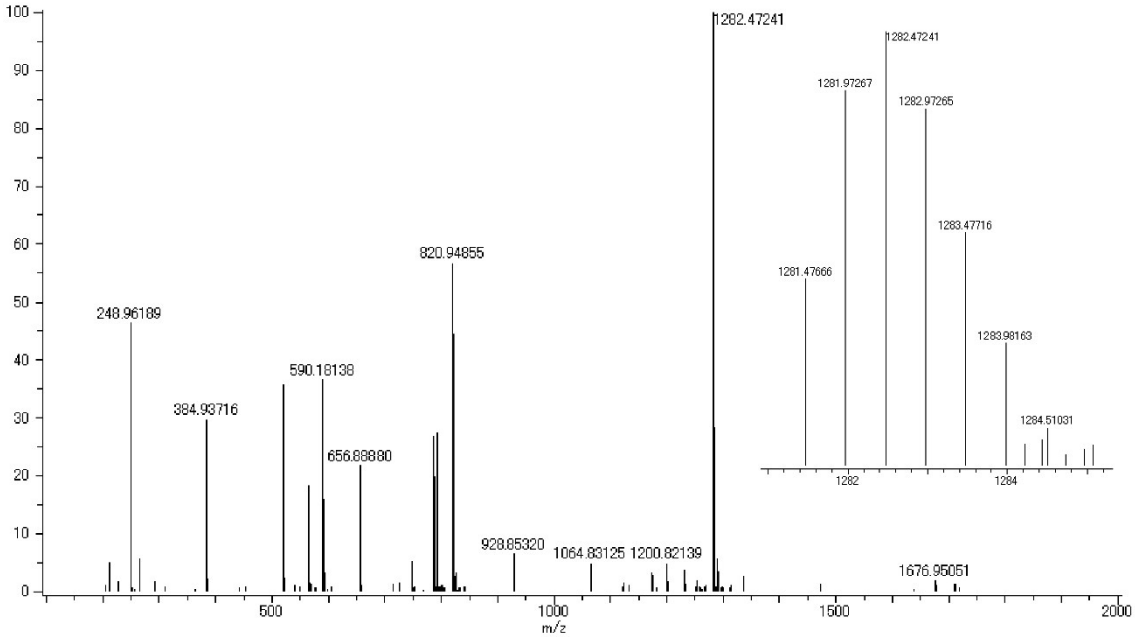

Figure S46. ESI-MS spectrum of **5b**·6HNEt$_3$ (MeOH).

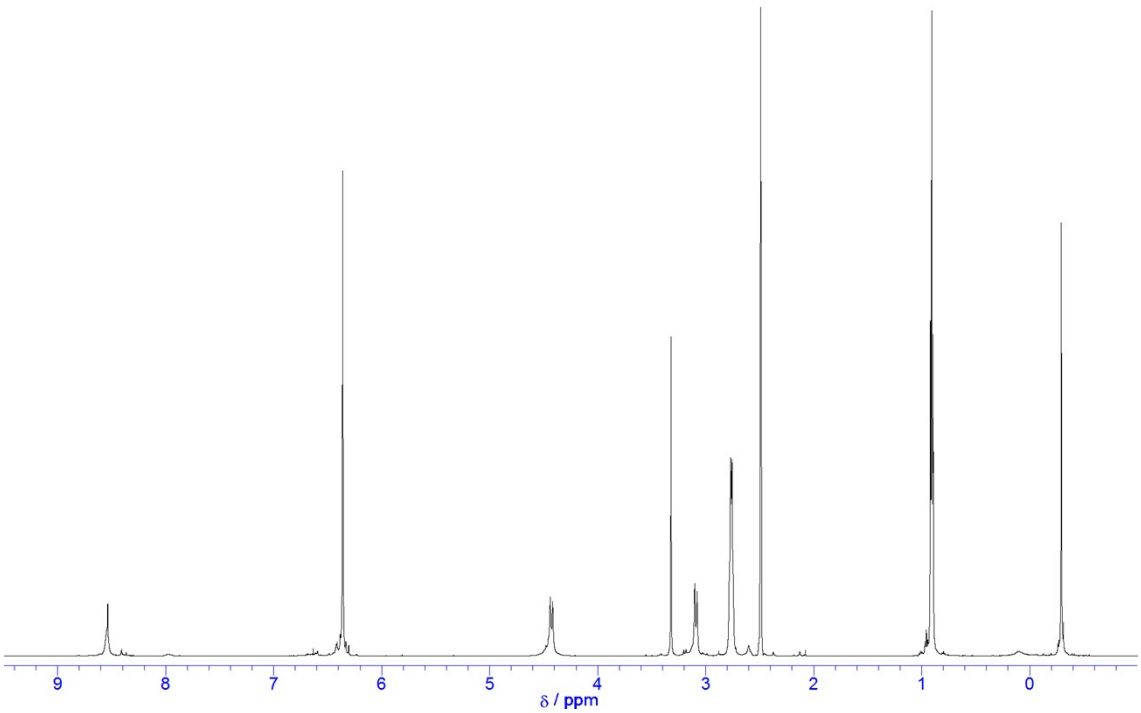

Figure S47. ^{1}H NMR spectrum of **5c**·6HNEt$_3$ (600 MHz, DMSO-d_6).

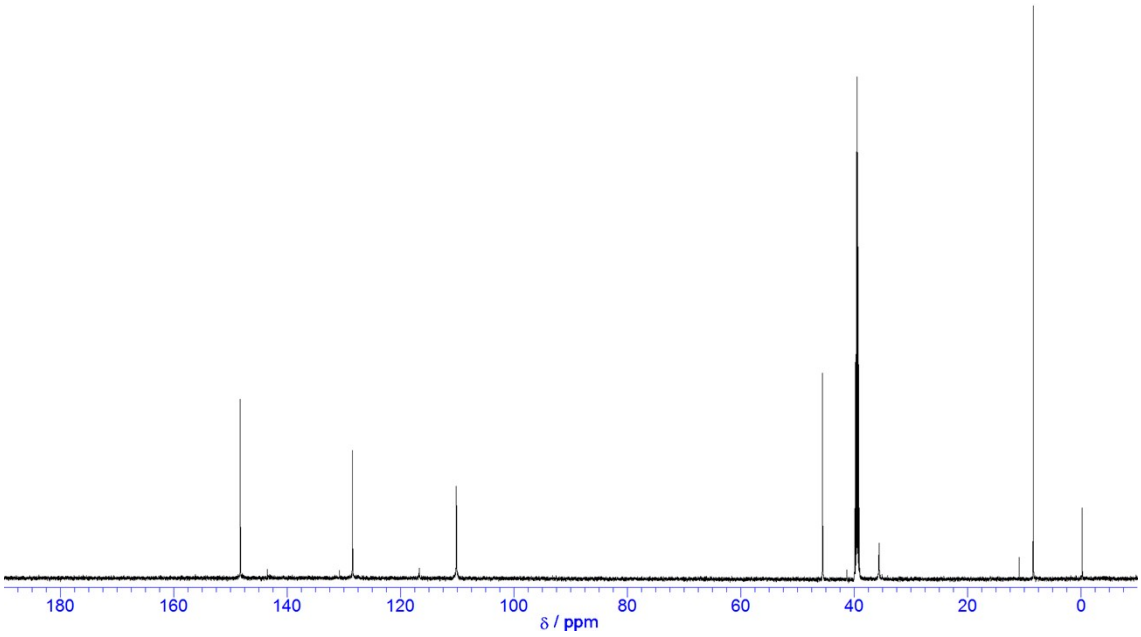

Figure S48. ^{13}C NMR spectrum of **5c**·6HNEt$_3$ (150 MHz, DMSO-d_6).

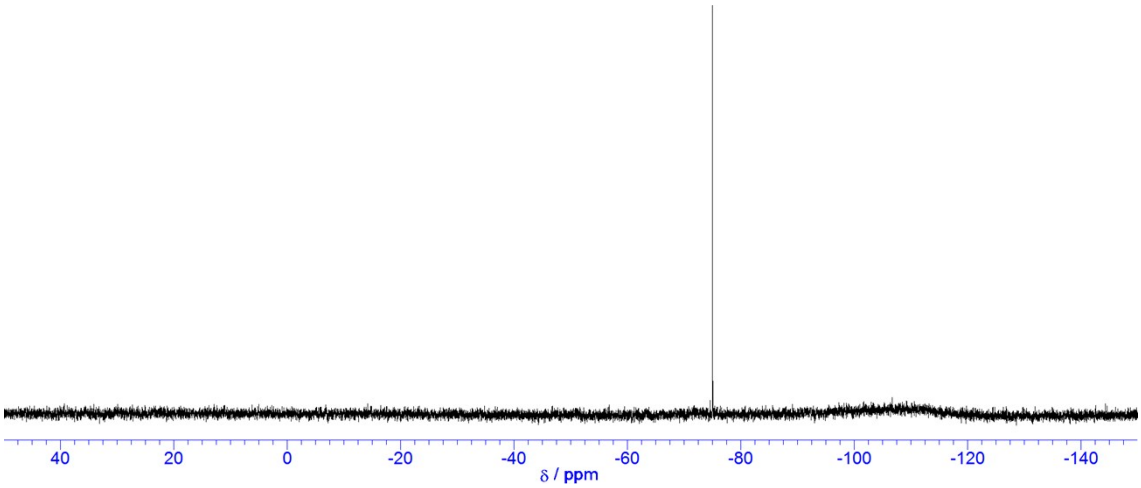

Figure S49. ^{29}Si NMR spectrum of **5c**·6HNEt$_3$ (120 MHz, DMSO-d_6).

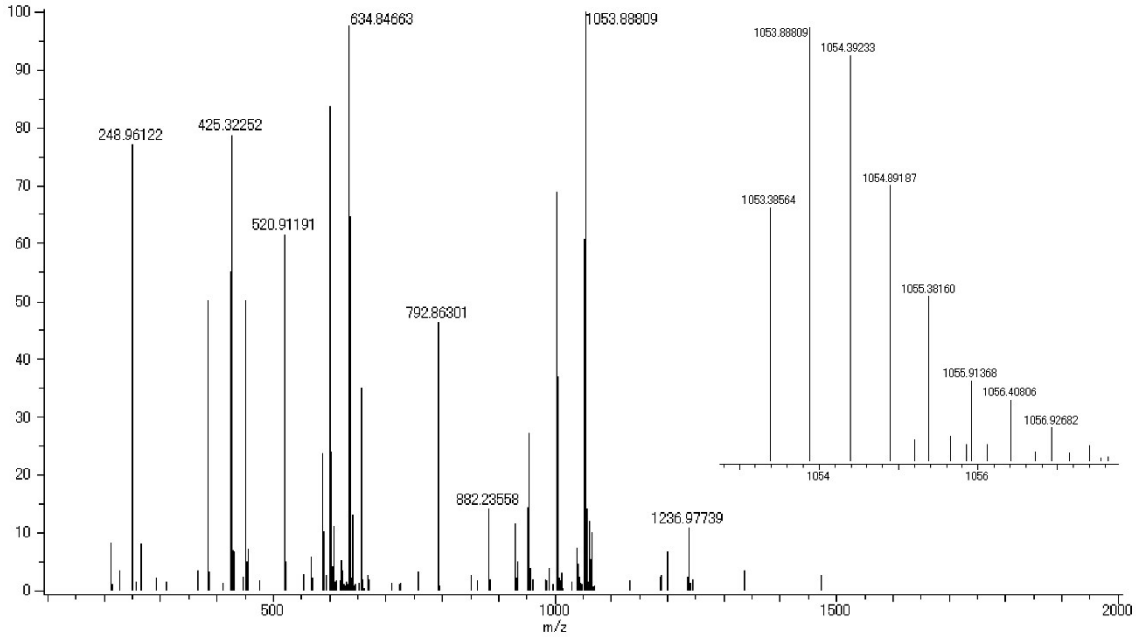

Figure S50. ESI-MS spectrum of **5c**·6HNEt$_3$ (MeOH).

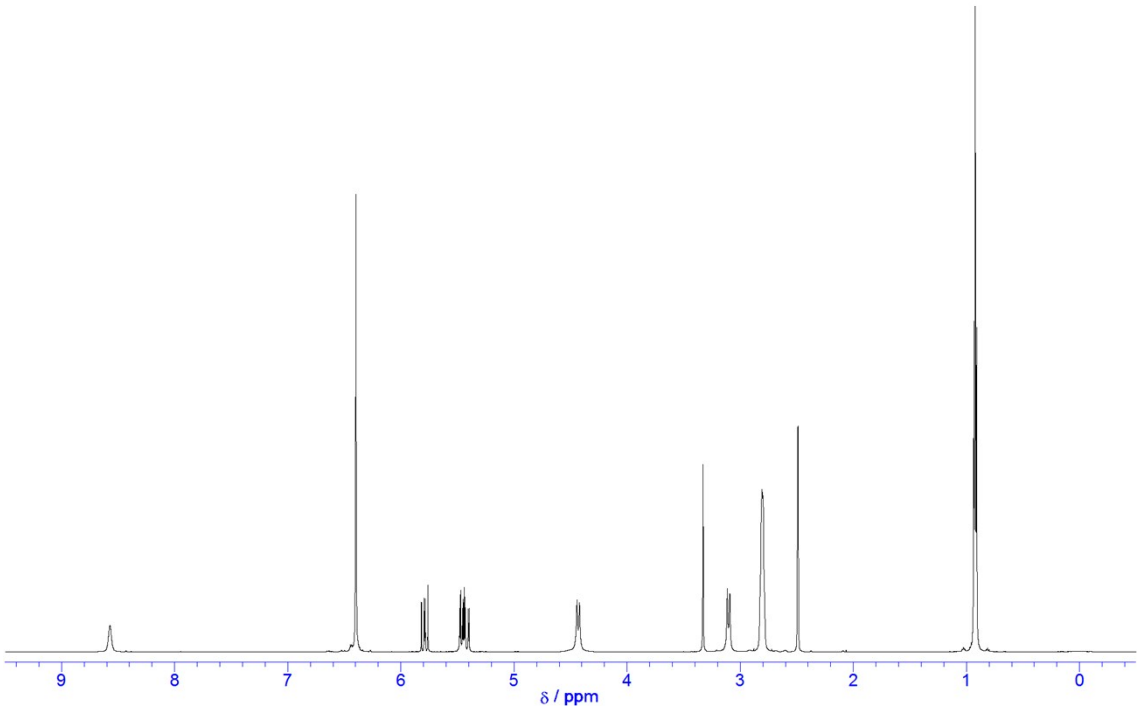

Figure S51. ^{1}H NMR spectrum of **5d**·6HNEt$_3$ (600 MHz, DMSO-d_6).

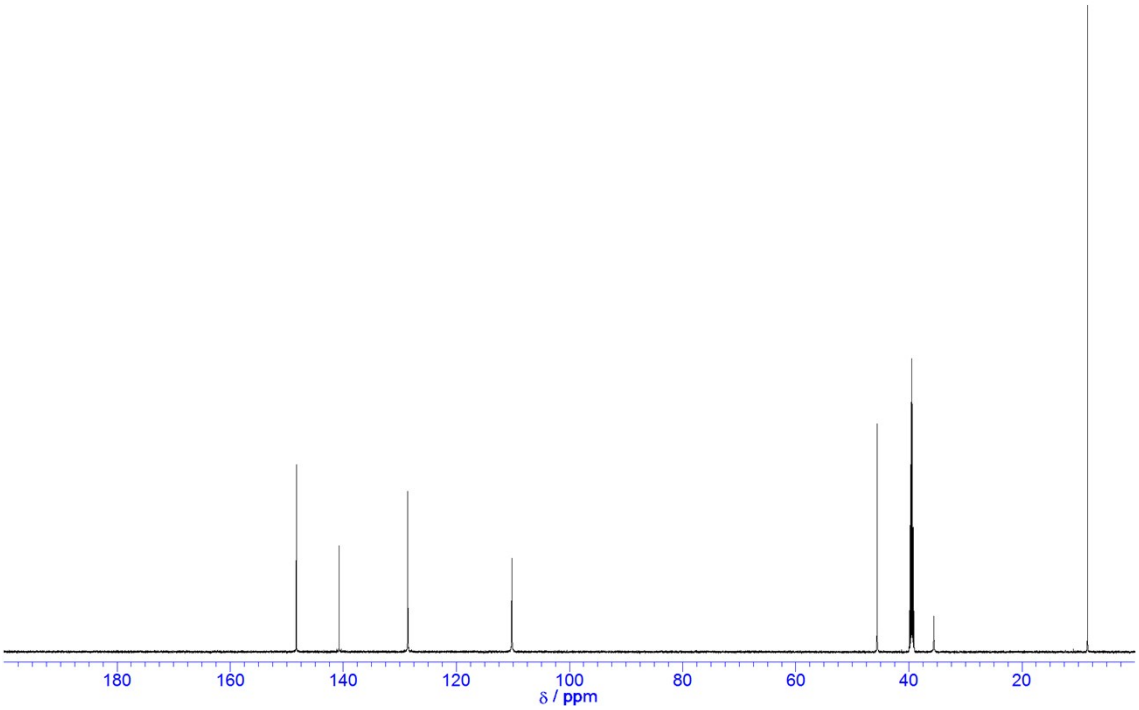

Figure S52. ^{13}C NMR spectrum of **5d**·6HNEt$_3$ (150 MHz, DMSO-d_6).

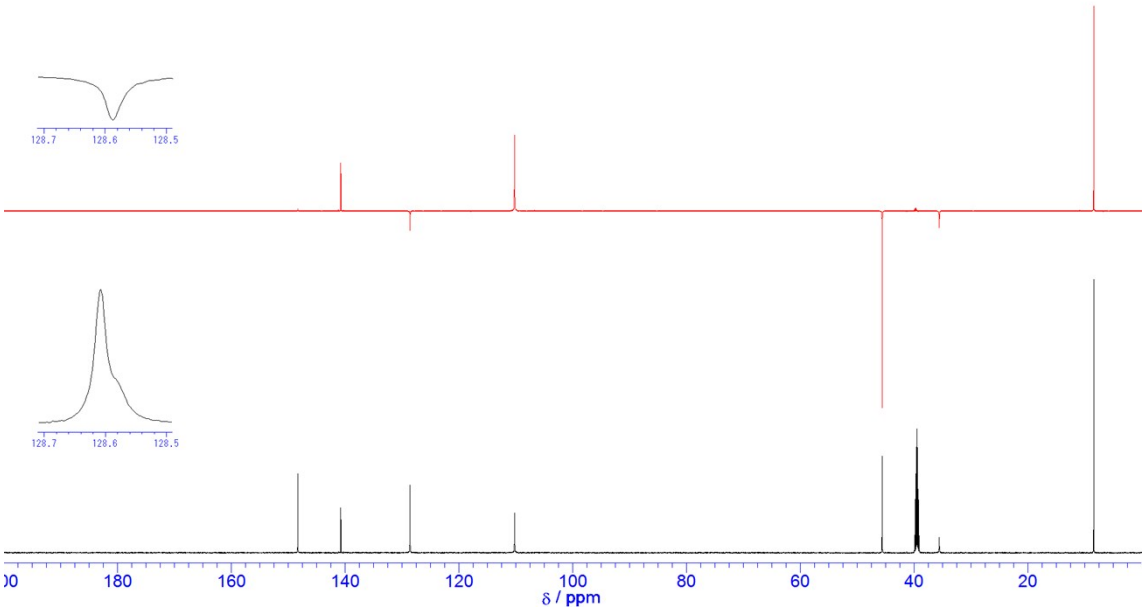

Figure S53. ^{13}C and DEPT135 NMR spectra of **5d**·6HNEt$_3$ (150 MHz, DMSO-d_6).

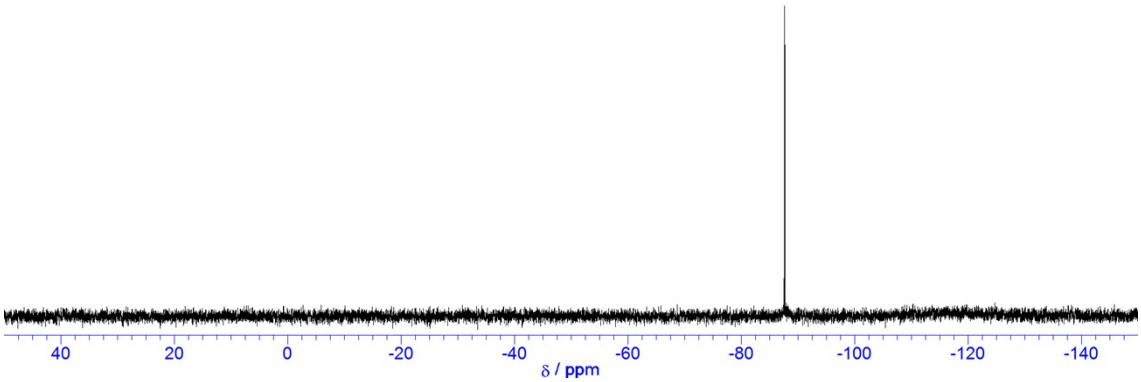

Figure S54. ^{29}Si NMR spectrum of **5d**·6HNEt$_3$ (120 MHz, DMSO-d_6).

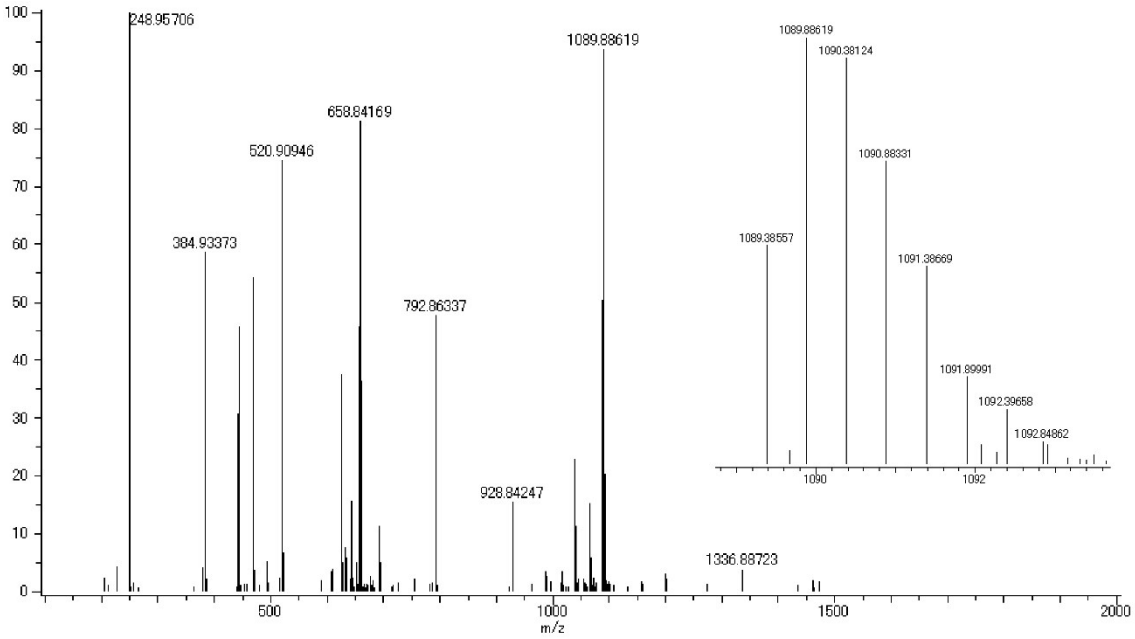

Figure S55. ESI-MS spectrum of **5d**·6HNEt$_3$ (MeOH).

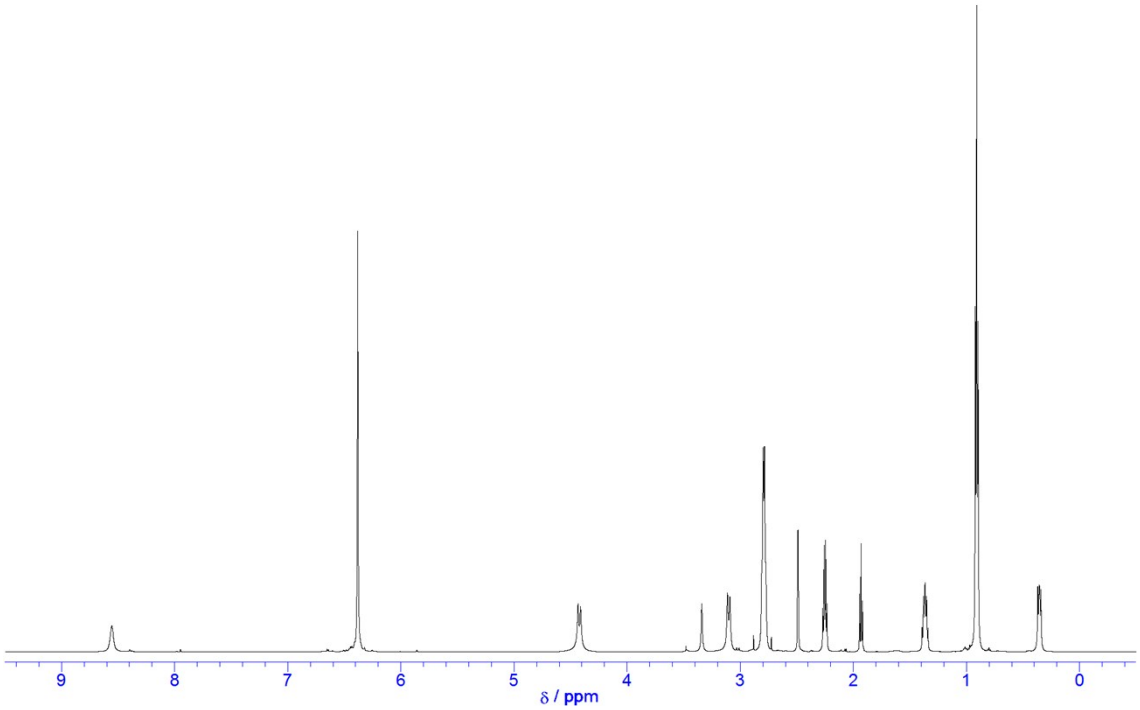

Figure S56. ^{1}H NMR spectrum of **5e**·6HNEt$_3$ (400 MHz, DMSO-d_6).

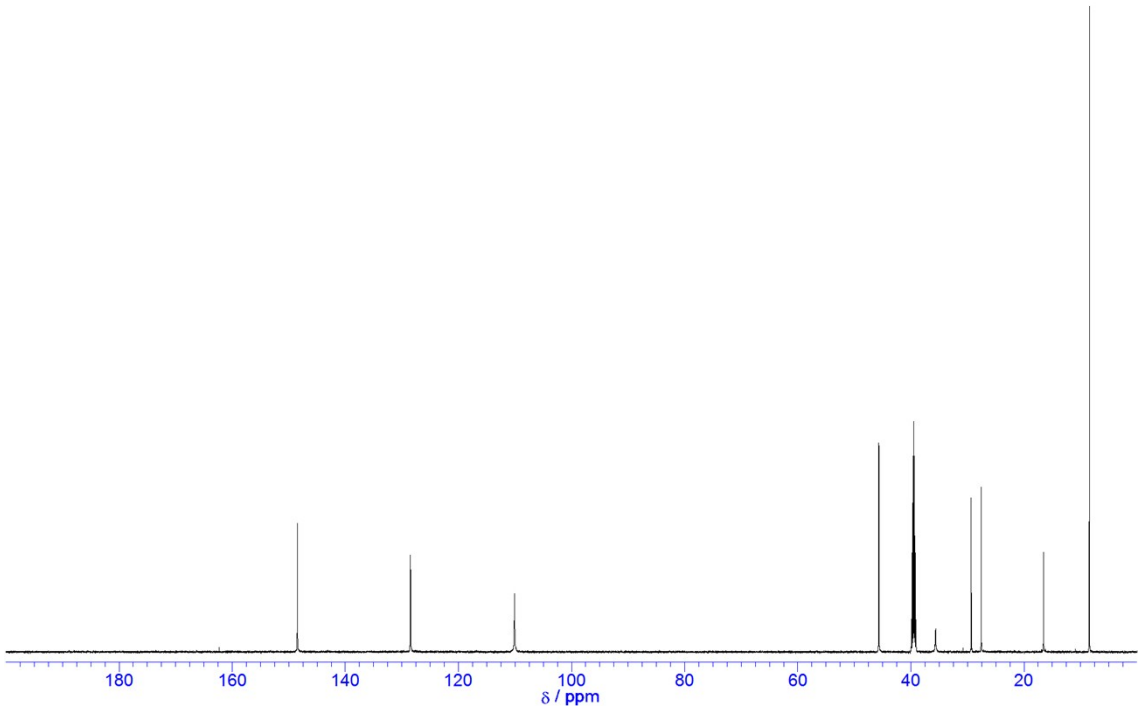

Figure S57. ^{13}C NMR spectrum of **5e**·6HNEt$_3$ (150 MHz, DMSO-d_6).

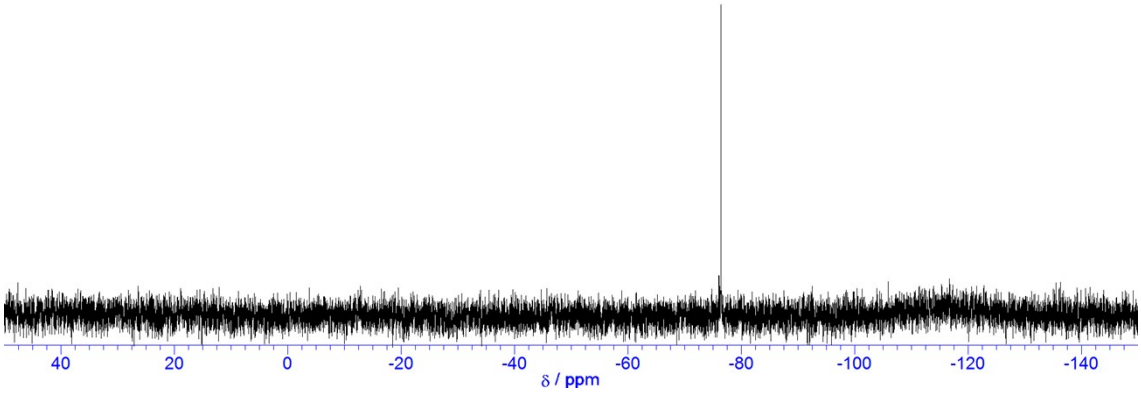

Figure S58. ^{29}Si NMR spectrum of **5e**·6HNEt$_3$ (120 MHz, DMSO-d_6).

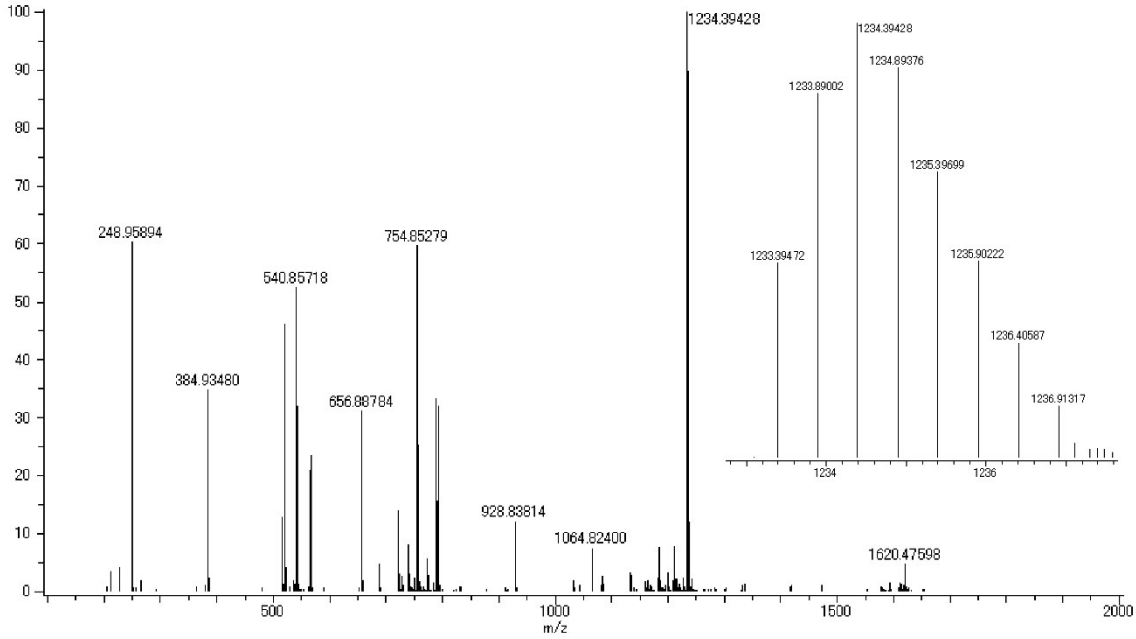

Figure S59. ESI-MS spectrum of **5e**·6HNEt$_3$ (MeOH).

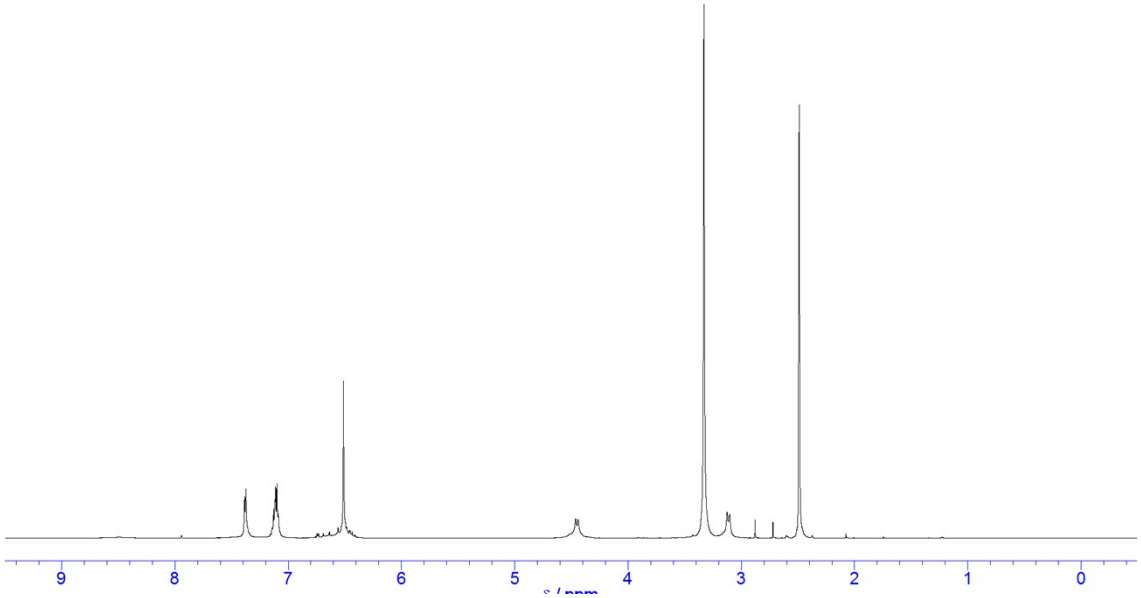

Figure S60. ^{1}H NMR spectrum of **5a**·6Na (600 MHz, DMSO-d_6).

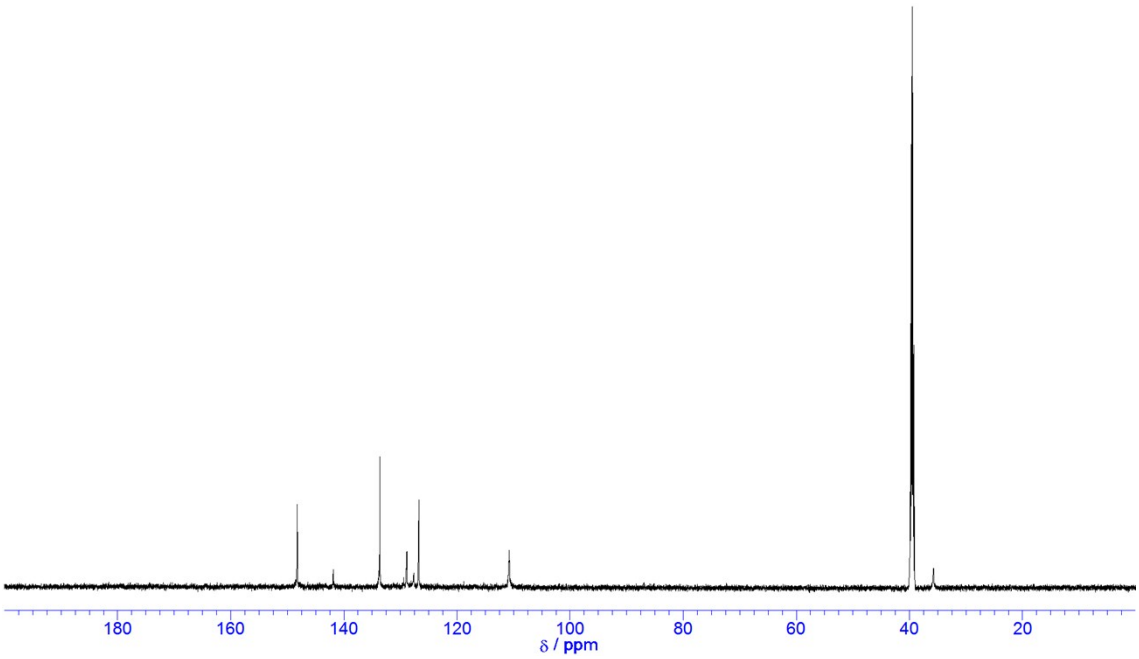

Figure S61. ^{13}C NMR spectrum of **5a**·6Na (150 MHz, DMSO-d_6).

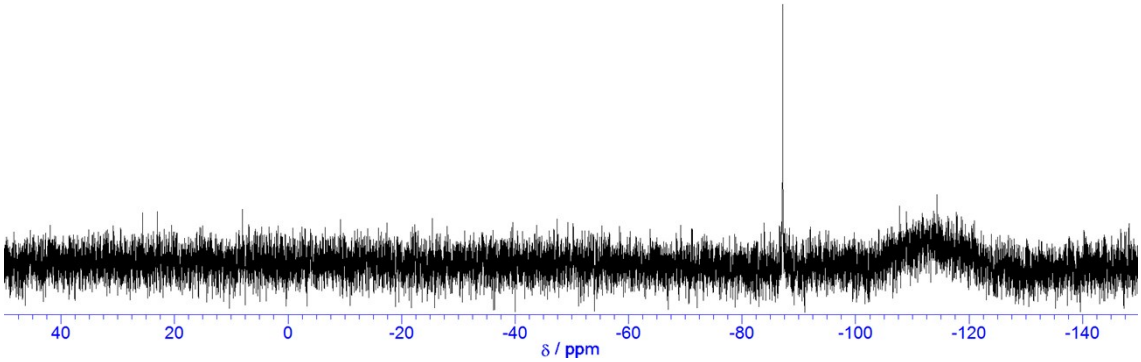

Figure S62. ^{29}Si NMR spectrum of **5a**·6Na (120 MHz, DMSO-d_6).

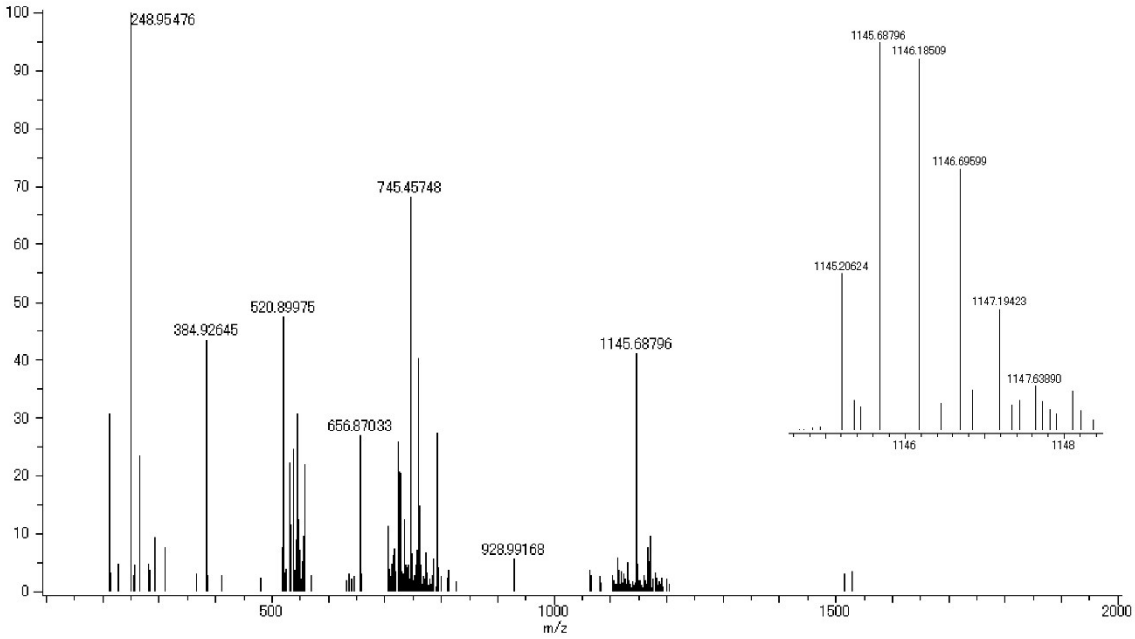

Figure S63. ESI-MS spectrum of **5a**·6Na (MeOH).

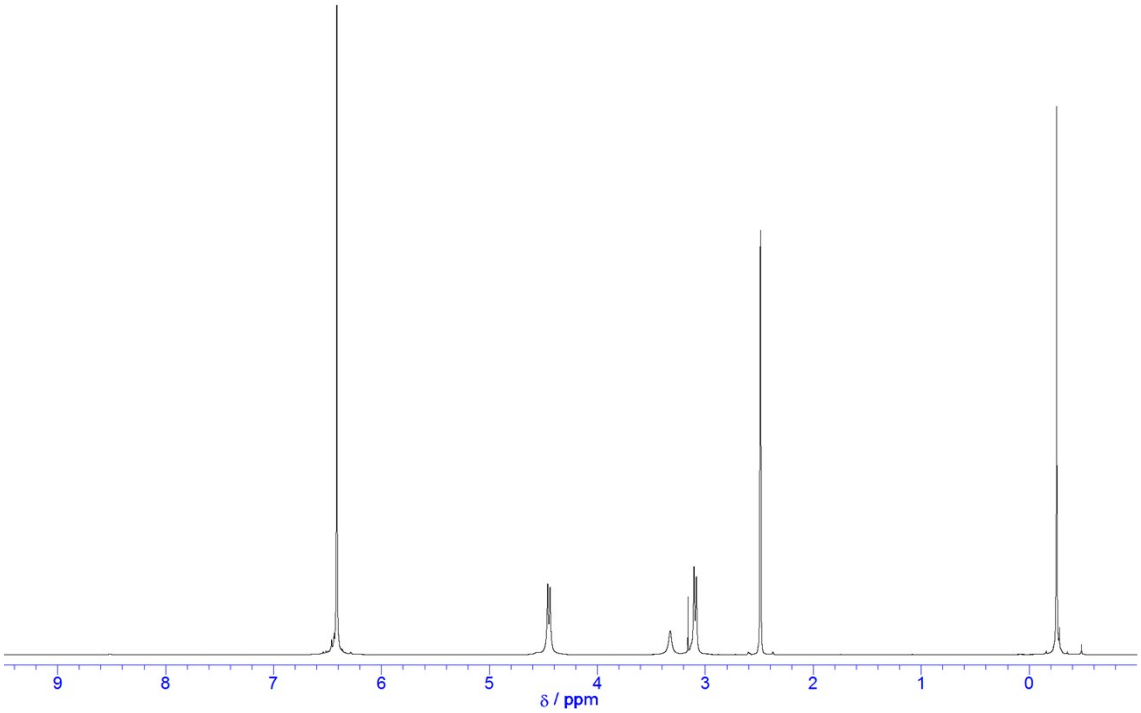

Figure S64. ^{1}H NMR spectrum of **5c**·6Na (600 MHz, DMSO-d_6).

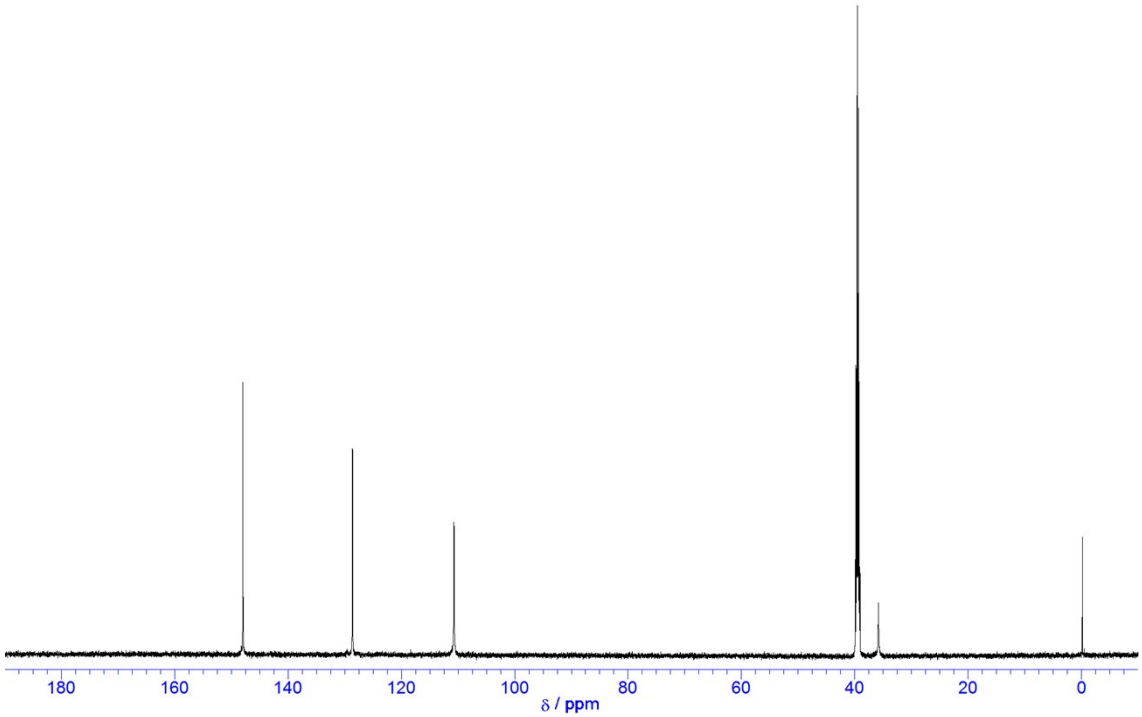

Figure S65. ^{13}C NMR spectrum of **5c**·6Na (150 MHz, DMSO-d_6).

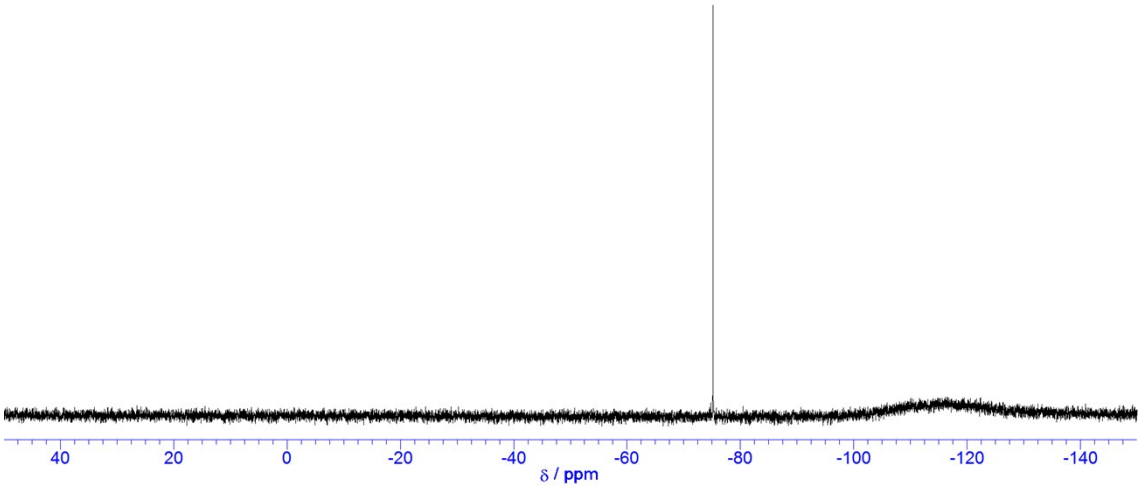

Figure S66. ^{29}Si NMR spectrum of **5c**·6Na (120 MHz, DMSO-d_6).

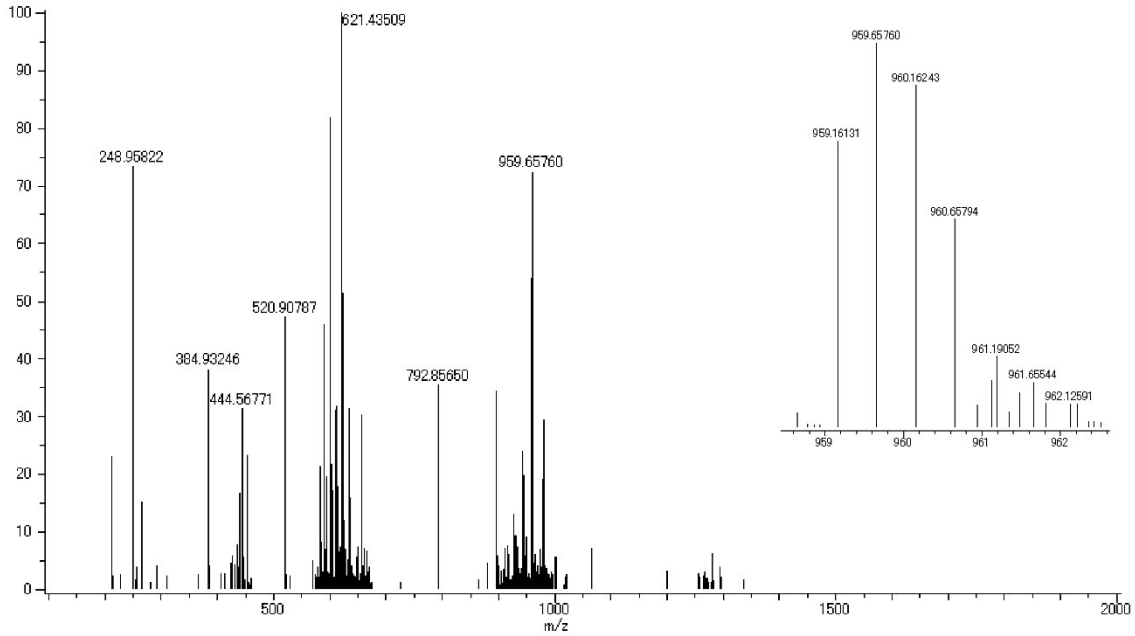

Figure S67. ESI-MS spectrum of **5c**·6Na (MeOH).

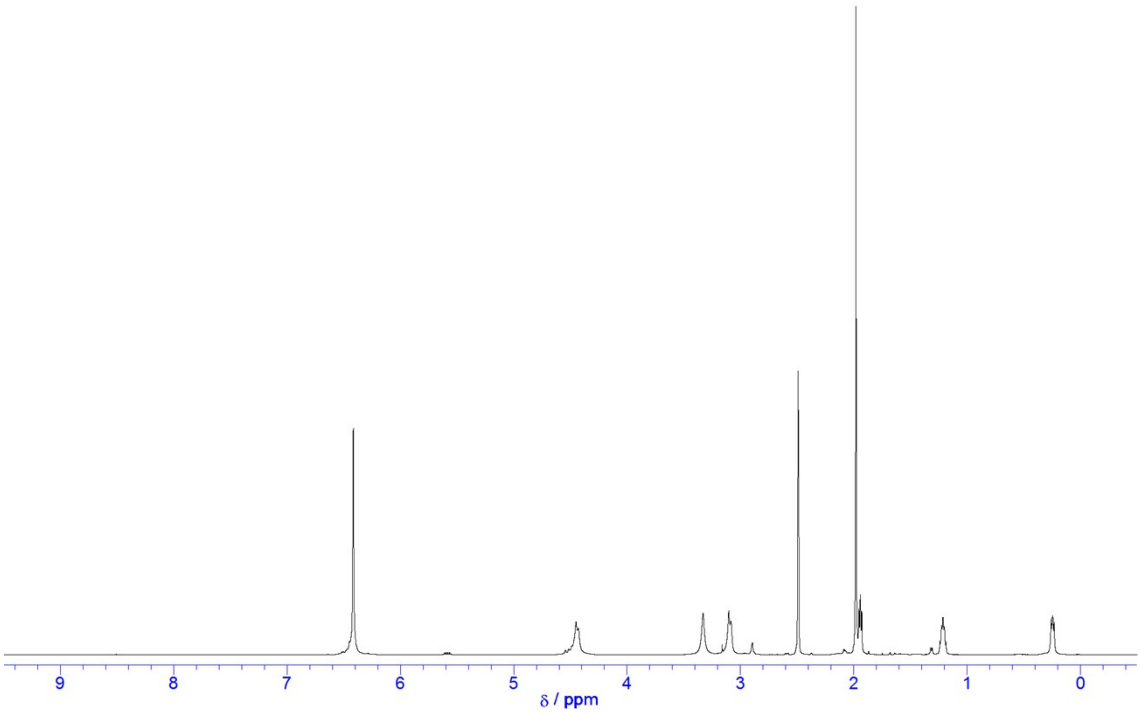

Figure S68. ^{1}H NMR spectrum of **5f**·6Na (600 MHz, DMSO-d_6).

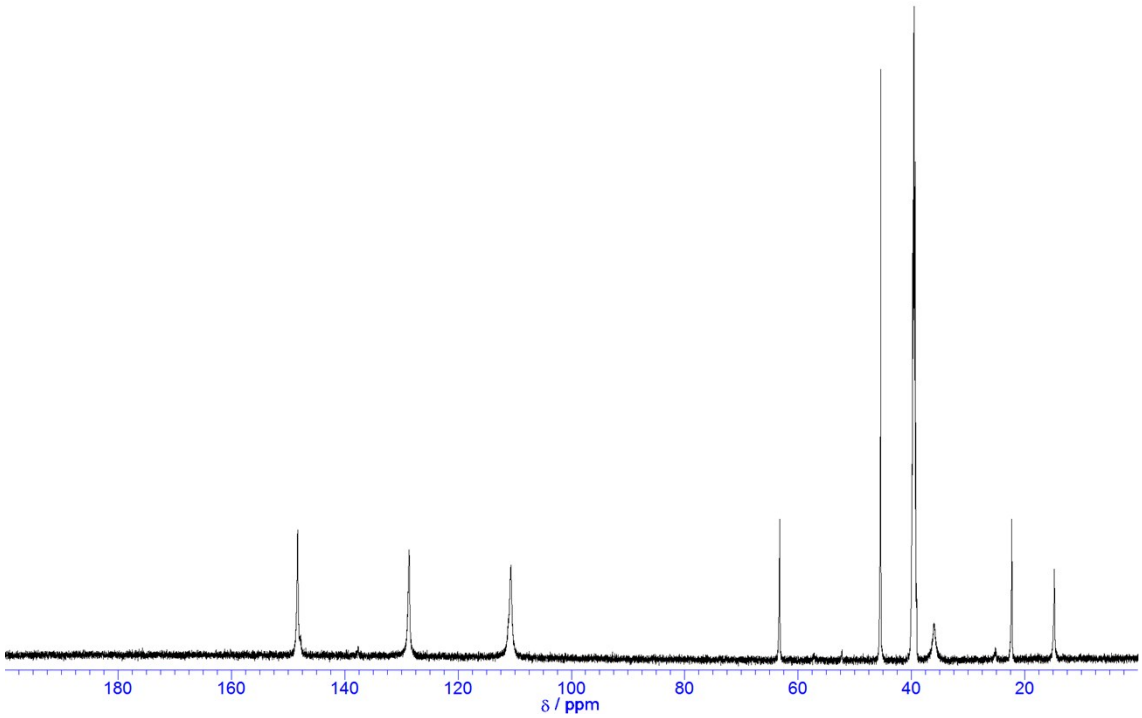

Figure S69. ^{13}C NMR spectrum of **5f**·6Na (150 MHz, DMSO-d_6).

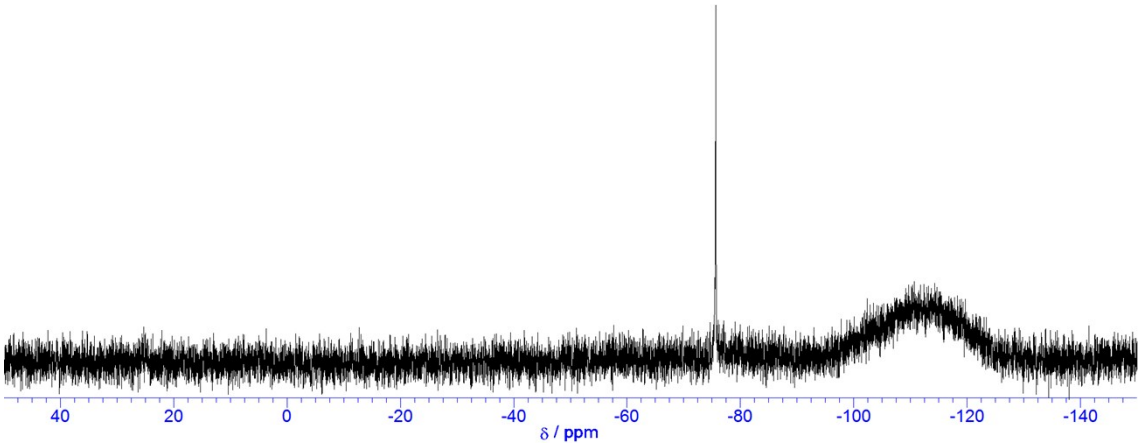

Figure S70. ^{29}Si NMR spectrum of **5f**·6Na (120 MHz, DMSO-d_6).

2.3. Structual assignment and spectral data of **5a**·6R_4N (R_4N = Me_4N, Et_4N, MePy and BuPy)

The cation exchange of **5a**·6$HNEt_3$ with Me_4NCl, Et_4NCl, MePyI and BuPyCl resulted in the formation of **5a**·6Me_4N, **5a**·6Et_4N, **5a**·6MePy and **5a**·6BuPy respectively. These cation-exchanged nanocages were fully characterized by ^{1}H, ^{13}C, and ^{29}Si NMR as well as ESI-mass spectroscopy (Figure S71-S86).

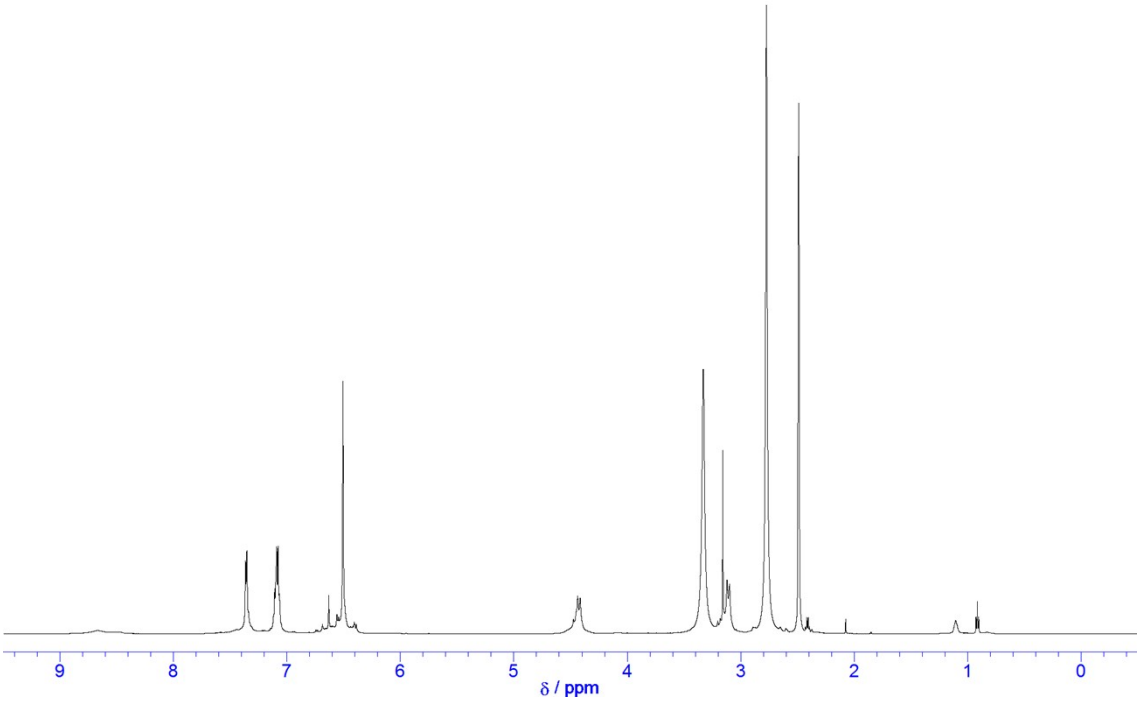

Figure S71. ^{1}H NMR spectrum of **5a**·6 Me_4N (600 MHz, DMSO-d_6).

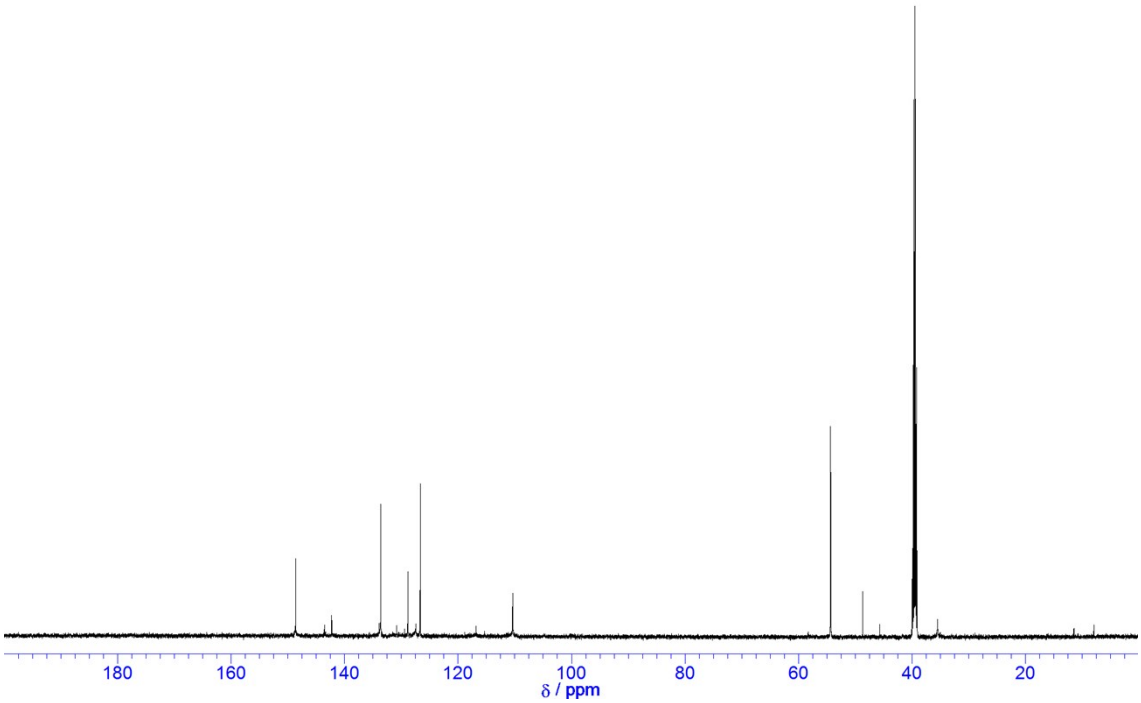

Figure S72. ^{13}C NMR spectrum of **5a**·6 Me_4N (150 MHz, DMSO-d_6).

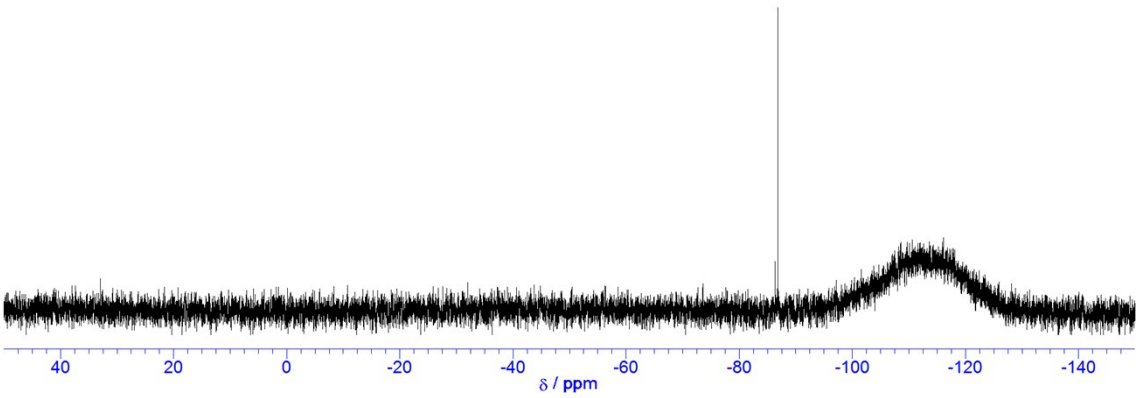

Figure S73. ^{29}Si NMR spectrum of **5a**·6 Me_4N (120 MHz, DMSO-d_6).

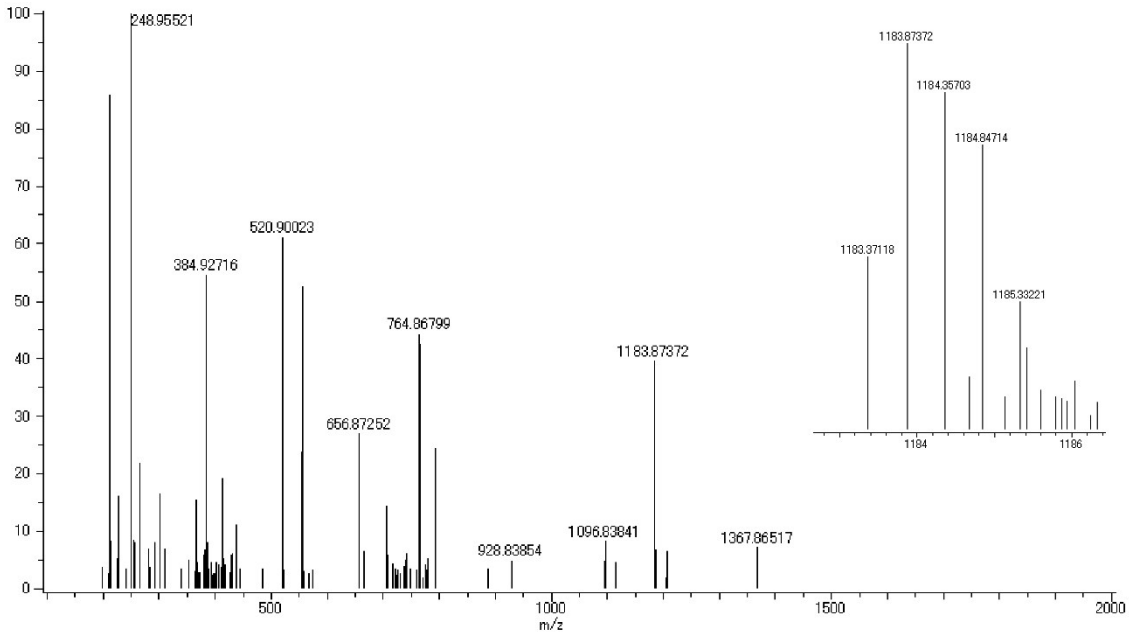

Figure S74. ESI-MS spectrum of **5a**·6Me_4N (MeOH).

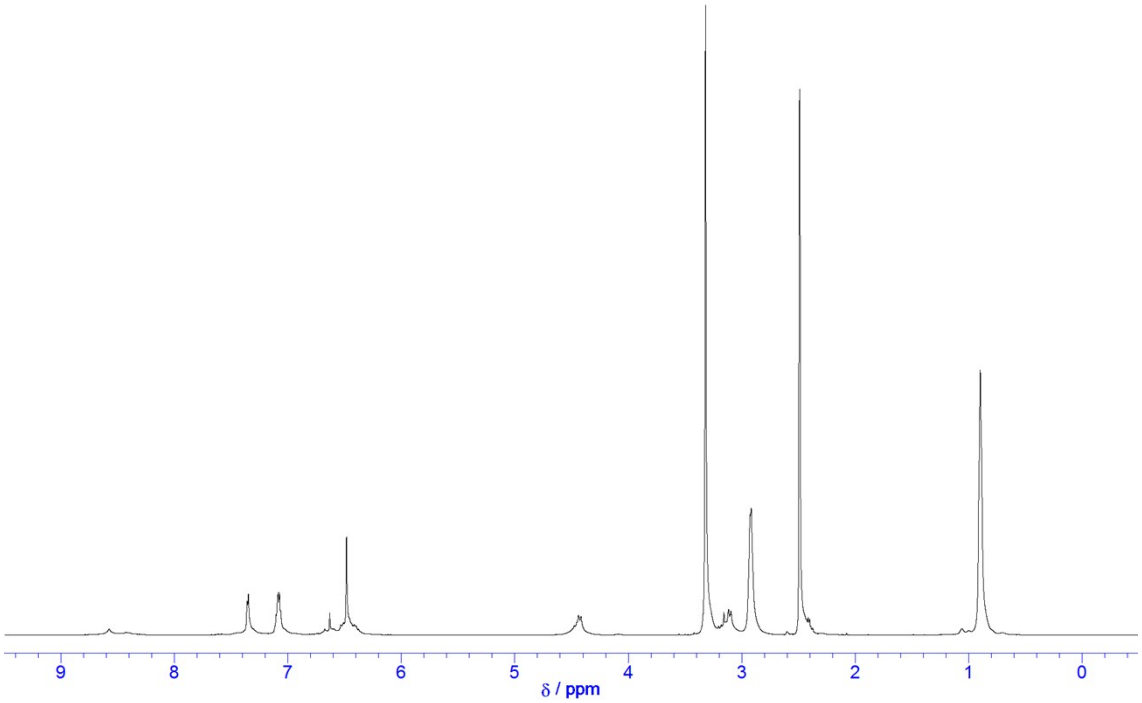

Figure S75. ^{1}H NMR spectrum of **5a**·6Et_4N (600 MHz, DMSO-d_6).

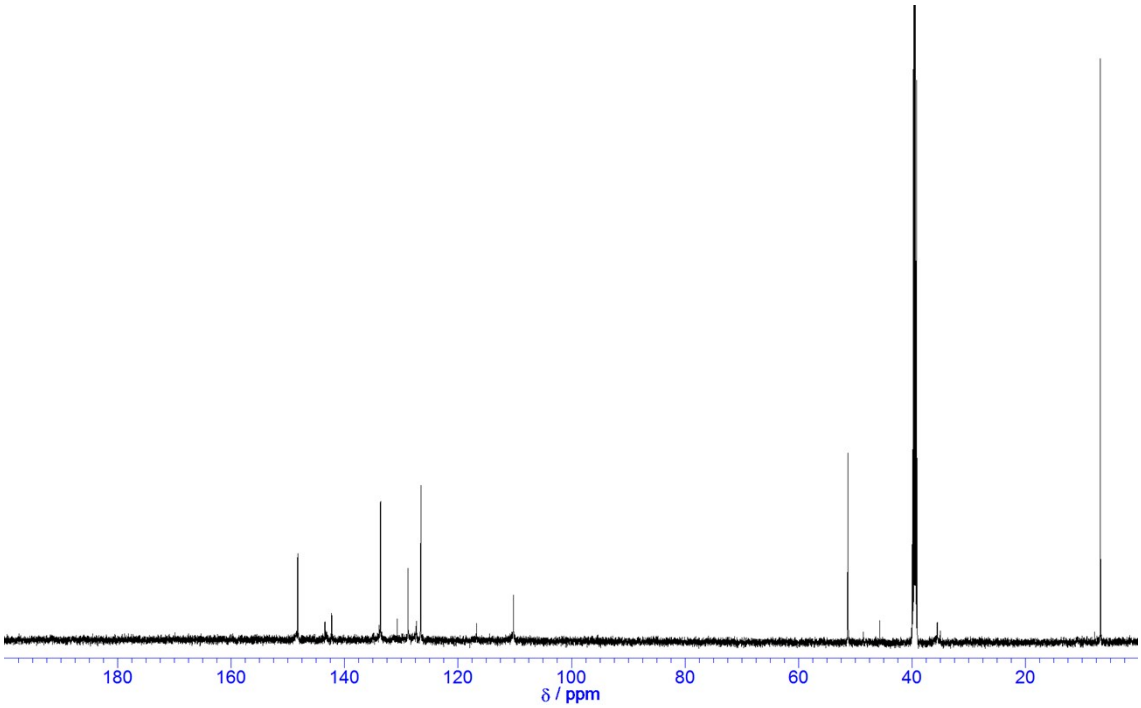

Figure S76. ^{13}C NMR spectrum of **5a**·6Et_4N (150 MHz, DMSO-d_6).

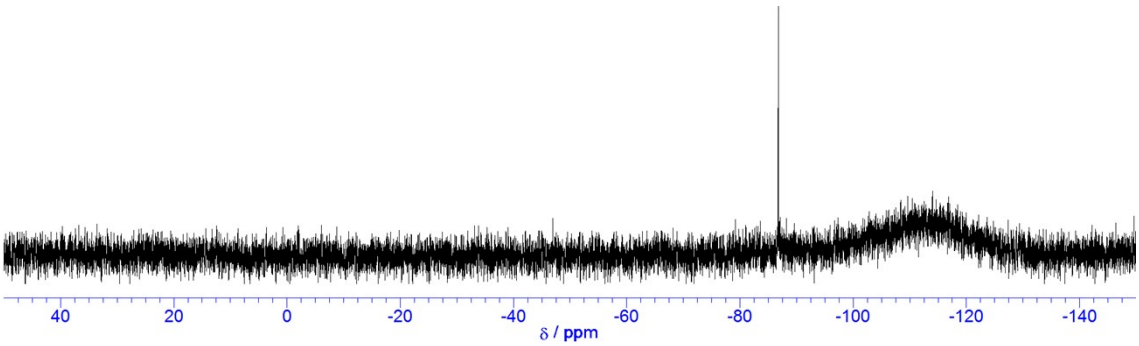

Figure S77. ^{29}Si NMR spectrum of **5a**·6Et_4N (120 MHz, DMSO-d_6).

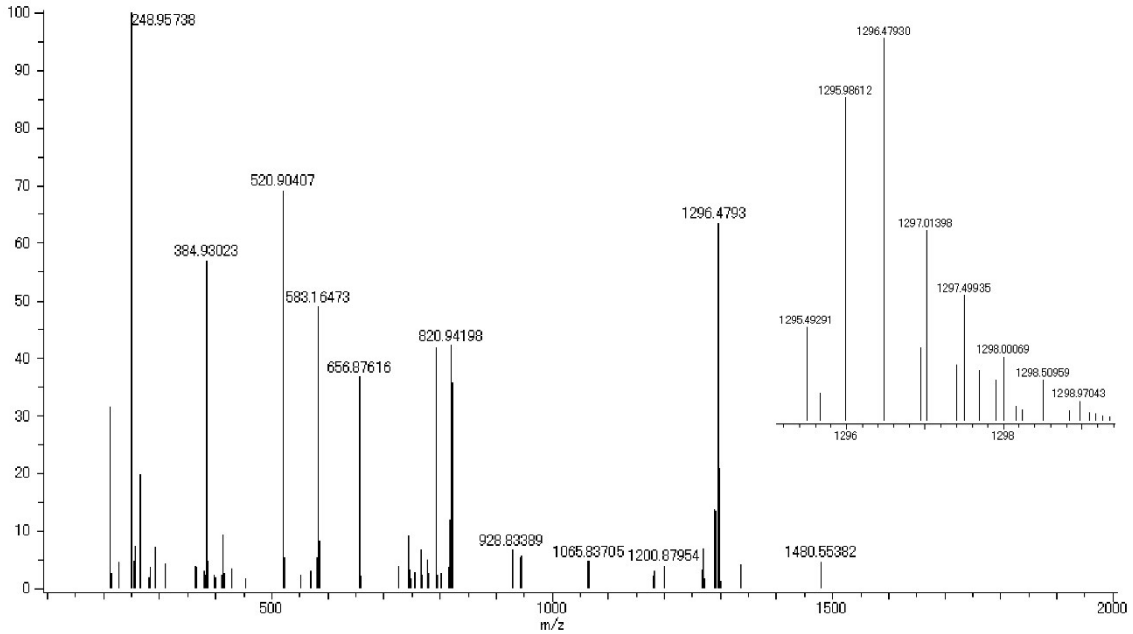

Figure S78. ESI-MS spectrum of **5a**·6Et$_4$N (MeOH).

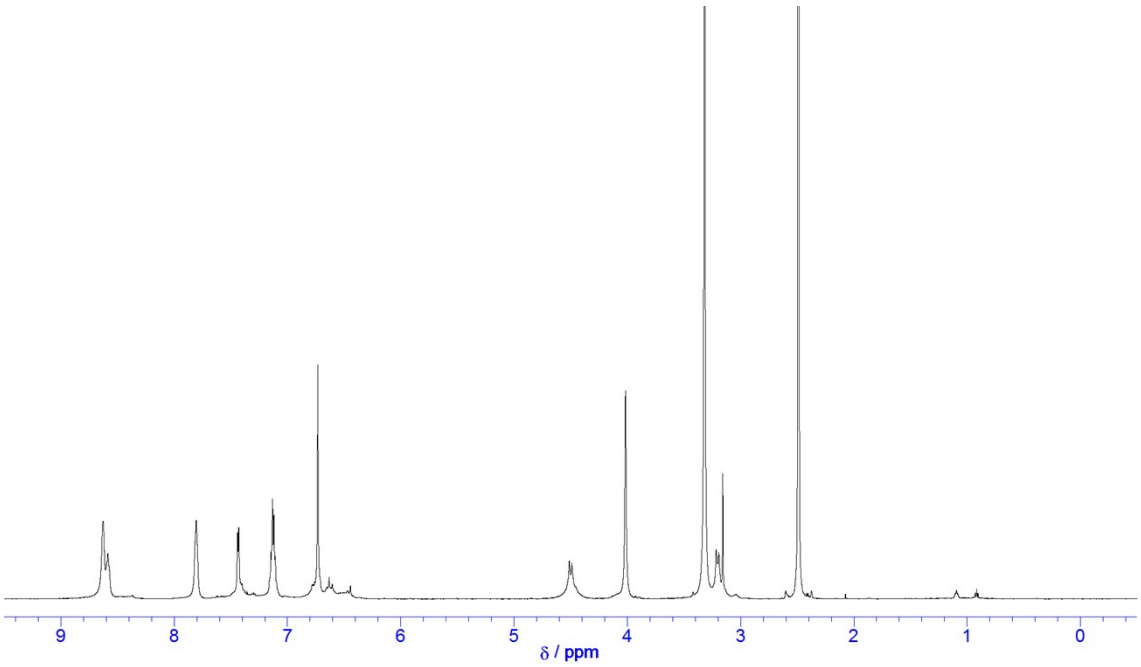

Figure S79. ^{1}H NMR spectrum of **5a**·6MePy (600 MHz, DMSO-d_6).

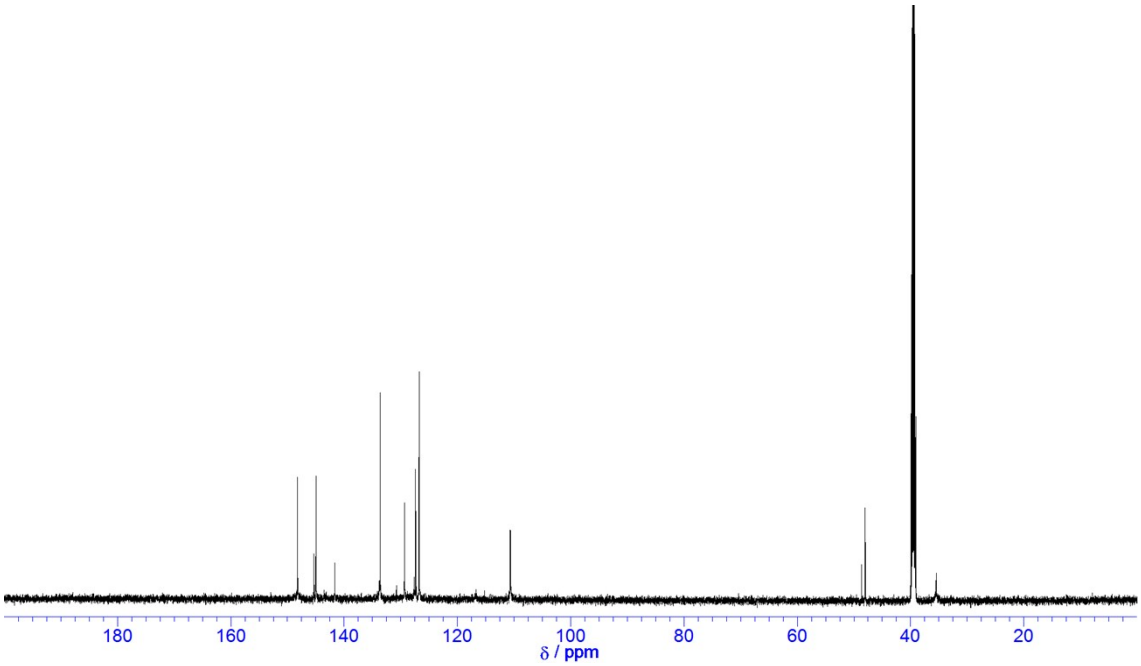

Figure S80. ^{13}C NMR spectrum of **5a**·6MePy (150 MHz, DMSO-d_6).

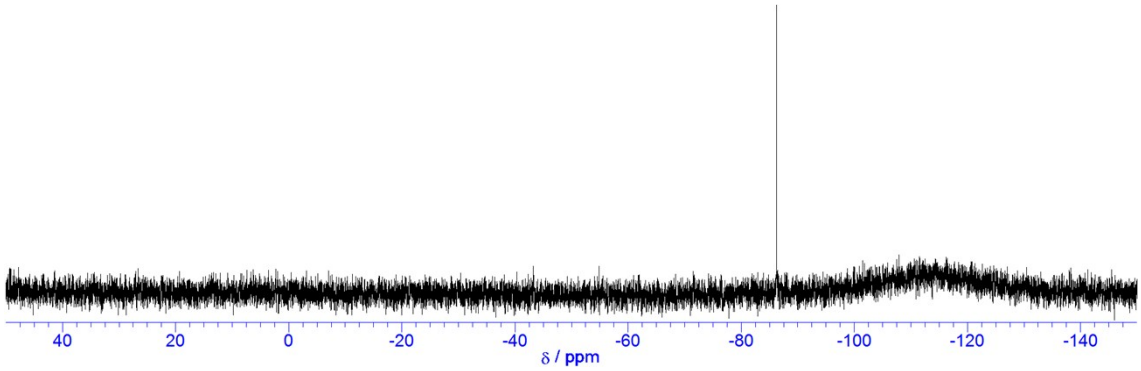

Figure S81. ^{29}Si NMR spectrum of **5a**·6MePy (120 MHz, DMSO-d_6).

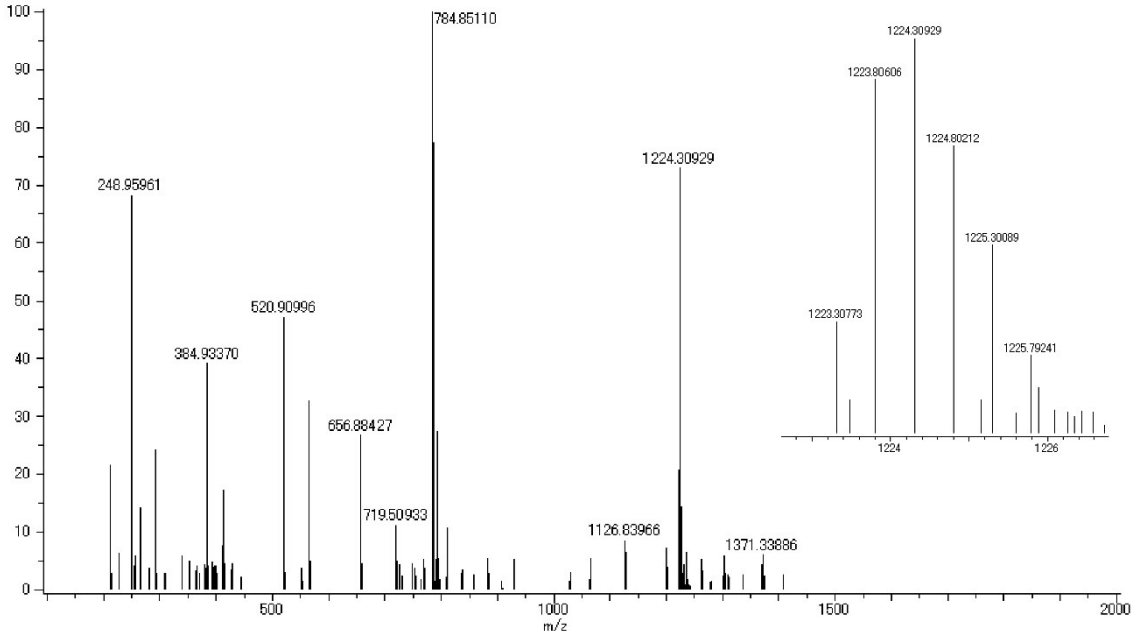

Figure S82. ESI-MS spectrum of **5a**·6MePy (MeOH).

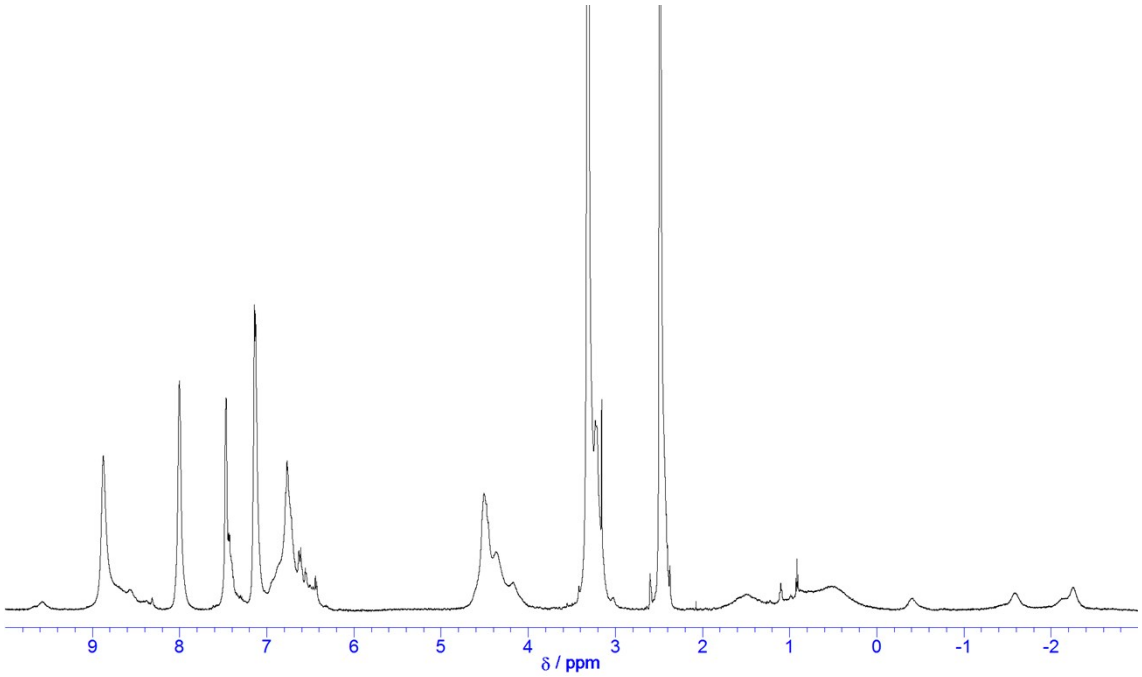

Figure S83. ^{1}H NMR spectrum of **5a**·6BuPy (600 MHz, DMSO-d_6).

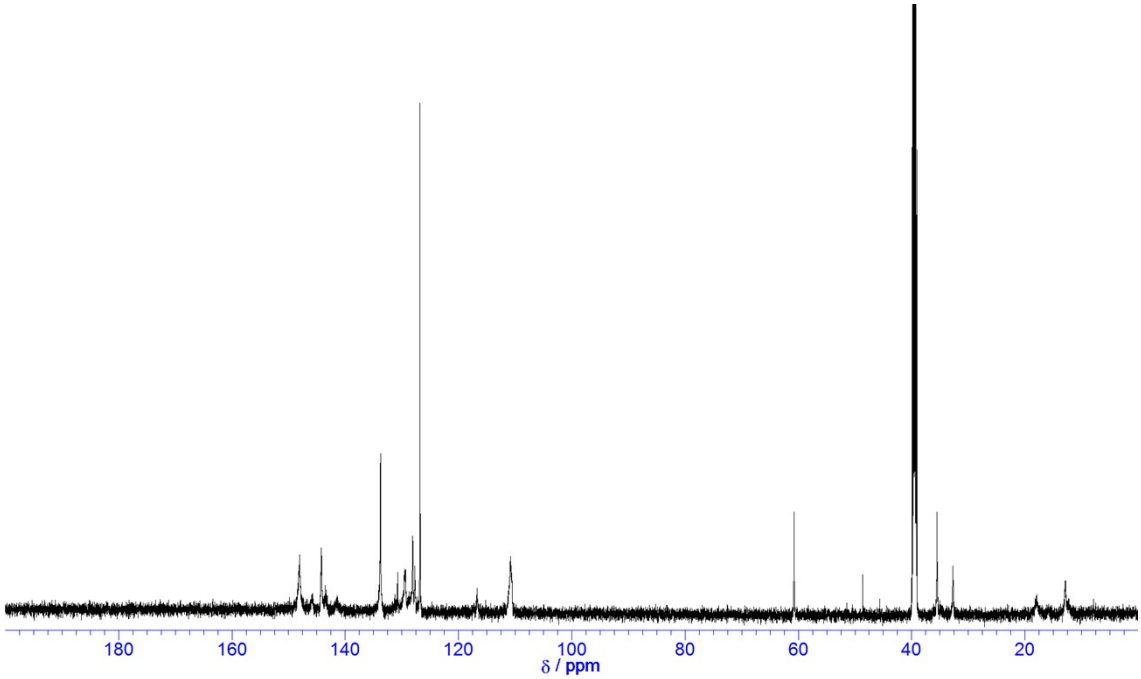

Figure S84. ^{13}C NMR spectrum of **5a**·6BuPy (150 MHz, DMSO-d_6).

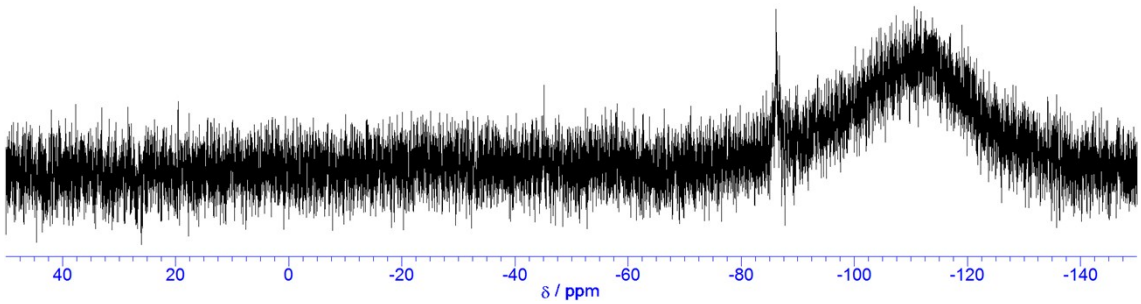

Figure S85. ^{29}Si NMR spectrum of **5a**·6BuPy (120 MHz, DMSO-d_6).

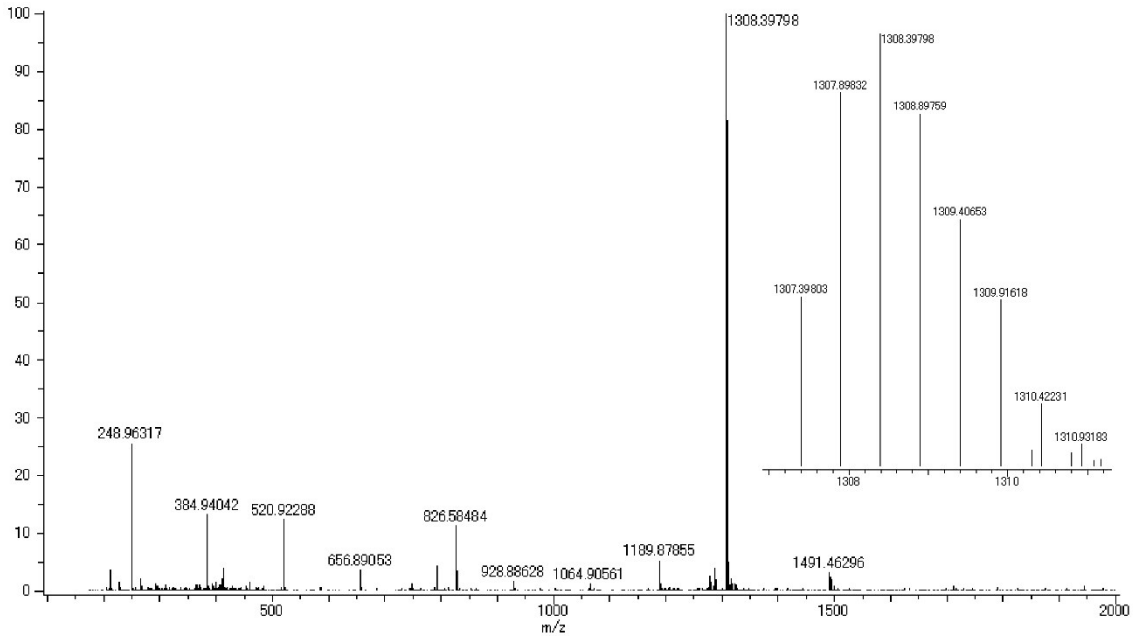

Figure S86. ESI-MS spectrum of **5a**·6BuPy (MeOH).

3. Crystallographic data

Single crystals of **4a**·4HNEt$_3$·8MeOH, **5a**·6Na·7THF·2DMF·2C$_6$H$_6$·23H$_2$O, and **8**@**4a**·14DMSO ·5H$_2$O suitable for X-ray diffraction analysis were mounted on a Rigaku VariMax with Saturn CCD diffractometer equipped with a Mo-K$_\alpha$ (graphite monochromated, λ = 0.71073) radiation. Crystal data and data statistics are summarized in Table S1. The structures were solved by direct methods (SHELXS-97 [8)] and SIR 2004 [9)]) using WinGX v1.70.01 as interface.[10)] The non-hydrogen atoms were refined anisotropically by the full-matrix least-square method (SHELXL-97).[8)] Hydrogen atoms were placed at calculated positions and kept fixed. In a subsequent refinement, the function $\Sigma\omega\ (F^2_o - F^2_c)^2$ was minimized, where $|F_o|$ and $|F_c|$ are the observed and calculated structure factor amplitudes, respectively. The agreement indices are defined as $R_1 = \Sigma\ (||F_o|-|F_c||)/\Sigma|F_o|$ and wR_2 = $[\Sigma\omega(F^2_o - F^2_c)^2/\Sigma(\omega F^4_o)]^{1/2}$.

The crystallographic data reported in this manuscript have been deposited with the Cambridge Crystallographic Data Centre as supplementary publication no. CCDC-1892127 for **4a**·4HNEt$_3$·8MeOH, 1892128 for **5a**·6Na·7THF·2DMF·2C$_6$H$_6$·23H$_2$O, and 1892129 for **8**@**4a**·14DMSO·5H$_2$O. Copies of these data can be obtained free of charge via the CCDC Website.

Table S1. Crystal data and data collection parameters of **4a**·4HNEt$_3$·8MeOH, **5a**·6Na·7THF·2DMF·2C$_6$H$_6$·23H$_2$O and **8**@**4a**·14DMSO·5H$_2$O.

	4a·4HNEt$_3$·8MeOH	**5a**·6Na·7THF·2DMF·2C$_6$H$_6$·23H$_2$O	**8**@**4a**·14DMSO·5H$_2$O
Empirical formula	$C_{128}H_{172}N_4O_{24}Si_4$	$C_{166}H_{206}N_2Na_6O_{56}Si_6$	$C_{80}H_{101}N_2O_{17.5}S_7Si_2$
Formula weight	2263.06	3431.81	1651.23
Temperature (K)	120 (2)	120 (2)	120 (2)
Wavelength (Å)	0.71073	0.71073	0.71073
Crystal system	Monoclinic	Monoclinic	Monoclinic
Space group	C2	P21/c	P21/c
a (Å)	43.040 (48)	19.998 (4)	15.993 (7)
b (Å)	9.038 (9)	34.746 (6)	21.486 (9)
c (Å)	20.978 (22)	24.908 (5)	27.205 (11)
α (deg)	90.00	90.00	90.00
β (deg)	114.772 (14)	101.563 (3)	107.14 (2)
γ (deg)	90.00	90.00	90.00
Volume (Å^3)	7409 (14)	16956 (5)	8934 (7)
Z	2	4	4
Density (calculated) (g/cm^3)	1.014	1.344	1.228
Absorption coefficient (mm^{-1})	0.099	0.152	0.266
F (000)	2432	7256	3500
Crystal size (mm)	0.38×0.31×0.16	0.18×0.16×0.12	0.23×0.20×0.10
Crystal color and habit	Colorless, Block	Colorless, Prism	Black, Prism
Solvent system	MeCN/MeOH, MeOH vapor	THF/Benzene	DMSO
Diffractometer	Rigaku Mercury CCD	Rigaku Mercury CCD	Rigaku Mercury CCD
Theta range for Data collection (deg)	3.05 to 27.45	3.05 to 27.45	3.01 to 27.43
Indexes	-55 ≦ h ≦ 55 -8 ≦ k ≦ 11 -27 ≦ l ≦ 25	-25 ≦ h ≦ 22 -45 ≦ k ≦ 44 -32 ≦ l ≦ 32	-20 ≦ h ≦ 20 -27 ≦ k ≦ 27 -35 ≦ l ≦ 35
Reflections collected	21709	188131	128180
Independent reflections	11432 (0.1466)	38521 (0.1104)	20240 (0.1023)

(Rint)			
Completeness to theta (%)	93.6 %	99.4 %	99.3 %
Absorption correction	None	None	None
Solution method	SHELXS-97 (Sheldrick, 2008)	SHELXS-97 (Sheldrick, 2008)	SHELXS-97 (Sheldrick, 2008)
Refinement method	Full-matrix least-squares on F^2 (SHELXS-97)	Full-matrix least-squares on F^2 (SHELXS-97)	Full-matrix least-squares on F^2 (SHELXS-97)
Data / restraints / parameters	11432 / 31 / 698	38521 / 77 / 2608	20240 / 6 / 1106
Goodness of Fit Indicator	1.345	1.082	1.784
Final R indices [I>2sigma(I)]	R1 = 0.1748, wR2 = 0.4365	R1 = 0.0964, wR2 = 0.2547	R1 = 0.1894, wR2 = 0.4934
R indices (all data)	R1 = 0.2062, wR2 = 0.4671	R1 = 0.1253, wR2 = 0.2819	R1 = 0.2191, wR2 = 0.5169
Largest diff peak and hole ($eÅ^{-3}$)	1.069 and -0.473	0.733 and -0.622	0.995 and -0.876

The X-ray crystal structure of **4a**·4HNEt$_3$·8MeOH showed an anionic macrocycle stack on top of one another cemented by ammonium cations to produce a tubular aggregate structure. Pyridinium cations were encapsulated inside the anionic macrocycle in **8**@**4a**·14DMSO·5H$_2$O, whereas the windows of the tetrahedral cage were closed outside by Na(H$_2$O)$_6^+$ in **5a**·6Na·7THF·2DMF·2C$_6$H$_6$·23H$_2$O, based on X-ray crystallographic analysis.

4. MeCN-promoted DCC conditions for the formation of 4a, 5a and 6a

In order to simulate the formation of macrocycle **4a** and nanocage **5a**, oligomers were grown in a stepwise fashion to generate key intermediates **A-1**-**A-3** and **B-1**, **B-2** as shown in Scheme S1 and S3. Once intermediates **A-1** and **B-1** are formed, they can cyclize into **4a** and **5a** respectively. Conformer **A-1** leads to **4a**, which can give rise to a tubular aggregate together with ammonium cations and/or template molecules and precipitate from the reaction mixture as the main product. In contrast, conformers **A-2** and **A-3** are assumed to lead to the formation of polymers. At this stage, MeCN can promote the conformational conversion among **A-1**, **A-2**, and **A-3** by accelerating the bond exchange equilibrium and pseudo-rotation (Scheme S2).

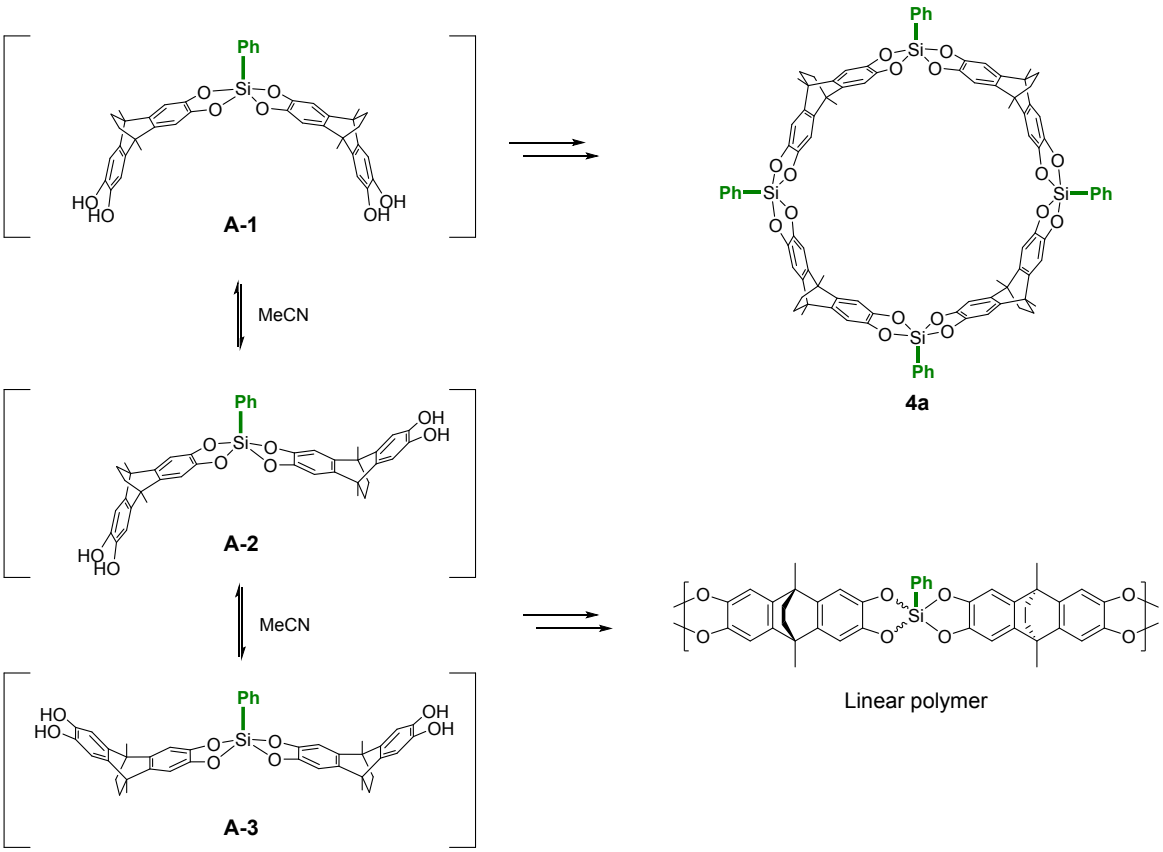

Scheme S1

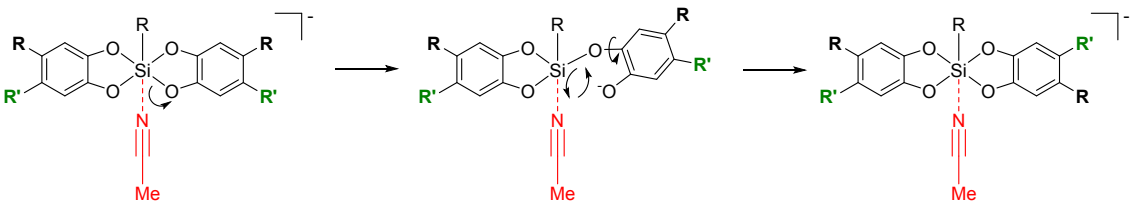

Scheme S2

Similarly, conformer **B-1** leads to the formation of nanocage **5a**, while **B-2** results in the formation of **6a**. Addition of MeCN as well as heating induces the conformational conversion between **B-1** and **B-2**, thus yielding **5a** as the exclusive product. In particular, although the time course NMR experiment of $PhSi(OMe)_3$ (**1a**) and EAT (**2**) was unsuccessful due to the precipitation of **4a**, that of **1a** and CTC (**3**) provided data to support that the first equilibrium can be reached with MeCN (see Figure S87-S90).

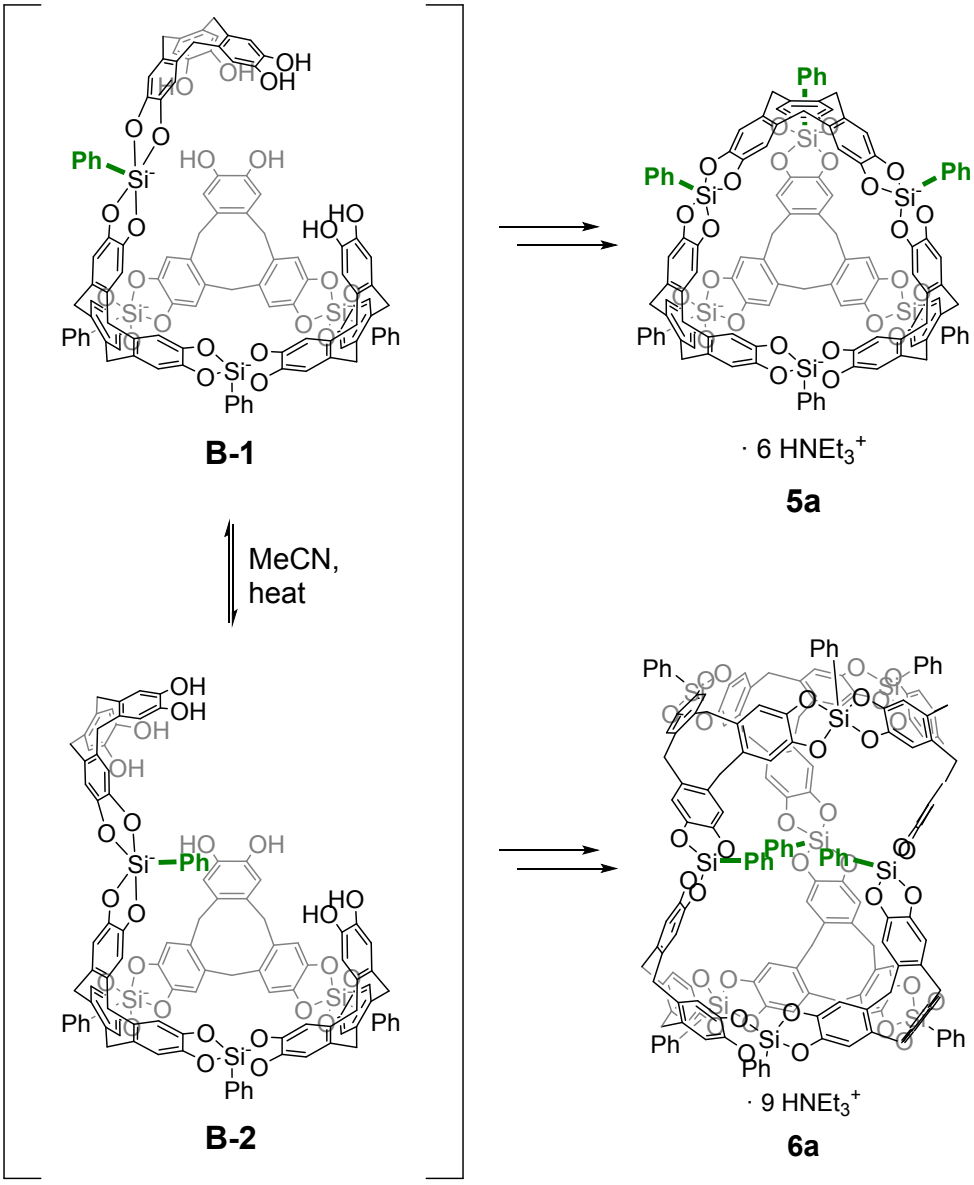

Scheme S3

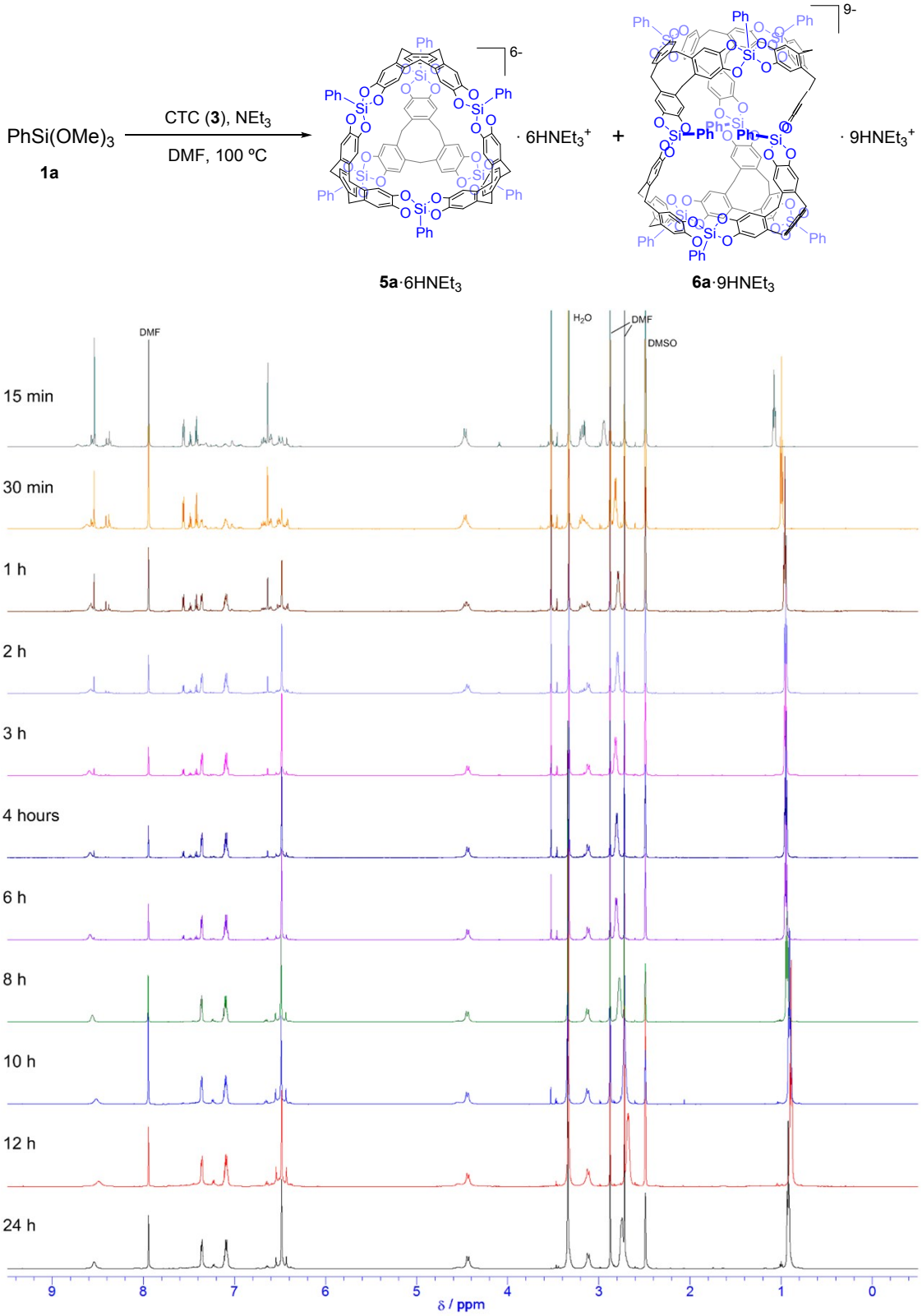

FigureS87. ^{1}H NMR spectra of the reaction mixture consisting of $PhSi(OMe)_3$ (**1a**), triscatechol (**3**), and NEt_3 without MeCN in DMF at 100 ºC (600 MHz, DMSO-d_6).

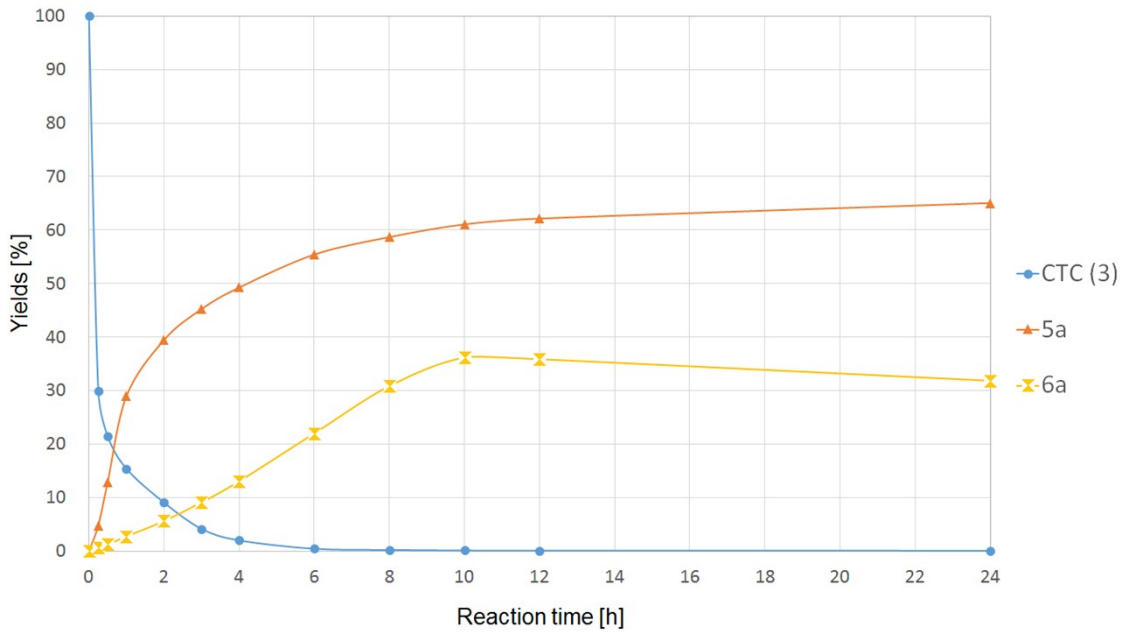

FigureS88. Time course of the reaction of $PhSi(OMe)_3$ (**1a**), triscatechol (**3**) and NEt_3 without MeCN in DMF at 100 ºC.

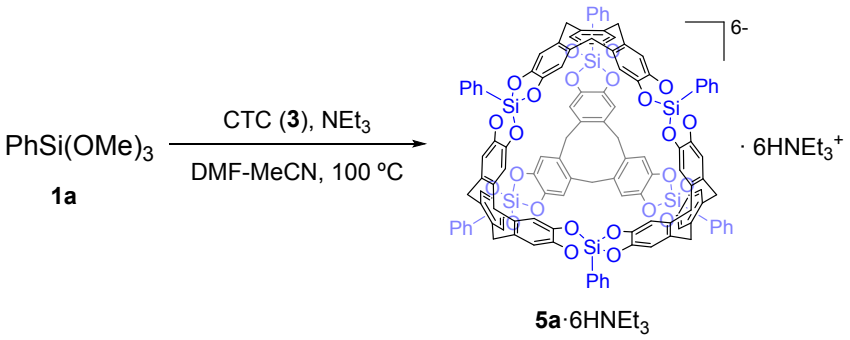

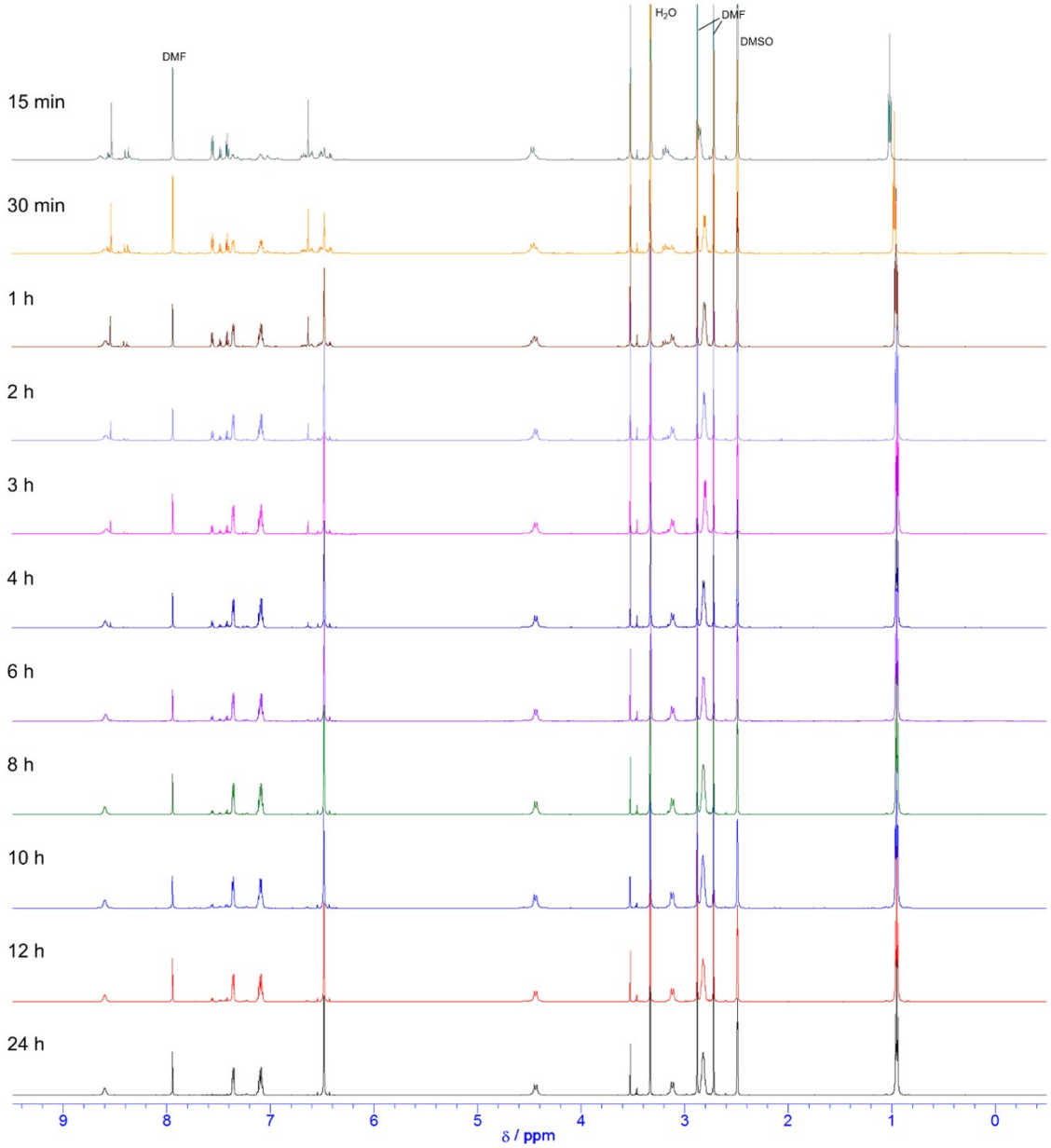

Figure S89. ^{1}H NMR spectra of the reaction mixture consisting of PhSi(OMe)$_3$ (**1a**), triscatechol (**3**), and NEt$_3$ with MeCN in DMF at 100 ºC (600 MHz, DMSO-d_6).

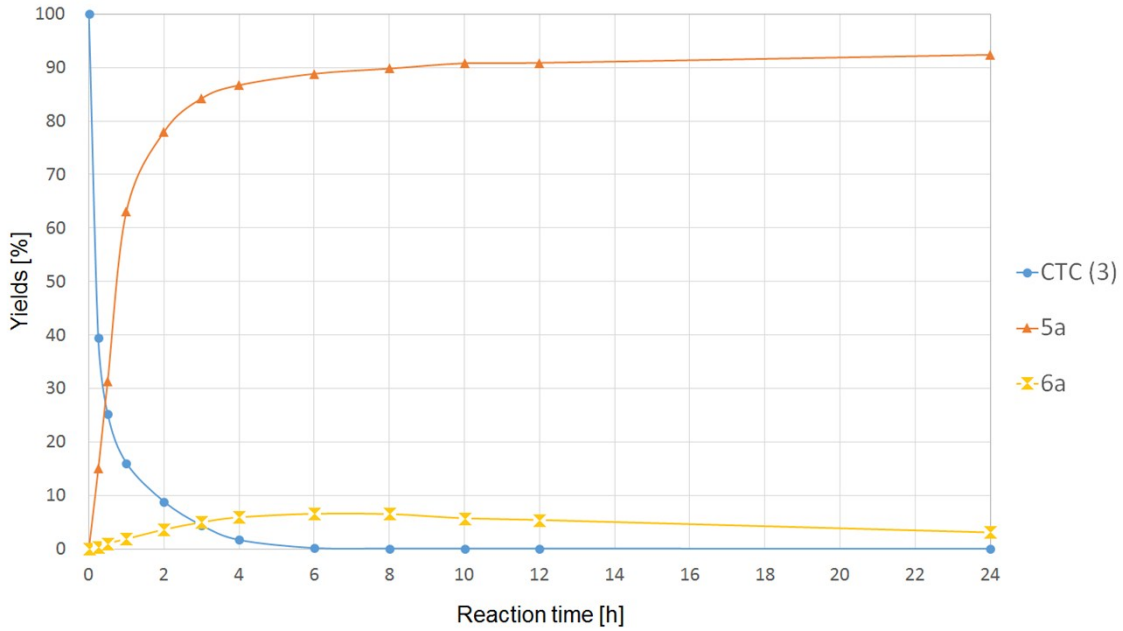

FigureS90. Time course of the reaction of $PhSi(OMe)_3$ (**1a**), triscatechol (**3**) and NEt_3 with MeCN in DMF at 100 ºC.

In order to datermine the temperature and solvent effects on the yields of **5a** and **6a**, the following reactions were performed.

Cyclotricatechylene (CTC) (**3**) (2.00 mmol, 0.733 g), $PhSi(OMe)_3$ (3.30 mmol, 0.614 g, 0.616 mL) and Et_3N (9.00 mmol, 0.911 g, 1.25 mL) were dissolved in a solvent (THF, THF/MeCN (3:1), THF/MeCN/MeOH (3:1:1), DMF, and DMF/MeCN (2:1), and the mixture was heated at a temperature lower than 100 ºC. When THF, THF/MeCN (3:1), and THF/MeCN/MeOH (3:1:1) were used as solvent, various oligomeric intermediates precipitated after several hours (Figure S91). In contrast, when the reaction was conducted in DMF or DMF/MeCN (2:1), a homogeneous solution was obtained. In these cases, the formation of **5a** and **6a** within the reaction mixture was monitored by ^{1}H NMR, as shown in Figure S92 and S93. The isolation of **5a** and **6a** was carried out as described above (section 1.10), followed by removal of the solvent under reduced pressure. Table S2 shows the reaction conditions and isolated yields of **5a** and **6a**. Upon a closer inspection of Table S2, it can be seen that the usage of MeCN and higher reaction temperatures increased the yield of **5a** compared to that of **6a**.

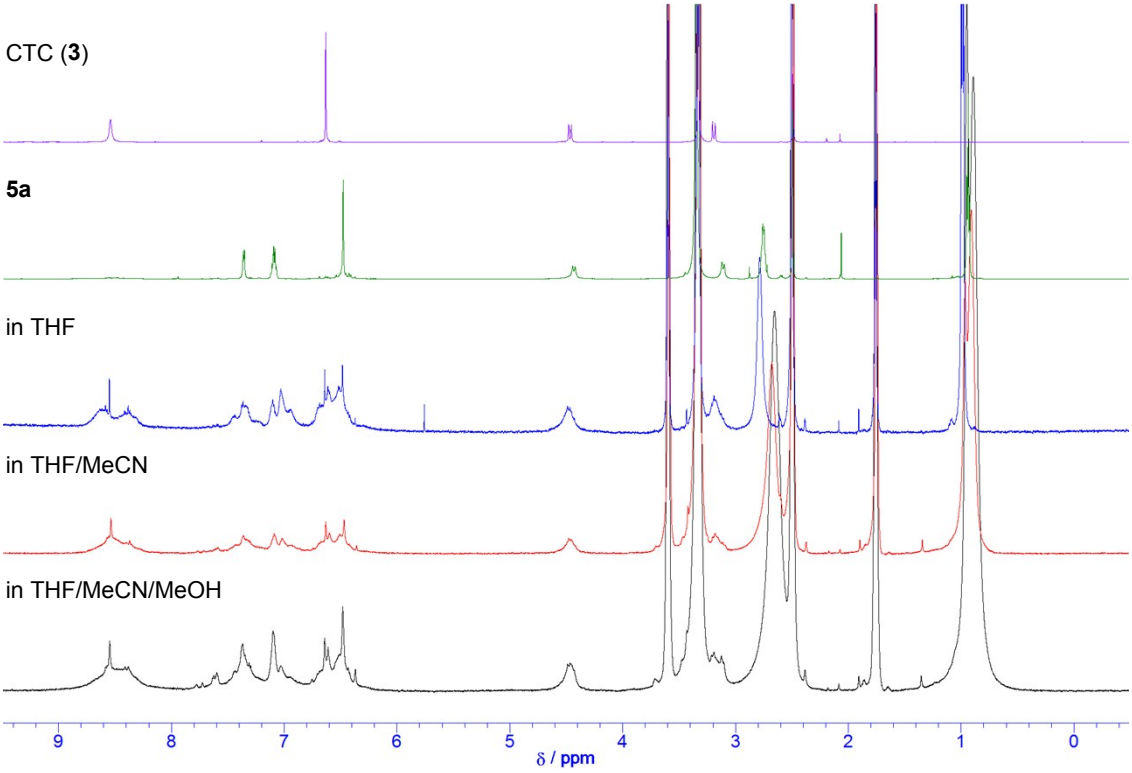

Figure S91. ^{1}H NMR spectra of the precipitates obtained from the reaction mixtures of $PhSi(OMe)_3$, CTC, and Et_3N in THF, THF/MeCN (3:1), and THF/MeCN/MeOH (3:1:1) under reflux (600 MHz, DMSO-d_6).

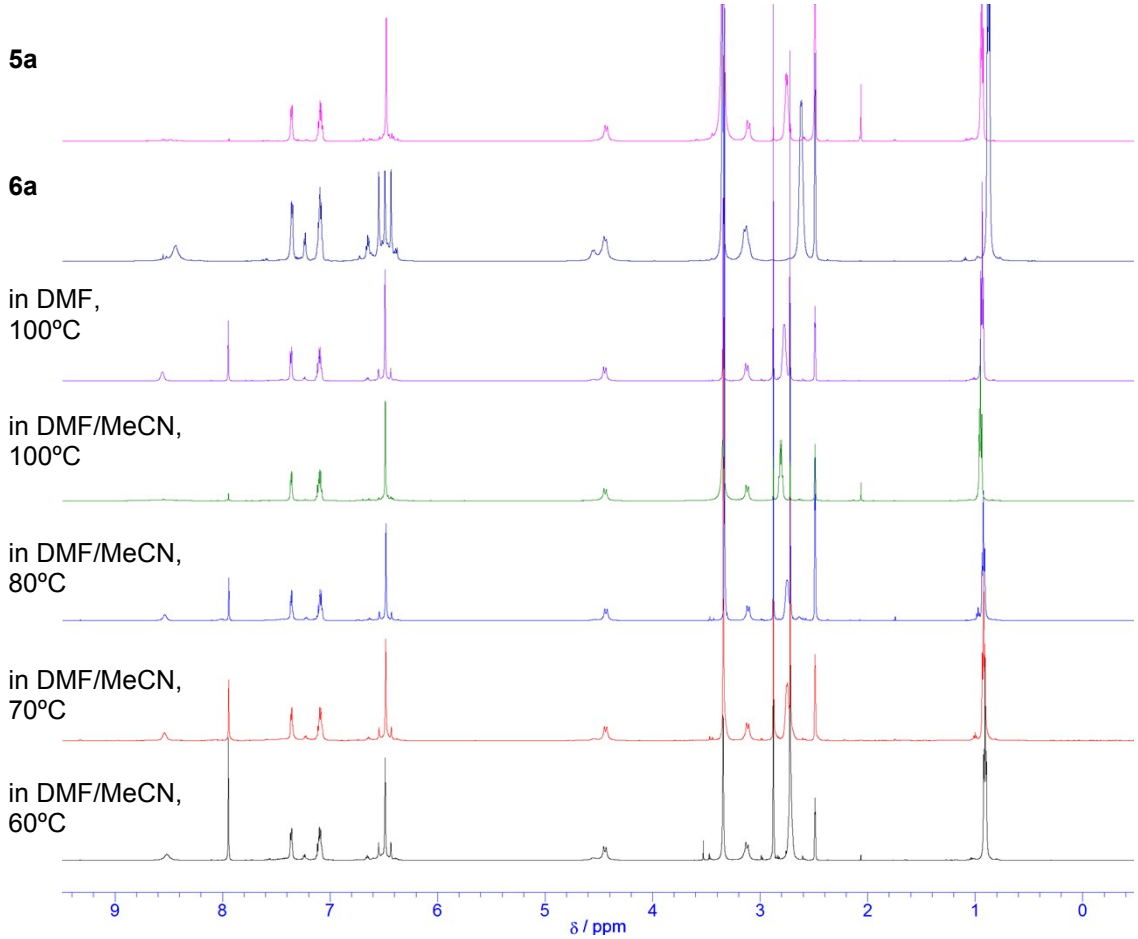

Figure S92. ^{1}H NMR spectra of the reaction mixtures of $PhSi(OMe)_3$, CTC and Et_3N in various solvents and temperatures (600 MHz, DMSO-d_6).

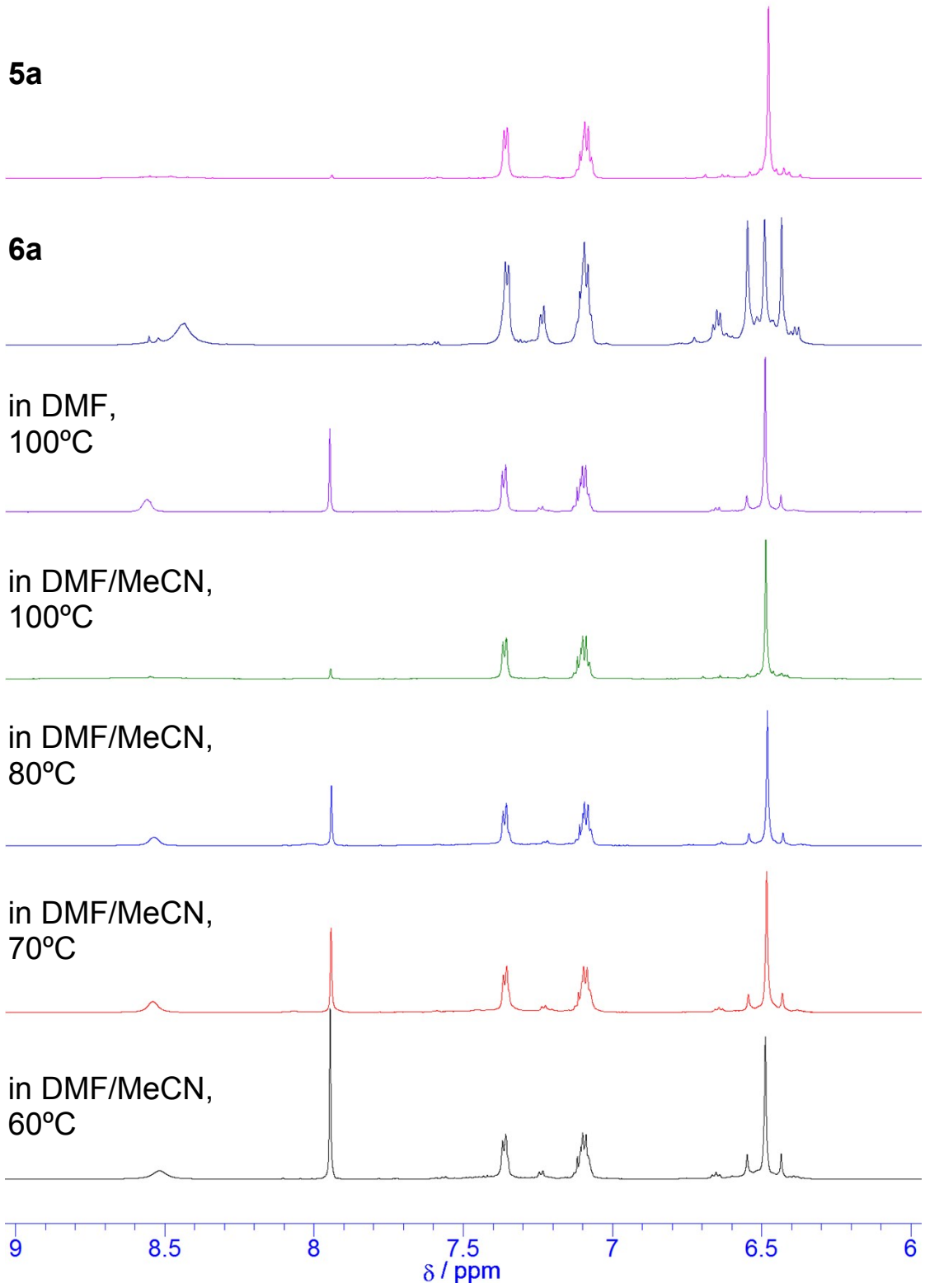

Figure S93. ^{1}H NMR spectra (6-9 ppm range)of the reaction mixtures of $PhSi(OMe)_3$, CTC, and Et_3N in various solvents and at different temperatures (600 MHz, DMSO-d_6).

Table S2. Solvent and temperature-dependent synthesis of silane catecholate nanocage **5a** and **6a**.

solvent	temp. (ºC)	time [a)]	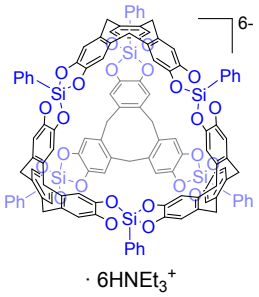 · 6HNEt$_3^+$	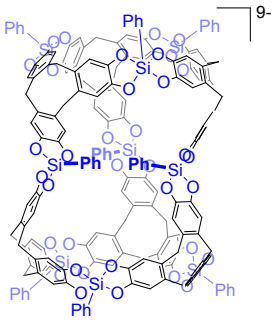 · 9HNEt$_3^+$
			5a ·6HNEt$_3$ [b)]	**6a**·9HNEt$_3$ [b)]
DMF	100	19 h	59.4	36.3
DMF/MeCN (2:1)	100	18 h	94.6	0.0
DMF/MeCN (2:1)	80	2 days	77.4	15.2
DMF/MeCN (2:1)	70	2 days	73.9	20.2
DMF/MeCN (2:1)	60	3 days	55.8	41.1

a) Reaction was performed until complete disappearance of the starting material and intermediates as determined by ^{1}H NMR analysis. b) Yields were calculated based on the starting CTC molecule.

5. ^{1}H NMR titrations

5.1. Titration of **5a**·6HNEt$_3$ with NBu$_4$Cl

Compound **5a**·6HNEt$_3$ (8.06 mg, 3.00 μmol) was dissolved in 6 mL of CD$_3$OD to afford a host solution (3 mM based on HNEt$_3$). NBu$_4$Cl (33.4 mg, 120 μmol) was dissolved in 2 mL of CD$_3$OD to give a guest solution (60 mM). Next, 600 μL of host solution was added to a NMR tube by using a microsyringe, and the corresponding ^{1}H NMR spectrum was recorded. The host solution was titrated by adding 5.00 μL incremental amounts (molar ratio) of the guest solution, as shown in Table S3. Gradual changes in resonance were monitored as shown in Figure S94.

Table S3. Added amounts (molar ratio) of $NBu_4 \cdot Cl$ to **5a**$\cdot 6HNEt_3$ and chemical shift changes of CTC, $HNEt_3^+$, and NBu_4^+ (600 MHz, CD_3OD).

$HNEt_3$: NBu_4	CTC	$HN(\underline{CH_2CH_3})_3^+$		$N(\underline{CH_2CH_2CH_2CH_3})_4^+$			
	ArH	NCH_2	CH_3	NCH_2	CH_2	CH_2	CH_3
$NBu_4 \cdot Cl$				3.239	1.664	1.419	1.030
$(SiPh)_6(CTC)_4 \cdot 6HNEt_3$	6.671	2.802	0.952				
6 : 1	6.664	2.860	1.005	3.136	1.544	1.284	0.827
6 : 2	6.657	2.901	1.042	3.145	1.554	1.287	0.847
6 : 3	6.651	2.933	1.072	3.154	1.562	1.290	0.867
6 : 4	6.648	2.957	1.092	3.162	1.572	1.295	0.890
6 : 5	6.645	2.978	1.110	3.170	1.580	1.307	0.905
6 : 6	6.643	2.996	1.124	3.178	1.593	1.333	0.928

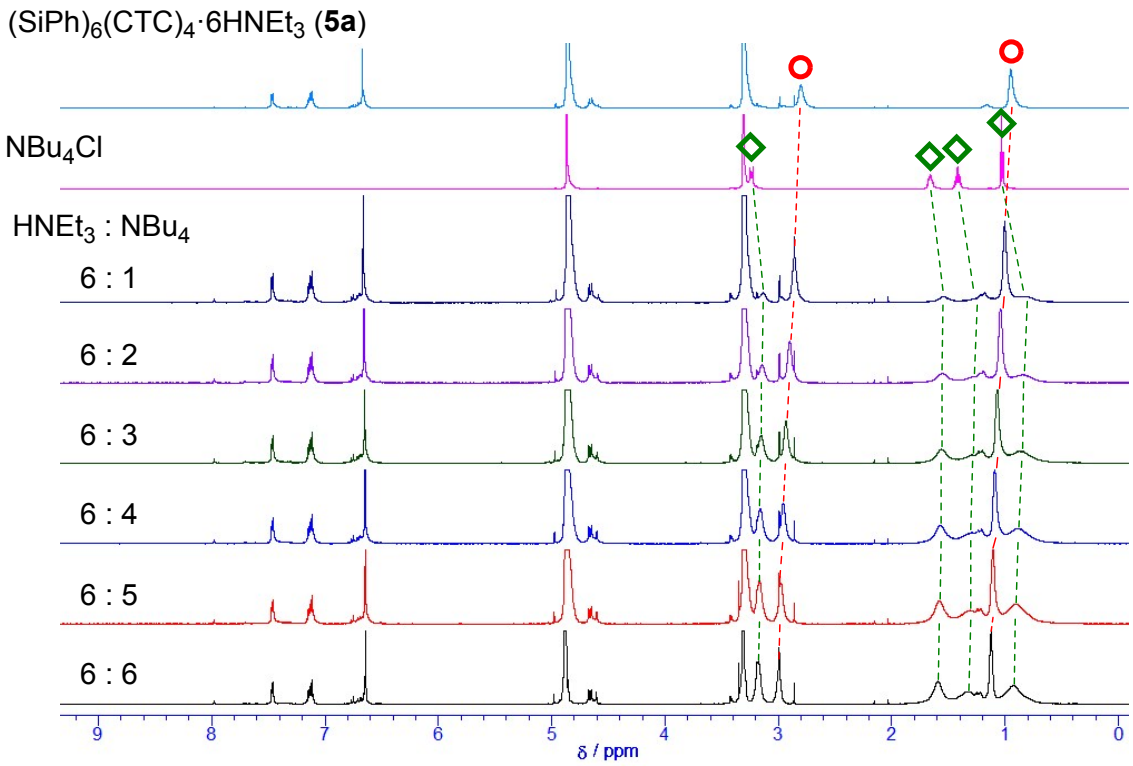

Figure S94. ^1H NMR titration of **5a**$\cdot 6HNEt_3$ with NBu_4Cl; circles indicate $HNEt_3^+$, while rhomboids stand for NBu_4^+ (600 MHz, CD_3OD).

5.2. For the titration of **5a**·6HNEt$_3$ with NEt$_4$Cl

Compound **5a**·6HNEt$_3$ (8.06 mg, 3.00 μmol) was dissolved in 6 mL of CD$_3$OD to afford a host solution (3 mM based on HNEt$_3$). NEt$_4$Cl (19.9 mg, 120 μmol) was dissolved in 2 mL of CD$_3$OD to give a guest solution (60 mM). Next, 600 μL of host solution was added to a NMR tube by using a microsyringe, and the corresponding ^{1}H NMR spectrum was recorded. The host solution was titrated by adding 5.00 μL incremental amounts (molar ratio) of the guest solution, as shown in Table S4. Gradual changes in resonance were monitored as shown in Figure S95.

Table S4. Added amounts (molar ratio) of NEt$_4$·Cl to **5a**·6HNEt$_3$ and chemical shift changes of CTC, HNEt$_3^+$, and NEt$_4^+$ (600 MHz, CD$_3$OD).

HNEt$_3$: NEt$_4$	CTC	HN(CH$_2$CH$_3$)$_3^+$		N(CH$_2$CH$_3$)$_4^+$	
	ArH	NCH$_2$	CH$_3$	NCH$_2$	CH$_3$
NBu$_4$·Cl				3.299	1.293
(SiPh)$_6$(CTC)$_4$ · 6HNEt$_3$	6.671	2.802	0.952		
6 : 1	6.673	2.939	1.063	2.581	0.773
6 : 2	6.672	3.005	1.120	2.745	0.877
6 : 3	6.672	3.043	1.157	2.859	0.953
6 : 4	6.671	3.077	1.186	2.947	1.015
6 : 5	6.670	3.093	1.203	3.002	1.054
6 : 6	6.670	3.108	1.219	3.048	1.088

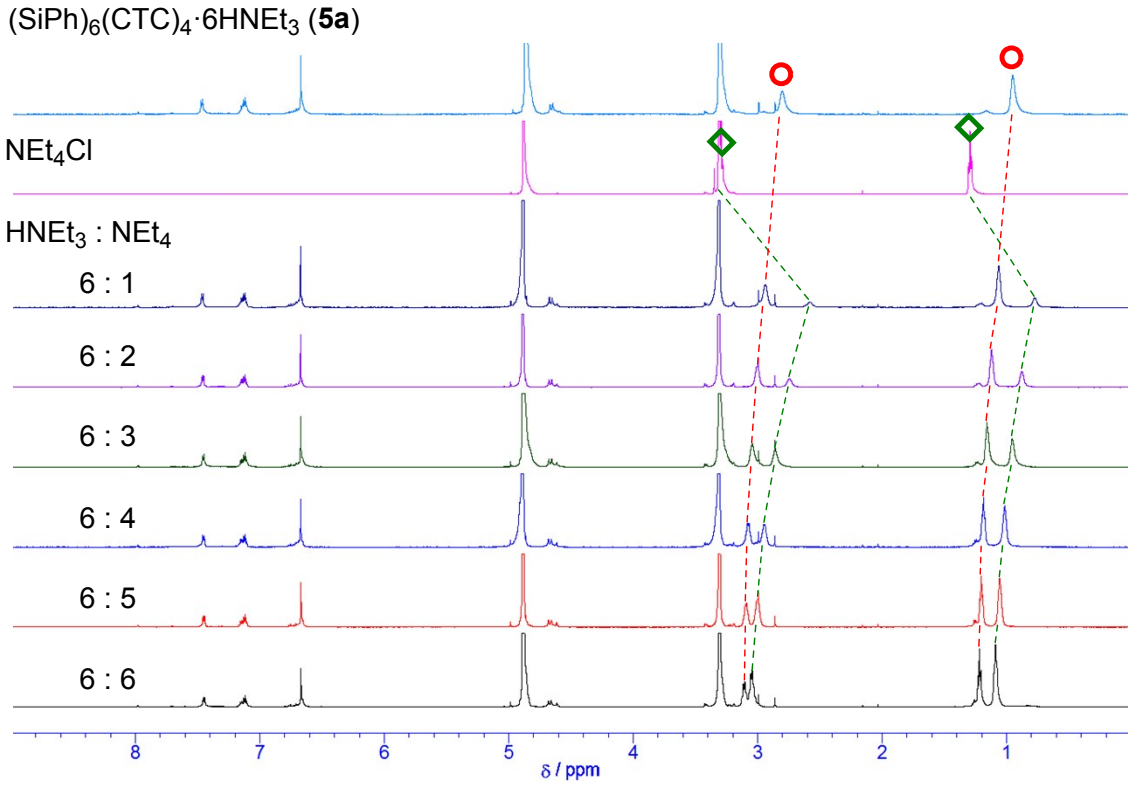

Figure S95. ^{1}H NMR titration of **5a**·6HNEt$_3$ with NEt$_4$Cl; circles indicate HNEt$_3^+$, while rhomboids stand for NEt$_4^+$ (600 MHz, CD$_3$OD).

5.3. For the titration of **5a**·6HNEt$_3$ with MePyI

Compound **5a**·6HNEt$_3$ (26.9 mg, 10.0 μmol) was dissolved in 2 mL of DMSO-d_6 to afford a host solution (30 mM based on HNEt$_3$). MePyI (33.2 mg, 150 μmol) was dissolved in 250 μL of DMSO-d_6 to give a guest solution (600 mM). Next, 600 μL of host solution was added to a NMR tube by using a microsyringe, and the corresponding ^{1}H NMR spectrum was recorded. The host solution was titrated by adding 5.00 μL incremental amounts (molar ratio) of the guest solution, as shown in Table S5. Gradual changes in resonance were monitored as shown in Figure S96.

Table S5. Added amounts (molar ratio) of MePy·I to **5a**·6HNEt$_3$ and chemical shift changes of CTC, HNEt$_3^+$, and MePy$^+$ (600 MHz, DMSO-d_6).

HNEt$_3$: C$_5$H$_5$NMe	CTC	HN(CH$_2$CH$_3$)$_3^+$		C$_5$H$_5$NCH$_3^+$	
	ArH	NCH$_2$	CH$_3$	NCH$_3$	NCH$_3$@**5a**
C$_5$H$_5$NMe·I				4.340	
(SiPh)$_6$(CTC)$_4$ · 6HNEt$_3$	6.492	2.733	0.939		
6 : 1	6.584	2.720	0.948	4.318	2.506
6 : 2	6.666	2.744	0.969	4.252	2.514
6 : 3	6.689	2.769	0.985	4.225	2.535
6 : 4	6.707	2.801	0.999	4.200	2.589
6 : 5	6.721	2.821	1.019	4.199	2.635
6 : 6	6.728	2.843	1.033	4.202	2.682

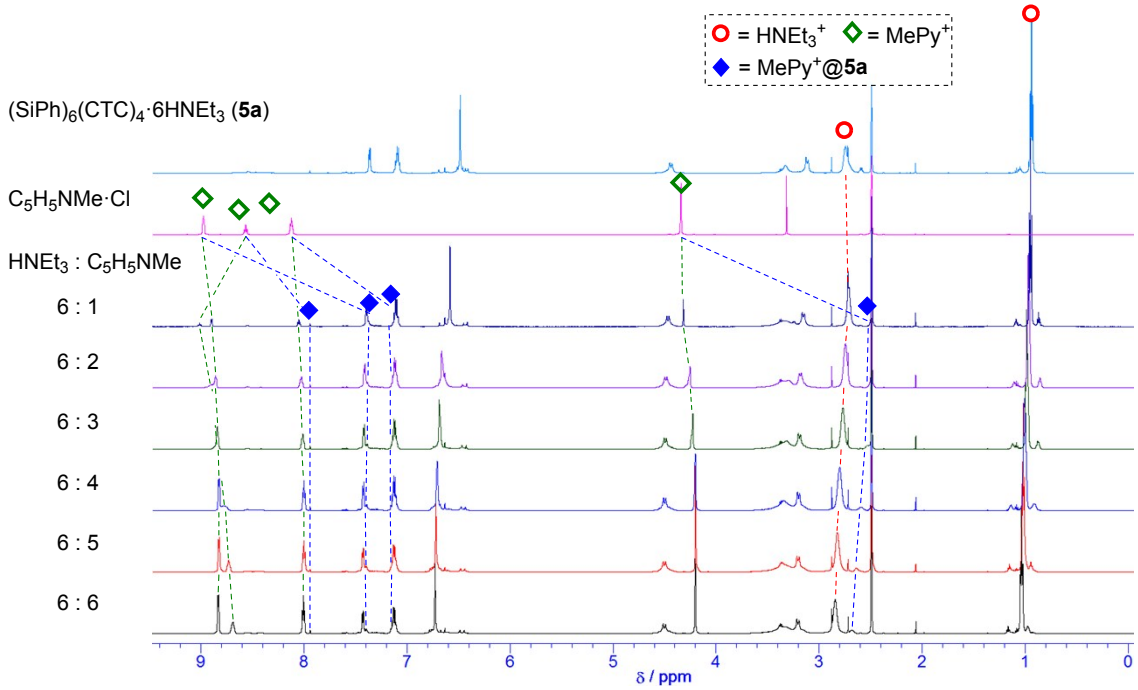

Figure S96. ^{1}H NMR titration of **5a**·6HNEt$_3$ with MePyI; circles indicate HNEt$_3^+$, while rhomboids stand for MePy$^+$ (600 MHz, DMSO-d_6).

5.4. For the titration of **5a**·6HNEt$_3$ with BuPyCl

Compound **5a**·6HNEt$_3$ (26.9 mg, 10.0 μmol) was dissolved in 2 mL of DMSO-d_6 to afford a host

solution (30 mM based on $HNEt_3$). BuPyCl (103 mg, 600 μmol) was dissolved in 250 μL of DMSO-d_6 to give a guest solution (600mM). Next, 600 μL of host solution was added to a NMR tube by using a microsyringe, and the corresponding ^{1}H NMR spectrum was recorded. The host solution was titrated by adding 5.00 μL incremental amounts (molar ratio) of the guest solution, as shown in Table S6. Gradual changes in resonance were monitored as shown in Figure S97.

Table S6. Added amounts (molar ratio) of BuPy·Cl to **5a**·6$HNEt_3$ and chemical shift changes of CTC, $HNEt_3^+$, and $BuPy^+$ (600 MHz, DMSO-d_6).

$HNEt_3$: PyBu	CTC	$HN(\underline{CH_2}CH_3)_3^+$		$C_5H_5N\underline{CH_2}CH_2CH_2CH_3^+$@**5a**			
	ArH	NCH_2	CH_3	NCH_2	CH_2	CH_2	CH_3
C_5H_5NBu·Cl				4.621	1.895	1.286	0.911
$(SiPh)_6(CTC)_4$ · 6$HNEt_3$	6.492	2.733	0.939				
6 : 1	6.609	2.777	0.987	-0.389	-1.569	-2.125	-2.244
6 : 2	6.719	2.854	1.047	-0.388	-1.571	-2.113	-2.240
6 : 3	6.743	2.896	1.080	-0.388	-1.572	-2.113	-2.242
6 : 4	6.763	2.933	1.110	-0.388	-1.576	-2.117	-2.245
6 : 5	6.775	2.948	1.125	-0.389	-1.574	-2.122	-2.244
6 : 6	6.781	2.958	1.136	-0.398	-1.578	-2.124	-2.246

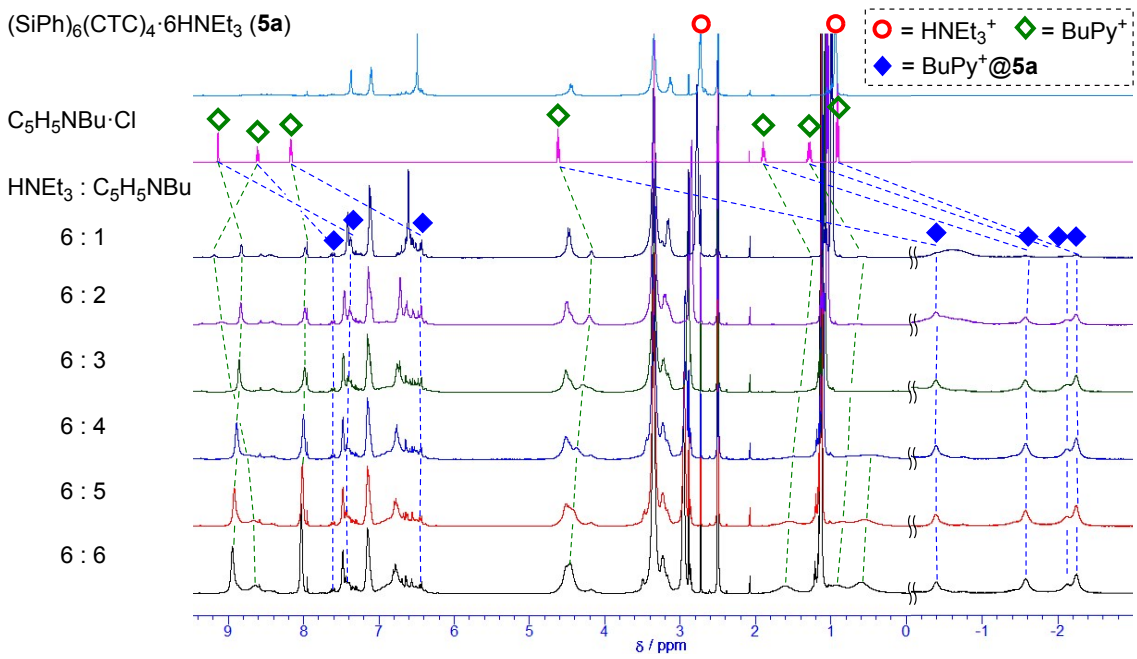

Figure S97. ^{1}H NMR titration of **5a**·6$HNEt_3$ with BuPyCl; circles indicate $HNEt_3^+$, while rhomboids stand for $BuPy^+$ (600 MHz, DMSO-d_6).

5.5. For the titration of **4a**·4TMEDAH with **7**·2PF_6

Compound **4a**·4TMEDAH (20.7 mg, 10.0 μmol) was dissolved in 2 mL of DMSO-d_6 to afford a host solution (20 mM based on TMEDAH). **7**·2PF_6 (53.0 mg, 75.0 μmol) was dissolved in 250 μL of DMSO-d_6 to give a guest solution (600 mM based on Pyridinium moiety). Next, 600 μL of host solution was added to a NMR tube by using a microsyringe, and the corresponding ^{1}H NMR spectrum was recorded. The host solution was titrated by adding 10.0 μL incremental amounts (molar ratio) of the guest solution, as shown in Table S7. Gradual changes in resonance were monitored as shown in Figure S98.

Table S7. Added amounts (molar ratio) of **7**·2PF_6 to **4a**·4TMEDAH and chemical shift changes of $\mathbf{7}^{2+}$, and TMEDAH$^+$ (600 MHz, DMSO-d_6).

4a : **7** [a]	EAT	$HN(\underline{CH_3})_2\underline{CH_2}$ $\underline{CH_2}N(\underline{CH_3})_2^+$		$C_6H_4(\underline{CH_2}N\underline{C_5}\underline{H_4}\underline{C_5}\underline{H_4}N)_2^{2+}$				
	ArH	NCH_2	NCH_3	CH_2N	3-CH	2-CH	2'-CH	3'-CH
7·2PF_6				5.866	9.320	8.628	7.992	8.859
$(SiPh)_4(EAT)_4$ · 4TMEDAH	6.410	2.586	2.296					
1 : 1 (4 : 2)	6.421	2.733	2.405	4.116	7.785	7.467	8.079	8.915
1 : 2 (4 : 4)	6.423	2.793	2.450	4.954	8.341	8.160	8.018	8.877
1 : 3 (4 : 6)	6.422	2.792	2.449	5.269	8.680	8.322	8.005	8.867
1 : 4 (4 : 8)	6.421	2.793	2.450	5.429	8.839	8.399	7.998	8.863

a) Molar ratio of **4a** and **7**. The values in parentheses represent the ratio of TMEDAH and pyridinium moiety in the **7**.

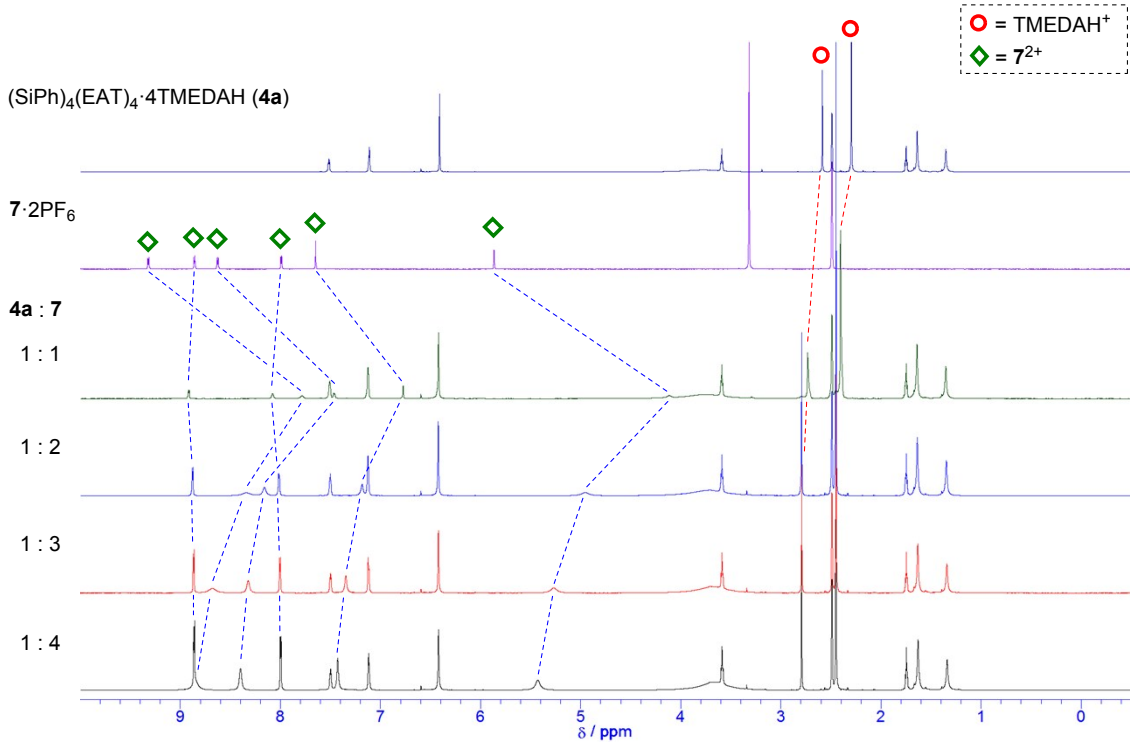

Figure S98. ^{1}H NMR titration of **4a**·4TMEDAH with **7**·2PF$_6$; circles indicate TMEDAH$^+$, while rhomboids stand for **7**$^{2+}$ (600 MHz, DMSO-d_6).

5.6. For the titration of **4a**·4TMEDAH with **8**·4PF$_6$

Compound **4a**·4TMEDAH (20.7 mg, 10.0 μmol) was dissolved in 2 mL of DMSO-d_6 to afford a host solution (20 mM based on TMEDAH). **8**·4PF$_6$ (33.0 mg, 30.0 μmol) was dissolved in 200 μL of DMSO-d_6 to give a guest solution (600 mM based on Pyridinium moiety). Next, 600 μL of host solution was added to a NMR tube by using a microsyringe, and the corresponding ^{1}H NMR spectrum was recorded. The host solution was titrated by adding 5.00 μL incremental amounts (molar ratio) of the guest solution, as shown in Table S8. Gradual changes in resonance were monitored as shown in Figure S99.

Table S8. Added amounts (molar ratio) of **8**·4PF$_6$ to **4a**·4TMEDAH and chemical shift changes of **8**$^{4+}$, and TMEDAH$^+$ (600 MHz, DMSO-d_6).

4a : **8** [a]	EAT	HN(CH$_3$)$_2$CH$_2$ CH$_2$N(CH$_3$)$_2^+$		(C$_6$H$_4$)$_2$(CH$_2$NC$_5$H$_4$C$_5$H$_4$N)$_2^{4+}$			
	ArH	NCH$_2$	NCH$_3$	C$_6$H$_4$	CH$_2$N	3-CH	2-CH
8·4PF$_6$				7.707	5.797	9.447	8.644
(SiPh)$_4$(EAT)$_4$ · 4TMEDAH	6.410	2.586	2.296				
1 : 0.25 (4 : 1)	6.445	2.711	2.390	6.845	5.989	8.634	7.584
1 : 0.50 (4 : 2)	6.446	2.788	2.447	6.936	5.848	8.459	7.427
1 : 0.75 (4 : 3)	6.536	2.788	2.447	6.998	5.785	8.442	7.383
1 : 1.00 (4 : 4)	6.623	2.788	2.447	7.042	5.757	8.426	7.404
1 : 1.25 (4 : 5)	6.695	2.788	2.446	7.068	5.747	8.418	7.449
1 : 1.50 (4 : 6)	6.736	2.788	2.447	7.094	5.747	8.415	7.478

a) Molar ratio of **4a** and **8**. The values in parentheses represent the ratio of TMEDAH and pyridinium moiety in the **8**.

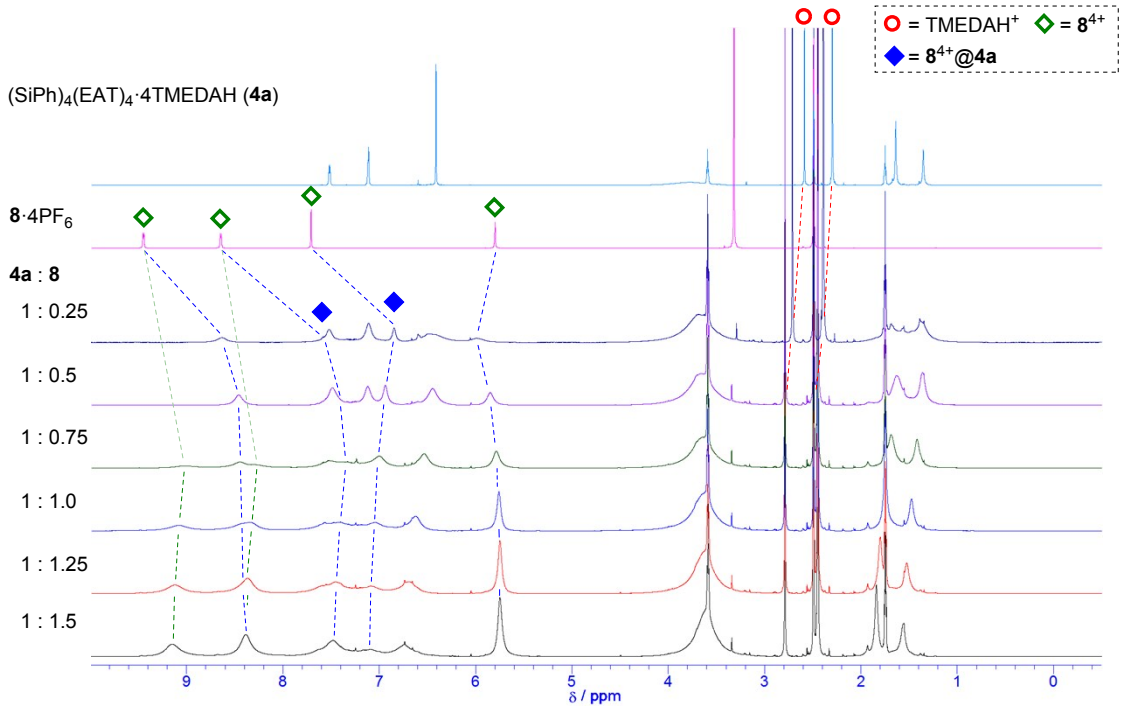

Figure S99. ^{1}H NMR titration of **4a**·4TMEDAH with **8**·4PF$_6$; circles indicate TMEDAH$^+$, while rhomboids stand for **8**$^{4+}$ (600 MHz, DMSO-d_6).

5.7. For the titration of **5a**·6HNEt$_3$ with **7**·2PF$_6$

Compound **5a**·6HNEt$_3$ (13.4 mg, 5.00 μmol) was dissolved in 1 mL of DMSO-d_6 to afford a host solution (30 mM based on HNEt$_3$). **7**·2PF$_6$ (53.0 mg, 75.0 μmol) was dissolved in 250 μL of DMSO-d_6 to give a guest solution (600 mM based on Pyridinium moiety). Next, 600 μL of host solution was added to a NMR tube by using a microsyringe, and the corresponding ^{1}H NMR spectrum was recorded. The host solution was titrated by adding 10.0 μL incremental amount (molar ratio) of the guest solution, as shown in Table S9. Gradual changes in resonance were monitored as shown in Figure S100.

Table S9. Added amounts (molar ratio) of **7**·2PF$_6$ to **5a**·6HNEt$_3$ and chemical shift changes of **7**$^{2+}$, and HNEt$_3^+$ (400 MHz, DMSO-d_6).

5a : **7** [a)]	CTC	HN($\underline{CH_2}\underline{CH_3}$)$_3^+$		C_6H_4($\underline{CH_2}$N$\underline{C_5H_4}\underline{C_5H_4}$N)$_2^{2+}$				
	ArH	NCH$_2$	CH$_3$	CH$_2$N	3-CH	2-CH	2'-CH	3'-CH
7·2PF$_6$				5.868	9.322	8.628	7.993	8.859
(SiPh)$_6$(CTC)$_6$ · 6HNEt$_3$	6.482	2.765	0.940					
1 : 1 (6 : 2)	6.468	2.905	1.034	----	9.038	7.868	7.355	8.002
1 : 2 (6 : 4)	6.465	2.964	1.076	5.238	8.925	7.903	7.360	8.247
1 : 3 (6 : 6)	6.463	2.989	1.097	5.551	8.883	7.920	7.356	8.375

a) Molar ratio of **5a** and **7**. The values in parentheses represent the ratio of HNEt$_3$ and pyridinium moiety in the **7**.

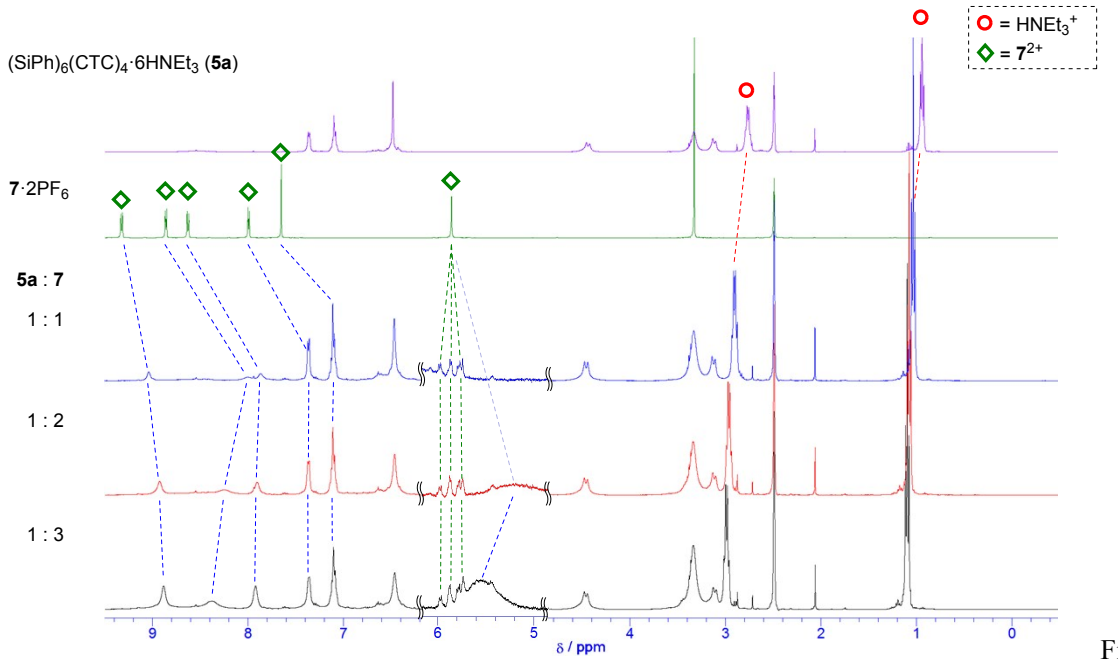

Figure S100. ^{1}H NMR titration of **5a**·6HNEt$_3$ with **7**·2PF$_6$; circles indicate HNEt$_3^+$, while rhomboids stand for **7**$^{2+}$ (400 MHz, DMSO-d_6).

5.8. For the titration of **5a**·6HNEt$_3$ with **8**·4PF$_6$

Compound **5a**·6HNEt$_3$ (13.4 mg, 5.00 μmol) was dissolved in 1 mL of DMSO-d_6 to afford a host solution (30 mM based on HNEt$_3$). **8**·4PF$_6$ (33.0 mg, 30.0 μmol) was dissolved in 200 μL of DMSO-d_6. 20 μL of this solution was diluted with 80 μL of DMSO-d_6 to give a guest solution (120 mM based on Pyridinium moiety). Next, 120 μL of host solution and 480 μL of DMSO-d_6 was added to a NMR tube by using a microsyringe, and the corresponding ^{1}H NMR spectrum was recorded (6 mM of host solution based on HNEt$_3$). The host solution was titrated by adding 10.0 μL incremental amounts (molar ratio) of the guest solution, as shown in Table S10. Gradual changes in resonance were monitored as shown in Figure S101.

Table S10. Added amounts (molar ratio) of **8**·4PF_6 to **5a**·6$HNEt_3$ and chemical shift changes of **8**$^{4+}$, and $HNEt_3^+$ (600 MHz, DMSO-d_6).

5a : **8** [a]	CTC	$HN(\underline{CH_2CH_3})_3^+$		$(C_6H_4)_2(\underline{CH_2}N\underline{C_5H_4C_5H_4}N)_2^{4+}$			
	ArH	NCH_2	CH_3	C_6H_4	CH_2N	3-CH	2-CH
8·4PF_6				7.707	5.797	9.448	8.645
$(SiPh)_6(CTC)_6$ · 6$HNEt_3$	6.474	2.775	0.947				
1 : 0.5 (6 : 2)	6.513	2.846	1.009	7.492	5.841	9.030	8.243
1 : 1.0 (6 : 4)	6.599	2.874	1.045	7.502	5.842	9.031	8.240
1 : 1.5 (6 : 6)	6.743	2.895	1.068	7.509	5.847	9.048	8.242

a) Molar ratio of **5a** and **8**. The values in parentheses represent the ratio of $HNEt_3$ and pyridinium moiety in the **8**.

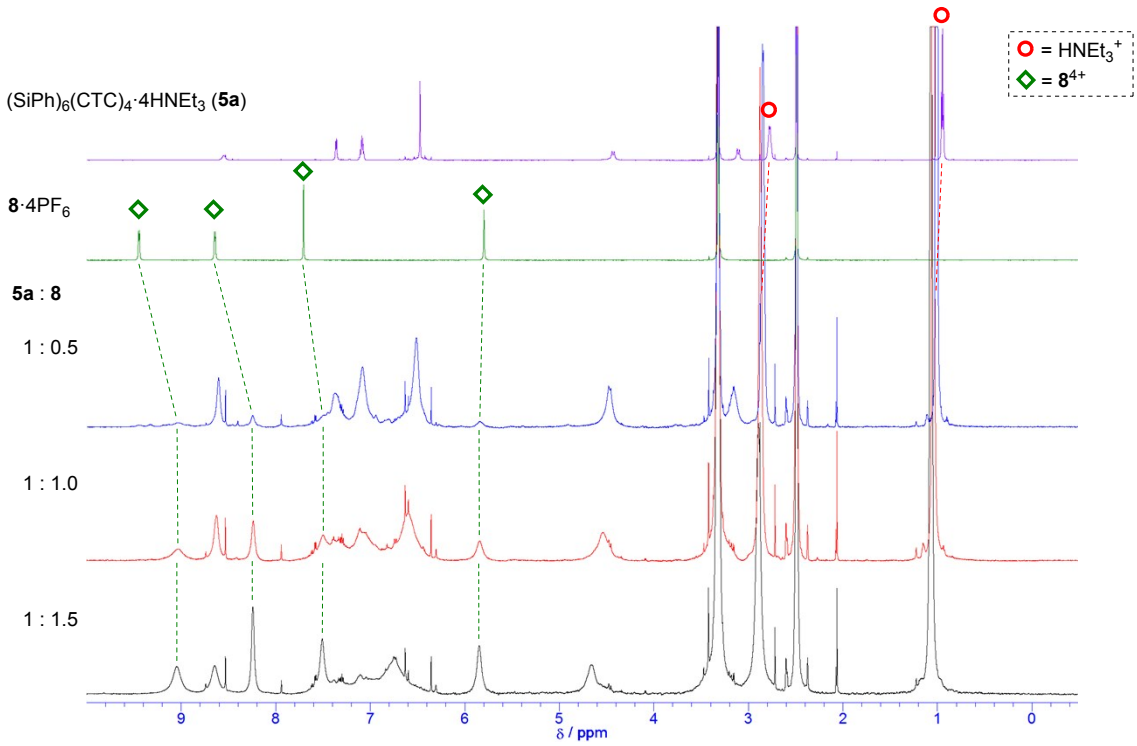

Figure S101. ^{1}H NMR titration of **5a**·6$HNEt_3$ with **8**·4PF_6; circles indicate $HNEt_3^+$, while rhomboids stand for **8**$^{4+}$ (600 MHz, DMSO-d_6).

6. Attempts to achieve gas-adsorption within 4a·4$HNEt_3$, 5a·6Na, and 5a·1.5(8)

Based on the X-ray analysis of **5a**·6$HNEt_3$, four significant electrom density peaks were observed inside the cage, which were tentatively assigned to four $HNEt_3$ cations (Figure S102 (left)). The ESI-

MS spectrum of **5a**·6HNEt$_3$ also exhibited a molecular ion that was consistent with [M+4HNEt$_3$]$^{2-}$ at m/z 1239.4 (Figure S102 (right)). Therefore, the N_2 gas adsorption-desorption analysis of **5a**·6HNEt$_3$ resulted in no porosity (Figure S103).

In the case of the X-ray analysis of **5a**·6Na, five or six water molecules were associated with each Na^+ (Figure S104 (left)). Since 6Na(H_2O)$_n^+$ (n = 5,6) is too large to enter the window of the tetrahedral cage, six Na(H_2O)$_n^+$ were located outside the negatively charged silicon centers to create an empty cavity. The ESI-MS spectrum of **5a**·6Na showed a molecular ion corresponding to [M+4Na+4MeOH]$^{2-}$ at m/z 1145.2 (Figure S104 (right)). Unfortunately, N_2 gas adsorption-desorption was not observed (Figure S105).

Finally, owing to of the poor solubility and crystallinity of **5a**·1.5(**8**) for X-ray analysis purposes, the molecular structure of **5a**·1.5(**8**) was not disclosed. However, since the ^{1}H NMR titration experiment showed no inclusion of **8** into **5a** leading to the generation of an empty cavity, N_2 gas adsorption-desorption analysis was also conducted. As a result, **5a**·1.5(**8**) did not show any porosity (Figure S106) in analogy to **5a**·6Na most likely due to a tight interaction between the cage anions and counter cations, as shown by NMR titration results. In addition, the disordered arrangement of **5a**·1.5(**8**) could disconnect the path of N_2 gas dispersion into the material.

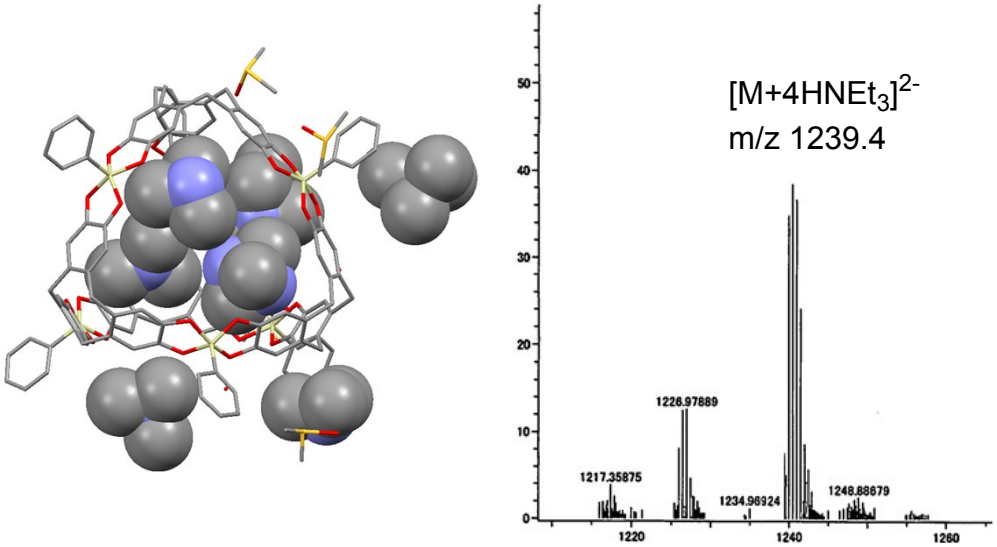

Figure S102. X-ray molecular structure (left) and ESI-MS spectrum (right) of **5a**·6HNEt$_3$. See also Figure S38 for the full range ESI-MS spectrum of **5a**·6HNEt$_3$.

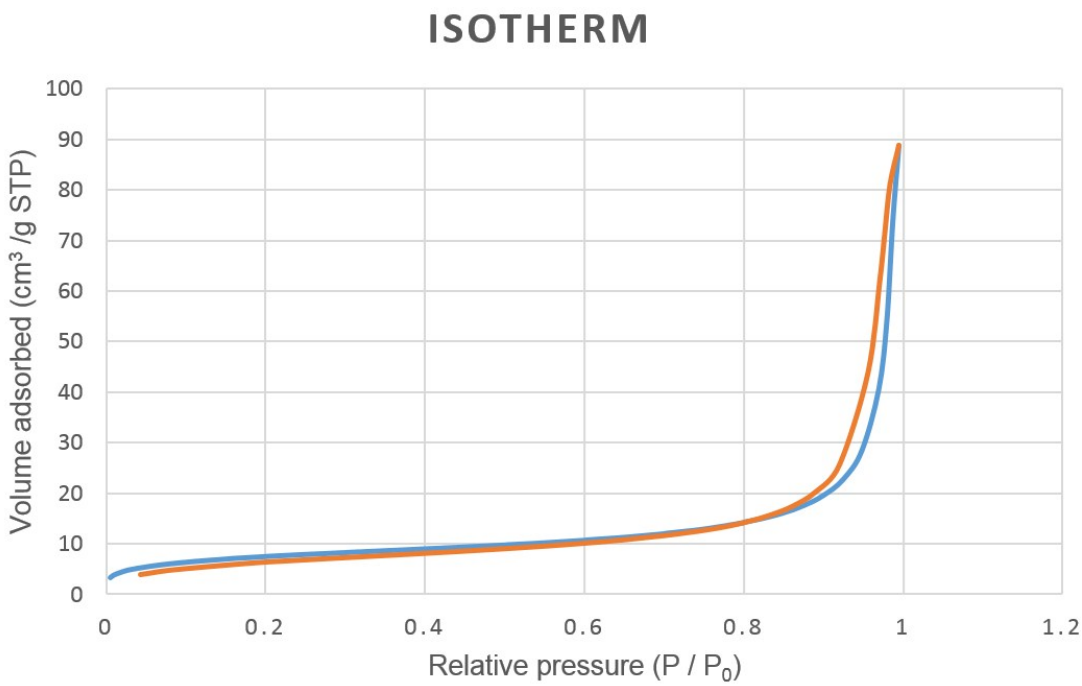

Figure S103. N_2 gas adsorption of **5a**·6HNEt$_3$.

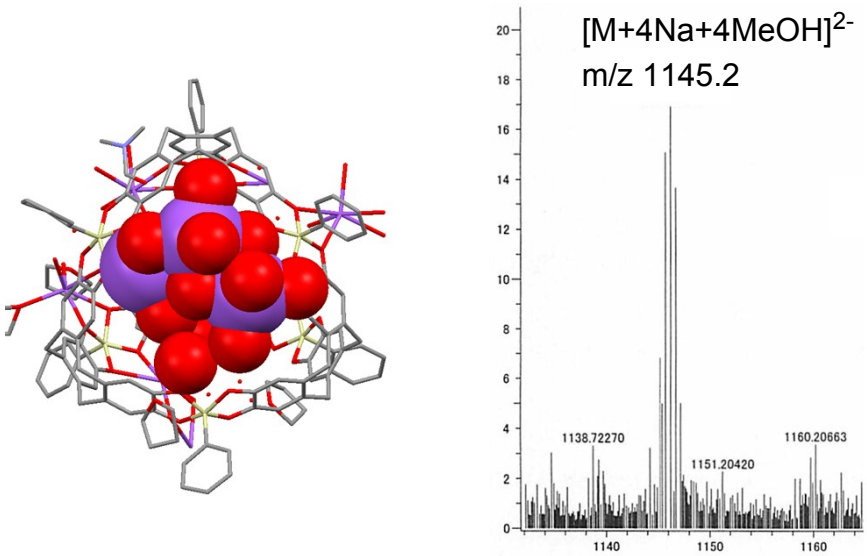

Figure S104. X-ray molecular structure (left) and ESI-MS spectrum (right) of **5a**·6Na. See also Figure S63 for the full range ESI-MS spectrum of **5a**·6Na.

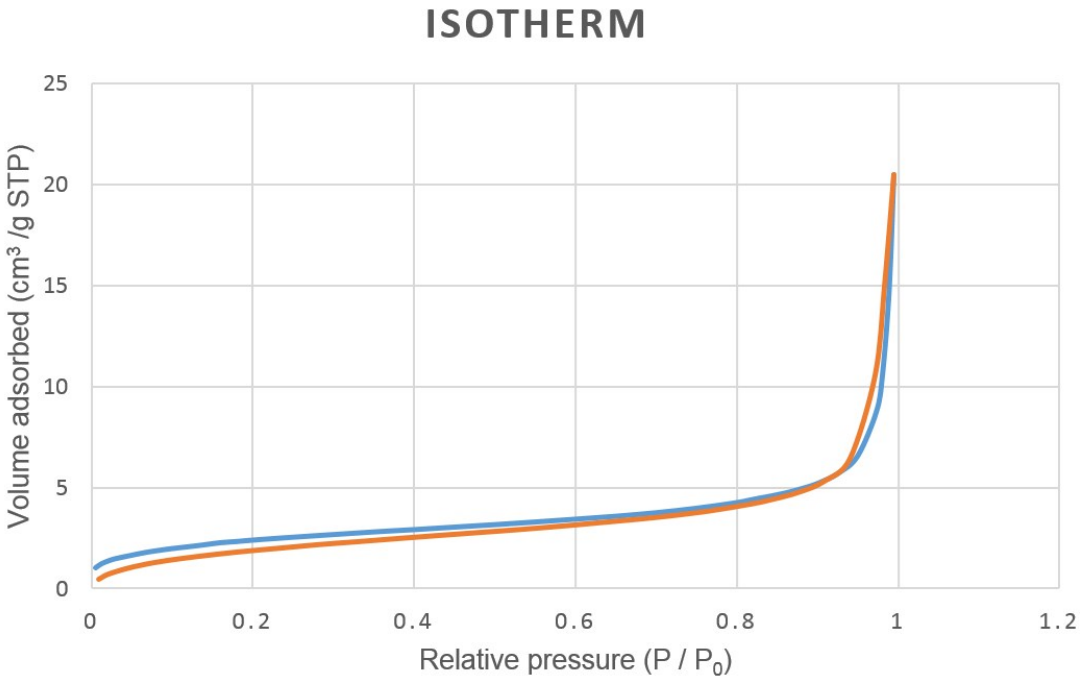

Figure S105. N_2 gas adsorption of **5a**·6Na.

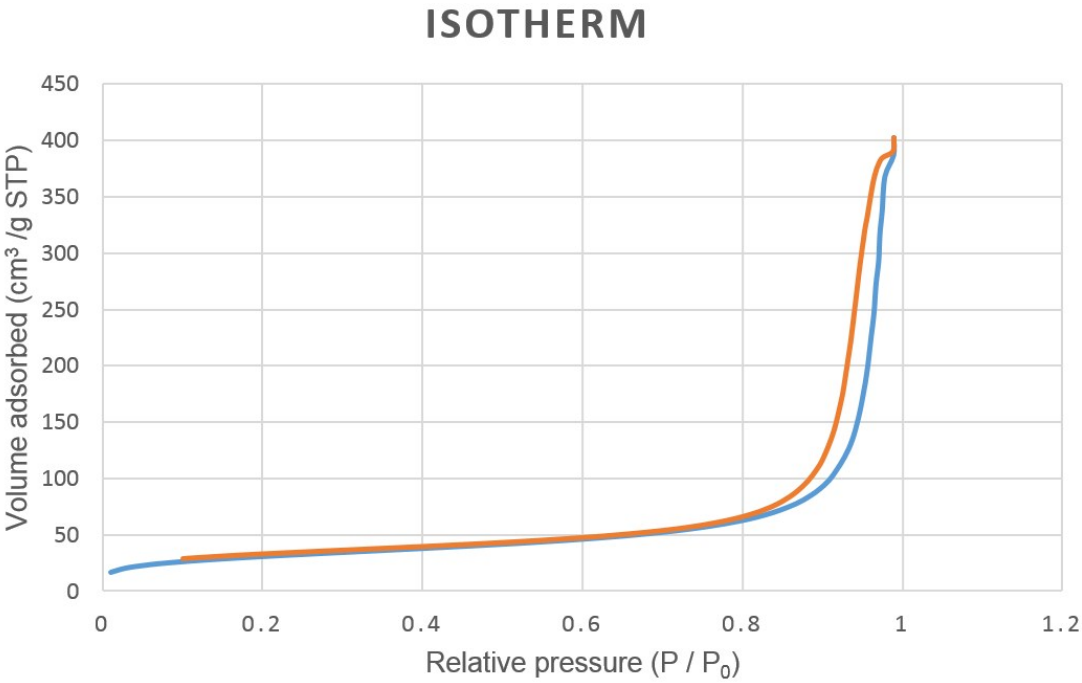

Figure S106. N_2 gas adsorption of **5a**·1.5(**8**)

7. Supporting references

1) D. Fritsch, G. Bengtson, M. Carta, N. B. McKeown, *Macromol. Chem. Phys.,* **2011**, *212*, 1137.
2) J. D. White and B. D. Gesner, *Tetrahedron Lett*., **1968,** *9*, 1591-1594.
3) Y. M. Vargas-Rodríguez, M. Vargas, R. Miranda, B. Francisco, O. Noguez, J. A. Morales-Serna, M. Salmón, *Org. Commun*., **2012**, *5*, 58-63.
4) J. A. Hyatt, *J. Org. Chem*., **1978**, *43*, 1808-1811.
5) A. Chakrabarti, H. M. Chawla, G. Hundal, N. Pant, *Tetrahedron*, **2005**, *61*, 12323-12329.
6) B. Odell, M. V. Reddington, A. M. Z. Slawin, N. Spencer, J. F. Stoddart, D. J. Williams, *Angew. Chem., Int. Ed.,* **1988**, *27*, 1547-1550.
7) M. Asakawa, W. Dehaen, G. L'abbe´, S. Menzer, J. Nouwen, F. M. Raymo, J. F. Stoddart, D. J. Williams, *J. Org. Chem.*, **1996**, *61*, 9591-9595.
8) G.M. Sheldrick, Program for the Solution of Crystal Structures, University of Göttingen, Germany.
9) M. C. Burla, R. Caliandro, M. Camalli, B. Carrozzini, G. L. Cascarano, L. De Caro, C. Giacovazzo, G. Polidori, R. Spagna, *J. Appl. Cryst.*, **2005**, *38*, 381–388.
10) L. J. Farrugia, *J. Appl. Cryst.*, **1999**, *32*, 837–838.